

2-P  
10/11/69

UNITED STATES

DEPARTMENT OF THE INTERIOR

GEOLOGICAL SURVEY

ORIGINAL CONTAINS  
COLOR ILLUSTRATIONS

INTERAGENCY REPORT NASA-149

MICROWAVE RADIOMETRIC STUDIES AND GROUND TRUTH MEASUREMENTS

OF THE NASA/USGS SOUTHERN CALIFORNIA TEST SITE

by

A.T. Edgerton

D.T. Trexler

S. Sakamoto

J.E. Jenkins

Aerojet-General Corporation

Space Division

El Monte, California

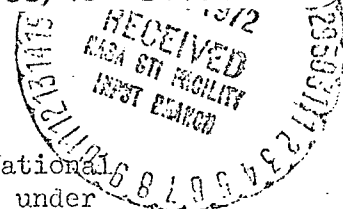
April 1969

(NASA-CR-126136) MICROWAVE RADIOMETRIC  
STUDIES AND GROUND TRUTH MEASUREMENTS OF  
THE NASA/USGS SOUTHERN CALIFORNIA TEST SITE A.T. Edgerton, et  
al (Aerojet-General Corp., El Monte,  
Calif.) Apr. 1969 109 p

N72-22368

Unclas  
24164

CSCL 08G G3/13



Prepared by the Geological Survey for the National Aeronautics and Space Administration (NASA) under contract No. W-12570, Task No. 160-75-01-32-10. Work performed under USGS/Geographic Applications Program Contract No. 14-08-0001-11425 with Aerojet-General Corp.

ORIGINAL CONTAINS  
COLOR ILLUSTRATIONS

## NOTICE

On reproduction of this report, the quality of the illustrations may not be preserved. As color illustrations are present, the black and white microfiche or facsimile copy may not reveal essential information. Full-size original copies of this report may be reviewed by the public at the libraries of the following U.S. Geological Survey locations:

U.S. Geological Survey  
1033 General Services Administration Bldg.  
Washington DC 20242

U.S. Geological Survey  
601 E. Cedar Avenue  
Flagstaff, Arizona 86002

U.S. Geological Survey  
345 Middlefield Road  
Menlo Park, California 94025

U.S. Geological Survey  
Bldg. 25, Denver Federal Center  
Denver, Colorado 80225

It is advisable to inquire concerning the timely availability of the original of this report and the possible utilization of local copying services (e. g., color reproduction) before visiting a particular library.

## FOREWORD

This report covers research conducted by the Geosciences Group, Microwave Systems Division of Aerojet-General Corporation, El Monte, California, for the Geographic Applications Program, United States Geological Survey, Washington, D. C. This work was performed in support of NASA Remote Sensing Mission 73, under Contract No. 14-08-0001-11425, "Microwave Radiometric Measurements and Geophysical Studies," between 15 May 1968 and 15 November 1968. This document represents the final technical report.

Several persons furnished cooperative support and assistance during the performance of this program. R. Alexander of the U. S. Geological Survey and Dr. L. Bowden of the University of California at Riverside were very helpful with planning and scheduling the investigations. Dr. W. Nordberg and Dr. W. Conoway of NASA's Goddard Space Flight Center are to be thanked for providing the 19.35 GHz microwave imagery. John Blinn of the Jet Propulsion Laboratory was helpful in providing reduced data from the Convair 240 MR 62 and MR 64 microwave radiometers.

R. Alexander of the Geographic Applications Program, U. S. Geological Survey, provided administrative and technical guidance to facilitate the research.

## ABSTRACT

During the weeks of 20 May and 3 June 1968, Aerojet-General Corporation participated in a joint NASA/USGS field measurement program conducted at the NASA/USGS Southern California Test Site. Ground truth data and multifrequency microwave brightness data were acquired by Aerojet's mobile field laboratory operating in conjunction with overflights by NASA's instrumented Convair 240 and 990 aircraft.

The ground-based investigations were performed at a number of locales representing a variety of terrains including open desert, cultivated fields containing several different types of crops, barren fields of varying composition and soil moisture content, portions of the San Andreas Fault Zone, and the Salton Sea. The measurements acquired ground truth data (temperature and moisture content at various depths, bearing strength, resistivity, and composition) and microwave brightness data at wavelengths of 0.8 cm, 2.2 cm, and 21 cm.

During the week of 20 May 1968, overflights were conducted by NASA's Convair 240 aircraft and radiometric brightness data were acquired along several flight lines and at wavelengths of 0.9 cm, 1.4 cm, 1.9 cm, and 3.2 cm. The airborne data acquired during the week of 3 June consisted of microwave imagery obtained by the electronically-scanned 1.55-cm microwave imager aboard NASA's Convair 990 aircraft.

One of the primary objectives of this program was to determine how effective microwave radiometers are for obtaining soil moisture data. Generally, the correlation between antenna brightness temperatures and the soil moisture content was good for the ground-based measurements. However, airborne data were inconclusive. The difficulty stems from the relatively large integration times used during the overflights coupled with the rather large fields of view of the instruments. These circumstances precluded good spacial resolution. Individual fields could not be resolved which tended to smooth the data so that there was no sharp distinction between fields of high moisture content and adjoining dry areas. This can be avoided by using shorter integration periods in future experiments.

Despite the problems encountered during these experiments, microwave radiometers, particularly imaging devices, have good potential as a tool for land use studies and geographic investigations. The imagery obtained with the Convair 990 aircraft indicates the usefulness of microwave radiometry as a tool for mapping terrain differences on the basis of microwave emission characteristics. The imagery also shows that surface conditions (sea state) of large areas of open water such as lakes and seas can be determined.

## TABLE OF CONTENTS

	<u>Page</u>
SECTION 1.0	INTRODUCTION AND SUMMARY. . . . . 1-1
SECTION 2.0	GROUND BASED STUDIES. . . . . 2-1
2.1	Soil Investigations . . . . . 2-5
2.1.1	Microwave Radiometric Measurements. . . . . 2-5
2.1.2	Geophysical Measurements on Soil Sites. . . . . 2-9
2.2	Crop Studies. . . . . 2-14
2.2.1	Summary . . . . . 2-14
2.2.2	Scattering by Vegetation. . . . . 2-14
2.2.3	Effect of Vegetation on Soil Moisture Determination. . . . . 2-16
2.3	Geologic Investigations . . . . . 2-19
2.3.1	San Andreas Fault Traverses . . . . . 2-19
2.3.2	Inclined Sediments. . . . . 2-20
SECTION 3.0	AIRBORNE MICROWAVE MEASUREMENTS . . . . . 3-1
3.1	Airborne Multifrequency Measurements. . . . . 3-2
3.1.1	USGS Flight Line 2 <sup>1</sup> . . . . . 3-2
3.1.2	USGS Flight Lines 5a and 5b . . . . . 3-5
3.2	1.55-cm (19.35 GHz) Microwave Imagery . . . . . 3-7
3.2.1	Instrumentation and Data Processing . . . . . 3-7
3.2.2	Agricultural and Desert Terrain . . . . . 3-10
3.2.3	Mexicali-Calexico Area. . . . . 3-12
3.2.4	Salton Sea. . . . . 3-14
SECTION 4.0	CONCLUSIONS . . . . . 4-1

## APPENDICES

APPENDIX A	MULTIFREQUENCY MICROWAVE LABORATORY AND GROUND TRUTH SYSTEM. . . . . A-1
APPENDIX B	DETAILED DESCRIPTION OF GROUND SITES INCLUDING PERTINENT GEOPHYSICAL AND MICROWAVE DATA. . . . B-1

## ILLUSTRATIONS

<u>FIGURE</u>		<u>Page</u>
1	Soil Moisture . . . . .	2-6
2	Comparison of Horizontal and Vertical Polarization Temperatures . . . . .	2-8
3	Physical Parameters of Site 1 . . . . .	2-10
4	Physical Parameters of Site 2 . . . . .	2-11
5	Physical Parameters of Site 3 . . . . .	2-12
6	Power Reflected vs. Water Content of Leaf . . . . .	2-15
7	Crop Comparisons. . . . .	2-17
8	Salton Sea and Vicinity Showing Location of NASA Convair 990 Aircraft Flight Line (7 June 1968) and Flight Lines 2 <sup>1</sup> , 5a, and 5b of NASA Convair 240A Aircraft (21 May 1968). . . . .	3-3
9	Microwave Radiometric Temperatures Along USGS Flight Line 2 <sup>1</sup> . . . . .	3-4
10	Antenna Brightness Temperatures Measured Along USGS Flight Lines 5a and 5b . . . . .	3-5
A-1	Close-up View of Radiometer . . . . .	A-2
A-2	Data Processing Flow Chart . . . . .	A-5
B-1	Site 1. . . . .	B-2
B-2a	Site 1 - Radiometric Brightness Temperature Measured at 21-cm Wavelength. . . . .	B-3
B-2b	Site 1 - Radiometric Brightness Temperature Measured at 2.2-cm Wavelength . . . . .	B-4
B-2c	Site 1 - Radiometric Brightness Temperature Measured at 0.8-cm Wavelength . . . . .	B-5
B-3	Site 2. . . . .	B-6
B-4	Site 3. . . . .	B-8
B-5a	Site 3 - Radiometric Brightness Temperature at 21-cm Wavelength. . . . .	B-10
B-5b	Site 3 - Radiometric Brightness Temperature Measured at 0.8-cm Wavelength . . . . .	B-11
B-5c	Site 3 - Radiometric Brightness Temperature Measured at 2.2-cm Wavelength . . . . .	B-12
B-6	Site 5. . . . .	B-14
B-7a	Site 5 - Radiometric Brightness Temperature Measured at 21-cm Wavelength. . . . .	B-15
B-7b	Site 5 - Radiometric Brightness Temperature Measured at 2.2-cm Wavelength . . . . .	B-16
B-7c	Site 5 - Radiometric Brightness Temperature Measured at 0.8-cm Wavelength . . . . .	B-17
B-8	Physical Parameters of Site 7 . . . . .	B-19
B-9a	Site 7 - Radiometric Brightness Temperature Measured at 2.2-cm Wavelength (Run 2) . . . . .	B-20
B-9b	Site 7 - Radiometric Brightness Temperature Measured at 0.8-cm Wavelength (Run 2) . . . . .	B-21

ILLUSTRATIONS - (Cont.)

<u>FIGURE</u>		<u>PAGE</u>
B-10a	Site 7 - Radiometric Brightness Temperature Measured at 2.2-cm Wavelength (Run 3) . . . . .	B-22
B-10b	Site 7 - Radiometric Brightness Temperature Measured at 0.8-cm Wavelength (Run 3) . . . . .	B-23
B-11	Sketch Map of Site 8. . . . .	B-24
B-12a	Site 8 - Radiometric Brightness Temperature Measured at 2.2-cm Wavelength . . . . .	B-25
B-12b	Site 8 - Radiometric Brightness Temperature Measured at 0.8-cm Wavelength . . . . .	B-26
B-13a	Site 10 - Radiometric Brightness Temperature Measured at 2.2-cm Wavelength . . . . .	B-29
B-13b	Site 10 - Radiometric Brightness Temperature Measured at 0.8-cm Wavelength . . . . .	B-30
B-14	Site 11 . . . . .	B-31
B-15a	Site 11 - Radiometric Brightness Temperature Measured at 21-cm Wavelength. . . . .	B-34
B-15b	Site 11 - Radiometric Brightness Temperature Measured at 2.2-cm Wavelength . . . . .	B-35
B-15c	Site 11 - Radiometric Brightness Temperature Measured at 0.8-cm Wavelength . . . . .	B-36
B-16	Site 12 . . . . .	B-37
B-17	Site 12 - Radiometric Brightness Temperature Measured at 21-cm Wavelength. . . . .	B-38
B-18	Site 13 . . . . .	B-40
B-19	Sites 14 and 15 . . . . .	B-41
B-20	San Andreas Fault Traverse. . . . .	B-43
B-21	Site 17 . . . . .	B-45
B-22	Microwave Brightness Temperatures at Three Wavelengths Taken During Traverse of Site 18. . . . .	B-47
B-23	Site 19 . . . . .	B-50
B-24	Site 20 . . . . .	B-52
B-25	Site 21 . . . . .	B-54



## Section 1

### INTRODUCTION AND SUMMARY

During the period of 21 May through 7 June 1968, Aerojet-General Corporation conducted multifrequency microwave radiometric measurements and ground truth investigations on the NASA/USGS Southern California Test Site, in conjunction with the U. S. Geological Survey Geographic Applications Program. These studies were conducted in various localities of the Coachella Valley/Salton Sea/Imperial Valley area of Southern California, as directed by the USGS technical officer. The resulting data have been reduced and interpreted in conjunction with airborne microwave data acquired by the NASA Convair 240 and Convair 990 aircraft. It is the purpose of this report to summarize all work performed and to present results of the microwave experiments.

The Southern California Test Site includes concentrations of agriculture and small towns in the Coachella and Imperial Valleys of the Salton Sea portion of the Colorado Desert, about one hundred miles from coastal Los Angeles. The Coachella Valley is adjacent to the San Bernardino and San Jacinto mountain ranges, and is bordered on the east by the San Andreas Fault.

During the week of 20 May 1968, ground truth investigations and multifrequency microwave measurements utilizing Aerojet's field laboratory, were performed in conjunction with overflights by the NASA Convair 240 remote sensor aircraft. Ground-based microwave radiometric measurements were taken at wavelengths of 21 cm (1.4 GHz), 2.2 cm (13.4 GHz), and 0.8 cm (37 GHz). Airborne measurements were taken at wavelengths of 3.2 cm (9.3 GHz), 1.9 cm (15.8 GHz), 1.4 cm (22.2 GHz) and 0.9 cm (34.0 GHz). Ground studies were conducted in farming areas along Jackson Road near Indio, on desert terrain northeast of the Salton Sea, and on various agricultural lands in the Imperial Valley, south of the Sea. Airborne measurements were conducted along a number of flight lines,

as outlined in the USGS/NASA Southern California Remote Sensing Program planning document.<sup>1</sup> Interpretation of the airborne microwave data has been confined to flight lines 2A, 5A, and 5B because of difficulties in reducing the raw data.

During the week of 3 June 1968, additional ground measurements were collected in conjunction with overflights by the NASA Convair 990 which was instrumented with an electronically scanned 1.55 cm (19.35 GHz) microwave imager. Ground studies were conducted on a variety of crop types in the Imperial Valley, and on desert terrain along the eastern side of the Salton Sea. Microwave imagery was collected along a number of flight lines across the Southern California Test Site. The quality of the resultant microwave images was very good. Consequently, a major share of the airborne data interpretation was of the imagery.

Some of the airborne data gathered during these investigations warrants further examination and analysis. However, due to the modest level of effort of this program, the investigators were unable to devote enough time for a thorough examination of all of the airborne data.

---

<sup>1</sup> NASA/USGS Southern California Test Site #76 Planning Document,  
Prepared for U. S. Geological Survey, May 1968.

## Section 2

### GROUND BASED STUDIES

#### 2.0 GENERAL

During the weeks of 20 May and 3 June 1968, ground truth investigations and multifrequency microwave measurements were performed on 21 sites within the Southern California Test Site. Microwave measurements were taken at both horizontal and vertical antenna polarizations, as a function of antenna viewing angle (elevation scans). In addition, microwave traverses were conducted at various fixed antenna viewing angles for selected crop types and terrains. These measurements were taken simultaneously at frequencies of 1.4 GHz (21 cm), 13.4 GHz (2.2 cm) and 37 GHz (0.8 cm). Ground truth investigations included acquisition of soil moisture data, thermal profiles, electrical resistivity and bearing strength measurements, photographic documentation of the study areas, and observations concerning soil and crop types.

The primary purpose of these measurements was to provide a sound basis for interpreting airborne microwave data acquired by the two NASA aircraft. For this reason measurements were taken of a variety of crops and barren fields with varying moisture conditions. Crops examined include beans, alfalfa, cotton, barley, sugar beets, and silage grass. Soil studies were conducted at six locations. These sites contained no vegetal cover, and moisture conditions ranged from substantially dry to saturated. Multifrequency microwave traverses were also conducted on three desert sites, including traverses across the San Andreas Fault and over a series of steeply dipping outcropping sediments. Additional measurements were also taken of the Salton Sea proper. Table 1 presents a description of each ground site and the type of measurements performed.

The mobile field laboratory used in conjunction with the ground studies is described in Appendix A. Detailed descriptions of each site, including pertinent geophysical and microwave data, are contained in Appendix B. The following discussions provide a comparison of data gathered for the various crop types and soil moisture conditions.

TABLE 1

## DESCRIPTION OF MICROWAVE AND GROUND TRUTH MEASUREMENTS

<u>Date</u>	<u>Time</u>	<u>Site No.</u>	<u>Site Description</u>	<u>Type of Measurement</u>	<u>Aircraft Overflight</u>
5/21/68	1070	1	Relatively dry plowed, fine sandy loam field along Jackson Street	Detailed elevation scans and ground truth	C-240 multifrequency microwave radiometer
5/21/68	1270	2	Recently irrigated field free of vegetal cover along Jackson Street	Detailed elevation scans and ground truth	C-24C multifrequency microwave radiometer
5/21/68	1420	3	Similar to Site 2, but dryer	Detailed elevation scans and ground truth	None
5/21/68	1570	4	Barren field recently irrigated	Fixed viewing angle traverse; $\theta = 60^\circ$ ; taken for statistical purposes	None
5/21/68	1700	5	Bean field	Detailed elevation scans and ground truth	None
5/22/68	1480	6	Desert terrain east of Salton Sea, in vicinity of San Andreas Fault	Fixed viewing angle traverse; $\theta = 45^\circ$	None
5/22/68	1890	7	Recently irrigated barren field and (see Sites 2-5) bean field	Detailed elevation scans in conjunction with sun-set overflights	C-240 multifrequency microwave radiometer
5/23/68	0600	7	As above	Detailed elevation scans in conjunction with sunrise overflights	Overflight cancelled

TABLE 1 (CONT.)

<u>Date</u>	<u>Time</u>	<u>Site No.</u>	<u>Site Description</u>	<u>Type of Measurement</u>	<u>Aircraft Overflight</u>
5/23/68	2100	8	Salton Sea adjacent to Calipatria Boat Ramp Causeway	Detailed elevation scans and water truth for use in improving calibration of C-240 radiometers	C-240 multifrequency microwave radiometer
5/23/68	2230	9	Saturated silt loam field (undergoing leaching)	Detailed elevation scans and ground truth and fixed viewing angle traverse; $\theta = 45^\circ$	C-240 multifrequency microwave radiometer
5/24/68	0030	10	Alfalfa field	Detailed elevation scans and fixed viewing angle traverse; $\theta = 45^\circ$ ground truth	C-240 multifrequency microwave radiometer
6/5/68	1403	11	Cotton field	Detailed elevation scan and ground truth	C-990 microwave imager
6/5/68	1555	12	Dry plowed field	Detailed elevation scans and ground truth	C-990 microwave imager
6/5/68	1680	13	Plowed field, relatively dry	Detailed elevation scans and ground truth	C-990 microwave imager
6/6/68	1362	14	Traverse across San Andreas Fault near Salton Parkside	Fixed viewing angle traverse; $\theta = 50^\circ$ and $30^\circ$ ; ground truth	C-990 microwave imager
6/6/68	1692	15	As above	Fixed viewing angle traverse; $\theta = 45^\circ$ ; ground truth	C-990 microwave imager
6/6/68	1734	16	Sedimentary series - attitude varied from flat-lying to near vertical	Fixed viewing angle traverse; $\theta = 45^\circ$	C-990 microwave imager

<u>Date</u>	<u>Time</u>	<u>Site No.</u>	<u>Site Description</u>	<u>Type of Measurement</u>	<u>Aircraft Overflight</u>
6/7/68	0983	17	Barley field - recently cut	Fixed viewing angle; traverse; $\theta = 45^\circ$ ; ground truth	C-990 microwave imager
6/7/68	1120	18	Alfalfa field, includes recently cut alfalfa and a mature crop	Fixed viewing angle traverse; $\theta = 50^\circ$ ; ground truth	C-990 microwave imager
6/7/68	1224	19	Mature sugar beet crop	Fixed viewing angle traverse; $\theta = 45^\circ$ , and elevation scans; ground truth	C-990 microwave imager
6/7/68	1314	20	Recently planted cotton field - 20% vegetal cover	Fixed viewing angle traverse; $\theta = 45^\circ$	C-990 microwave imager
6/7/68	1443	21	Silage grass - 80% vegetal cover	Fixed viewing angle traverse; $\theta = 45^\circ$ ; elevation scan; ground truth	C-990 microwave imager

## 2.1 Soil Investigations

### 2.1.1 Microwave Radiometric Measurements

Microwave brightness temperatures of soils are dependent upon a number of physical properties. These include moisture content, surface roughness, (including microrelief, particle or fragment size and shape, vegetal cover, etc.), thermometric temperature, and stratigraphy (layering, etc.). Compositional variations are of less importance in determining the microwave characteristics of soils, except in circumstances where significant amounts of metallic or magnetic minerals are present. With the exception of the thermometric temperature dependence, these parameters are all associated with the dielectric properties of the soils. Other factors which must be considered in determining the microwave characteristics of natural materials include: observational frequency or wavelength, antenna polarization, and antenna viewing angle. Soil moisture content is one of the most influential variables contributing to brightness temperature variations. Soil measurements taken on Sites 1, 2, 3, and 9 bear out this point.

Figure 1 shows microwave brightness temperatures measured as a function of antenna viewing angle for wavelengths of 0.8 cm, 2.2 cm, and 21 cm. Site 1 was driest, followed by Site 3. Site 2 was quite moist, and Site 9 was saturated (Table 1). At all three wavelengths, the microwave brightness temperatures are a function of moisture content with radiometric temperatures decreasing for increasing moisture values.

Soil moisture variations can best be distinguished by examining microwave data acquired for low antenna viewing angles (0 to 20 degrees or so above nadir). At higher viewing angles, brightness temperatures, particularly the horizontally polarized components, are more strongly influenced by surface roughness variations. Roughness effects are most conspicuous in the short 0.8 cm wavelength data.

The depth of investigation of a particular radiometer is dependent on the sensor wavelength. Longer wavelength systems are capable of greater penetration. Consequently, by utilizing multiwavelength systems it is

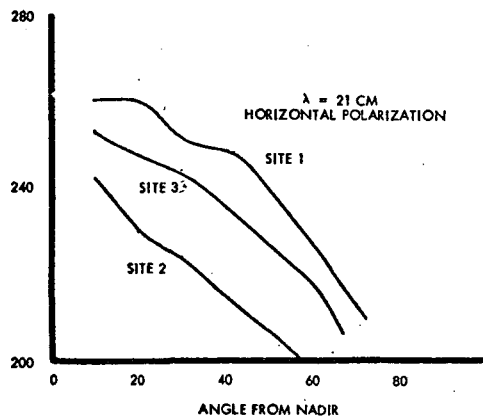
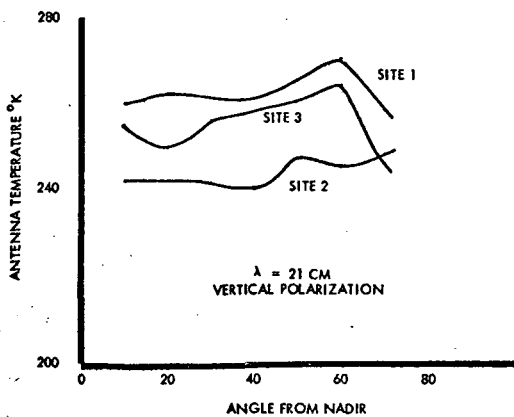
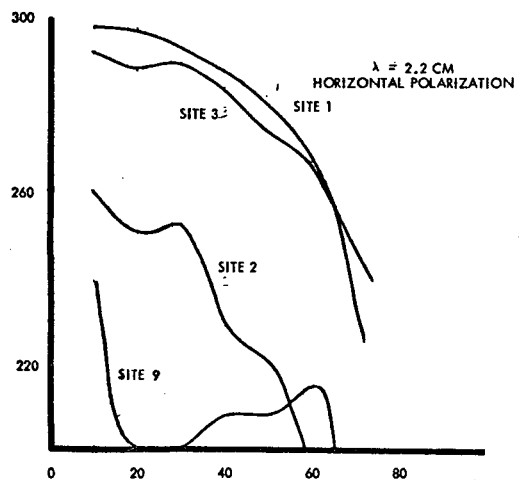
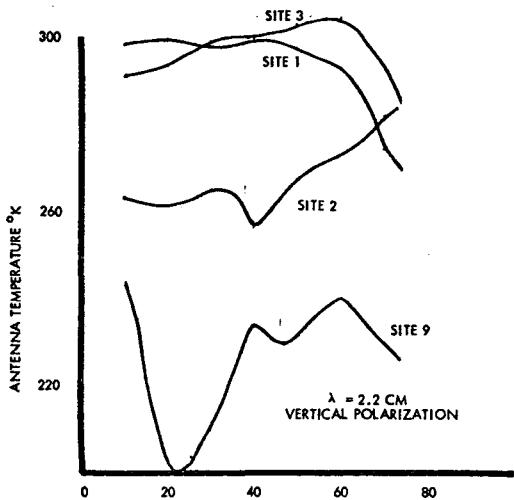
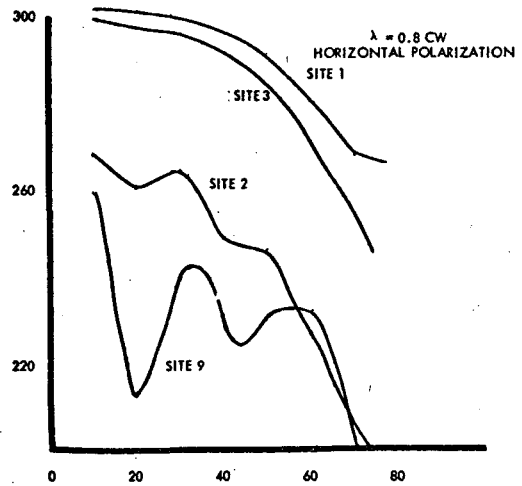
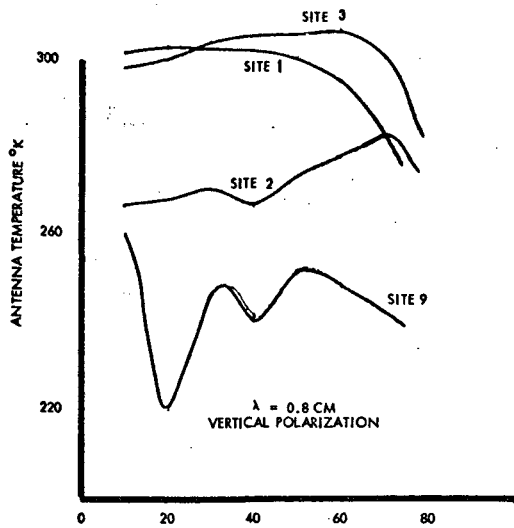


Figure 1. Soil Moisture



possible to construct a picture of the vertical distribution of soil moisture in the upper interval of soil. Soils on Sites 2 and 9 contained substantial amounts of moisture on and below the surface in contrast with Sites 1 and 3 which were relatively dry on the surface. Brightness temperatures measured at all three wavelengths were conspicuously colder on the moist sites, whereas measured temperatures on Sites 1 and 3 were quite similar. Site 9 was a field undergoing leaching near the south end of the Salton Sea. The leach basins were separated by earthen dikes. The large variations in the Site 9 scans correspond to alternately viewing the very moist leach basins, and the somewhat drier dikes separating the leach ponds.

Vertical polarization brightness temperatures are compared with horizontal polarization temperatures for barren fields with varying moisture, grain size and surface texture (Figure 2). Two angles,  $10^\circ$  and  $45^\circ$  from nadir, were selected to show displacement of the curve to the left with increasing angle of observation while the slope of the curves remains nearly equal. The slope of the lines represents the ratio of horizontal polarization emissivity to vertical polarization emissivity. This relationship is obtained by analyzing the basic radiometric temperature formulas to determine the slope of the curves.

$$\text{Slope} = \frac{T_{v\theta}}{T_{h\theta}} = \frac{\epsilon_v T_g + \rho_v T_s}{\epsilon_h T_g + \rho_h T_s}$$

where:

$T_{h\theta}$  = Horizontal polarization brightness temperature at angle  $\theta$

$T_{v\theta}$  = Vertical polarization brightness temperature at angle  $\theta$

$\epsilon_{h\theta}$  = Emissivity for horizontal polarization at angle  $\theta$

$\epsilon_{v\theta}$  = Emissivity for vertical polarization at angle  $\theta$

$\rho_h$  = Horizontal polarization reflection coefficient

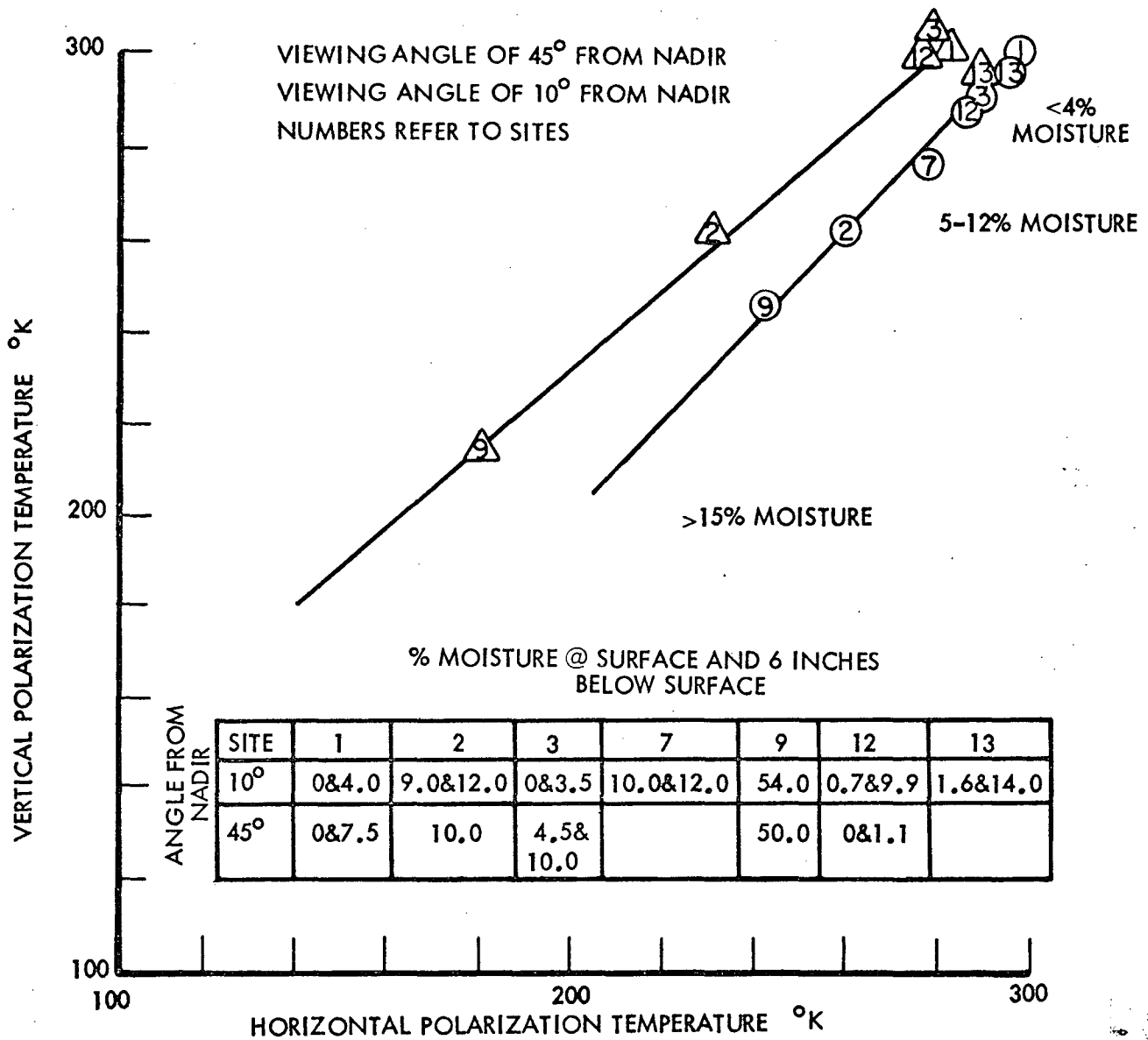


Figure 2. Comparison of Horizontal and Vertical Polarization Temperatures

$\rho_v$  = Vertical polarization reflection coefficient

$T_s$  = Radiometric sky temperature

$T_g$  = Thermometric ground temperature

$\rho T_s$  is small compared to  $\epsilon T_g$  and can be disregarded. Therefore,

$$\frac{\epsilon_v T_g}{\epsilon_h T_g} \text{ can be reduced to } \frac{\epsilon_v}{\epsilon_h} .$$

The curves show that the ratio of  $\frac{\epsilon_v}{\epsilon_h}$  does not change appreciably with increasing angle of observation. In plotting the points, no attempt was made to correct any of the radiometric temperatures for the effects of grain size or surface texture (roughness). Note that, in the case of Site 13, a warmer horizontal polarization brightness temperature ( $\theta = 45^\circ$ ) causes the point to be shifted to the right. This warmer horizontal polarization brightness temperature is indicative of temperatures obtained from diffuse surfaces. The soil surface at Site 13 is moderately rough with clods approaching 6 inches in maximum dimension.

The influence of variations in soil thermometric temperature ( $T_g$ ) can be eliminated by comparing vertical and horizontal polarization temperatures. This permits direct comparison of variations in soil from site to site, independent of variations in thermometric temperature.

### 2.1.2 Geophysical Measurements on Soil Sites

Geophysical measurements conducted on each soil site included measurement of the vertical temperature profile, moisture as a function of depth at several points along each scan path, bearing strength observations, electrical resistivity measurements, and determination of soil type and texture. Figures 3, 4, and 5 are plots of the thermal gradient moisture content, bearing strength and electrical resistivity as a function of distance along the scan path. On these plots data are shown as a function of antenna viewing angle for convenience in relating to the microwave measurements.

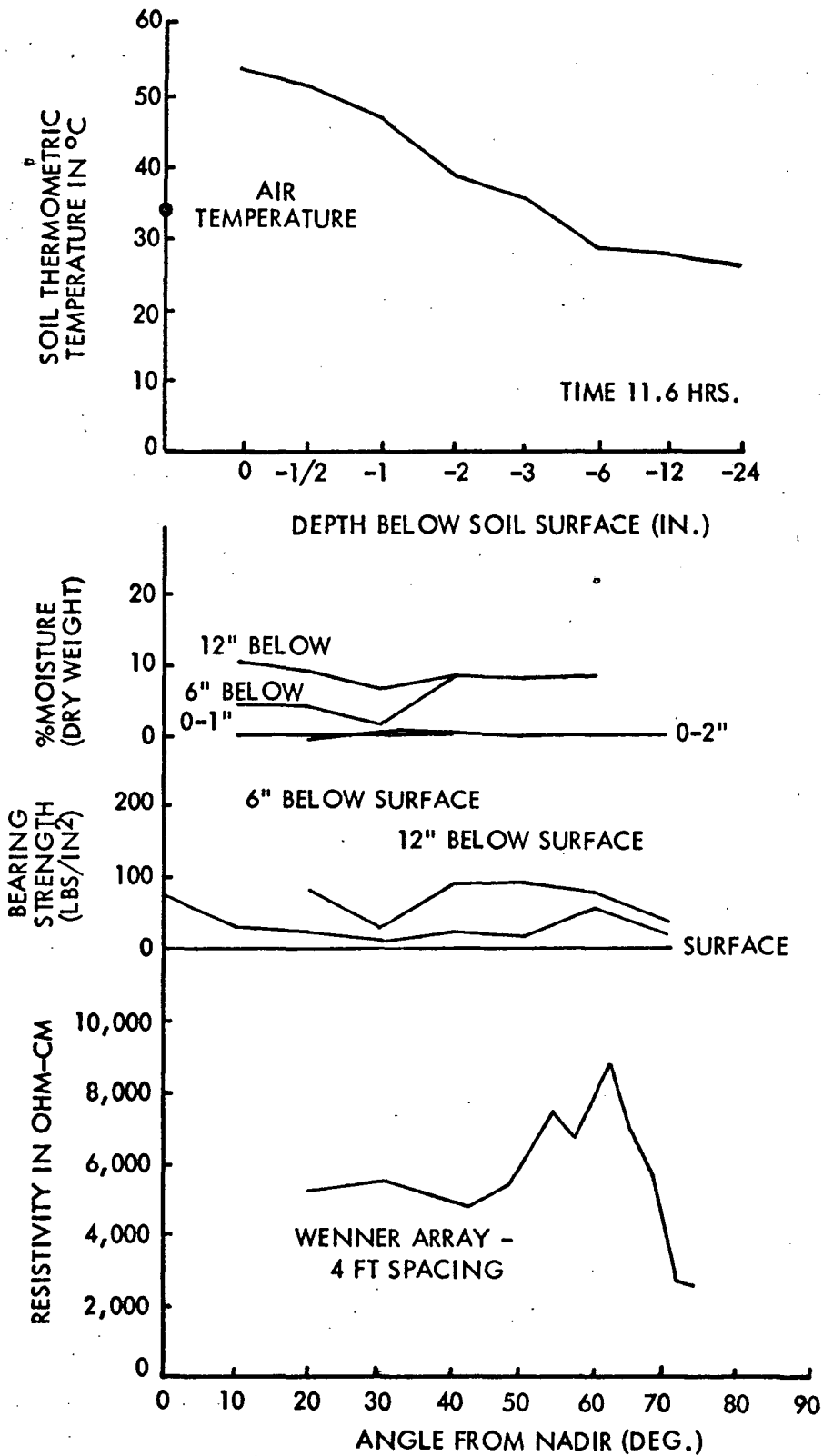


Figure 3. Physical Parameters of Site 1

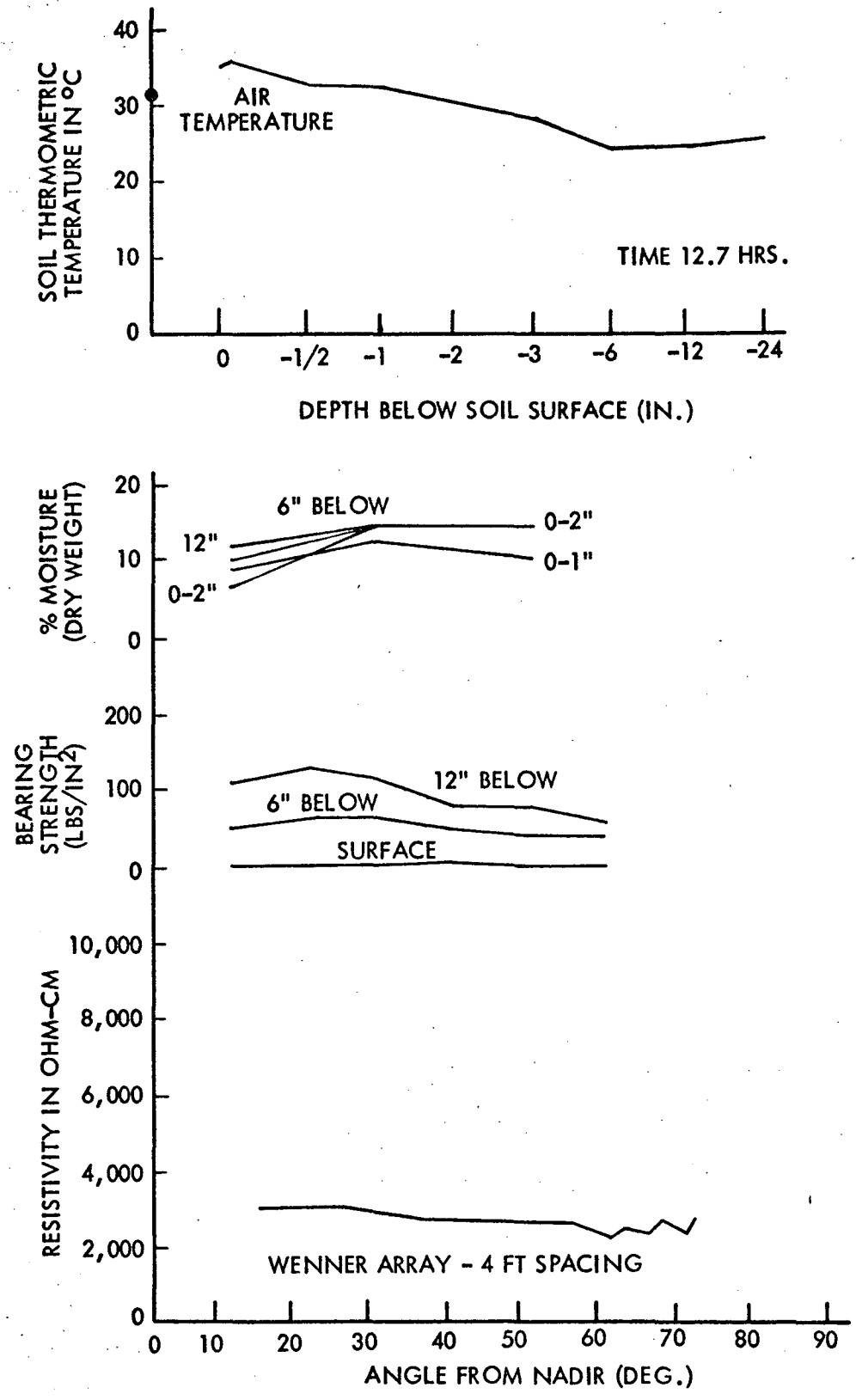


Figure 4. Physical Parameters of Site 2

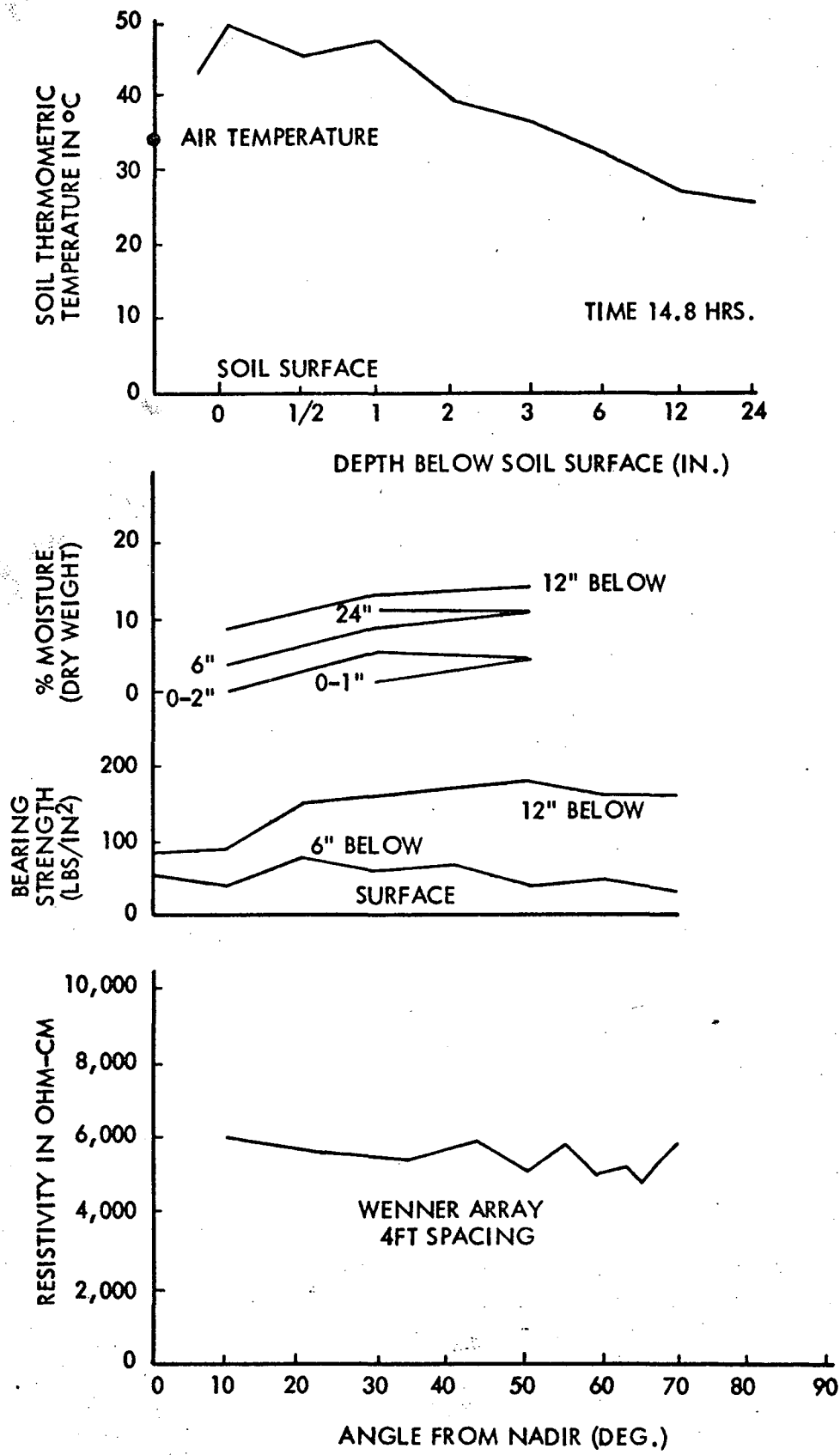


Figure 5. Physical Parameters of Site 3

Sites 1 and 3 were quite warm on the surface with temperatures above 50°C, Table 2. Site 2, which was very moist, was somewhat cooler with a surface temperature of 35°C. Site 9 was saturated and contained standing water in places. Temperature on the surface of Site 9 was 16°C. On all four sites the temperatures measured at a depth of 24 inches were on the order of 25°C.

TABLE 2

SOIL MOISTURE AND TEMPERATURE DATA FOR  
SITES 1, 2, 3, & 9

	Depth, in.	Site No.			
		1	2	3	9
Avg. Moisture Content Along Scan Path	0-1	0%	11%	3%	54%
	6	6%	13½%	7½%	54%
	12	8%	12½%	13%	54%
	24	-	-	11%	-
Soil Temp., °C	-½	51	33	45	25
	-2	38	30	37	20
	-6	28	25	32	18

Soil moisture content along the various scan paths was somewhat variable, ranging from a low of 0 percent on the surface of Site 1 to above 50 percent on Site 9. Site 1 represents the driest material examined. Site 2 was relatively moist, and Site 3 was intermediate between the two. Site 9 was saturated. Bearing strengths and electrical resistivity along the scan path were somewhat erratic on Site 1, indicating that soils were

variable in lateral extent. On Sites 2 and 3 these properties were more uniform, indicating that the soils were more consistent there.

The soil constituting Site 1 was a fine sandy loam. Soils in the vicinity of Sites 2 and 3 were of similar character. Site 9 was situated on a fine textured silt loam.

## 2.2 Crop Studies

### 2.2.1 Summary

Due to time limitations, the crop study measurements were confined to collecting basic radiometric data. This work provided a limited catalog of crop data which have been examined for uniqueness and for effects of vegetal cover on microwave soil moisture determination. Crops of alfalfa, barley, beans, cotton, silage grass and sugar beets were examined.

### 2.2.2 Scattering by Vegetation

Water, a good reflector at microwave frequencies, is the dominant constituent of foliage. Thus, a single leaf (the surface of which is typically smooth, relative to observational wavelength) can be approximated by an equivalent film of water. Then, the microwave characteristics of the leaves are determined by the orientation of the equivalent moisture film relative to the sensor, the surface roughness of the film, the film thickness, and the physical temperature of the film. Figure 6 presents the results of an unpublished study performed by J. E. Jenkins and G. T. Chalfin<sup>2</sup>. Leaf specimens were collected from seven types of trees and the power reflection coefficients were measured at 19.35 GHz (1.55 cm), using a slotted-line waveguide insertion technique. Measurements were repeated periodically as the specimens dried out. Results are shown on Figure 6 as percent of power reflected vs. moisture content of the foliage. These results show that the individual leaves are good reflectors. The high degree of scattering typical of vegetation

---

2. Jenkins, J. E., & Chalfin, G. T., Unpublished Study, Space-General Corp., 1966.



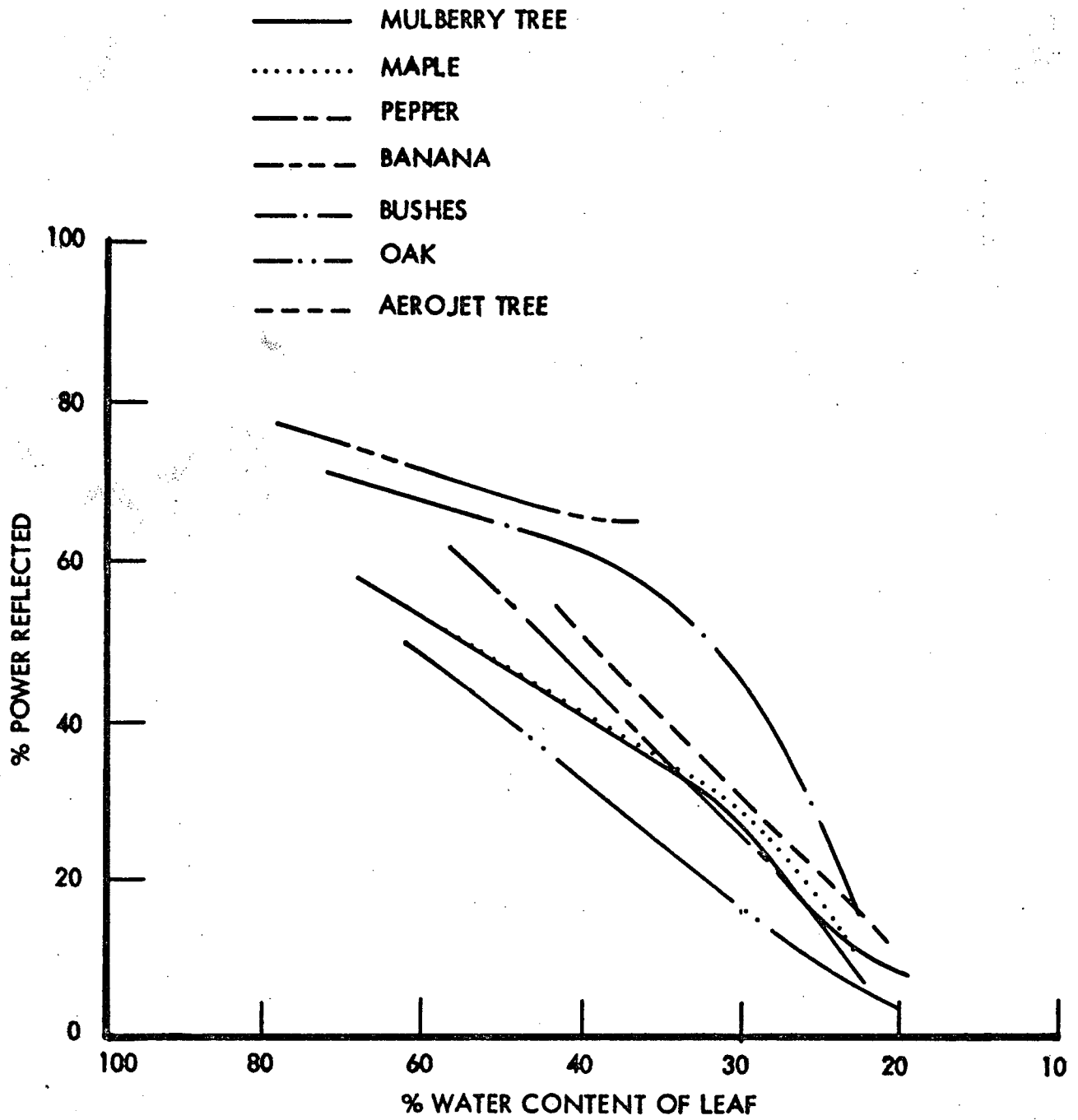


Figure 6. Power Reflected vs. Water Content of Leaf.

arises from the spacial distribution of leaves (individual reflectors) relative to the sensor. Vegetal surfaces commonly have abundant radii of curvature which are not small in comparison to microwave sensor wavelengths so that emitted and reflected microwave energy tends to be scattered. The resulting microwave radiometric signatures tend to be quite warm (emissivities approach unity) and unpolarized, with little dependence on antenna viewing angle. The closer the radii of curvature of the vegetal cover approaches observational wavelength, the more intense the scattering. These surfaces are classified as diffuse or rough surfaces.

Thus, a very dense crop such as alfalfa (leaf dimensions on the order of 0.5 cm to 1.5 cm) will exhibit no appreciable polarization difference ( $T_v - T_h \rightarrow 0$ ) for observational wavelengths of 0.8 cm and 2.2 cm. Figure 7 presents 0.8-cm and 2.2-cm antenna temperatures as a function of antenna viewing angle for alfalfa, beans, cotton and sugar beets. Antenna temperatures are shown on an expanded scale so that polarization differences can be examined. Note that the alfalfa exhibits substantially no polarization and that other crops exhibit very little polarization.

Differences in absolute values of the antenna brightness temperatures of the various crops reflect the fact that some crops, such as the beans, were measured during midday when the foliage temperature was high. Other crops, such as alfalfa, were measured at night when foliage temperatures were cooler. The physical temperature of vegetation varies in close correspondence with the air temperature, and diurnal variations of foliage brightness temperatures are on the order of the changes in air temperature. Exposed soils typically attain thermometric temperatures in excess of the air temperature in the day time due to solar radiation. Therefore, exposed soils commonly exhibit greater diurnal brightness temperature variations than vegetation.

### 2.2.3 Effect of Vegetation on Soil Moisture Determination

One of the purposes of the crop investigations was to determine the effect of vegetal cover on soil moisture determination by means of microwave radiometry. The foregoing discussion reviews the importance of

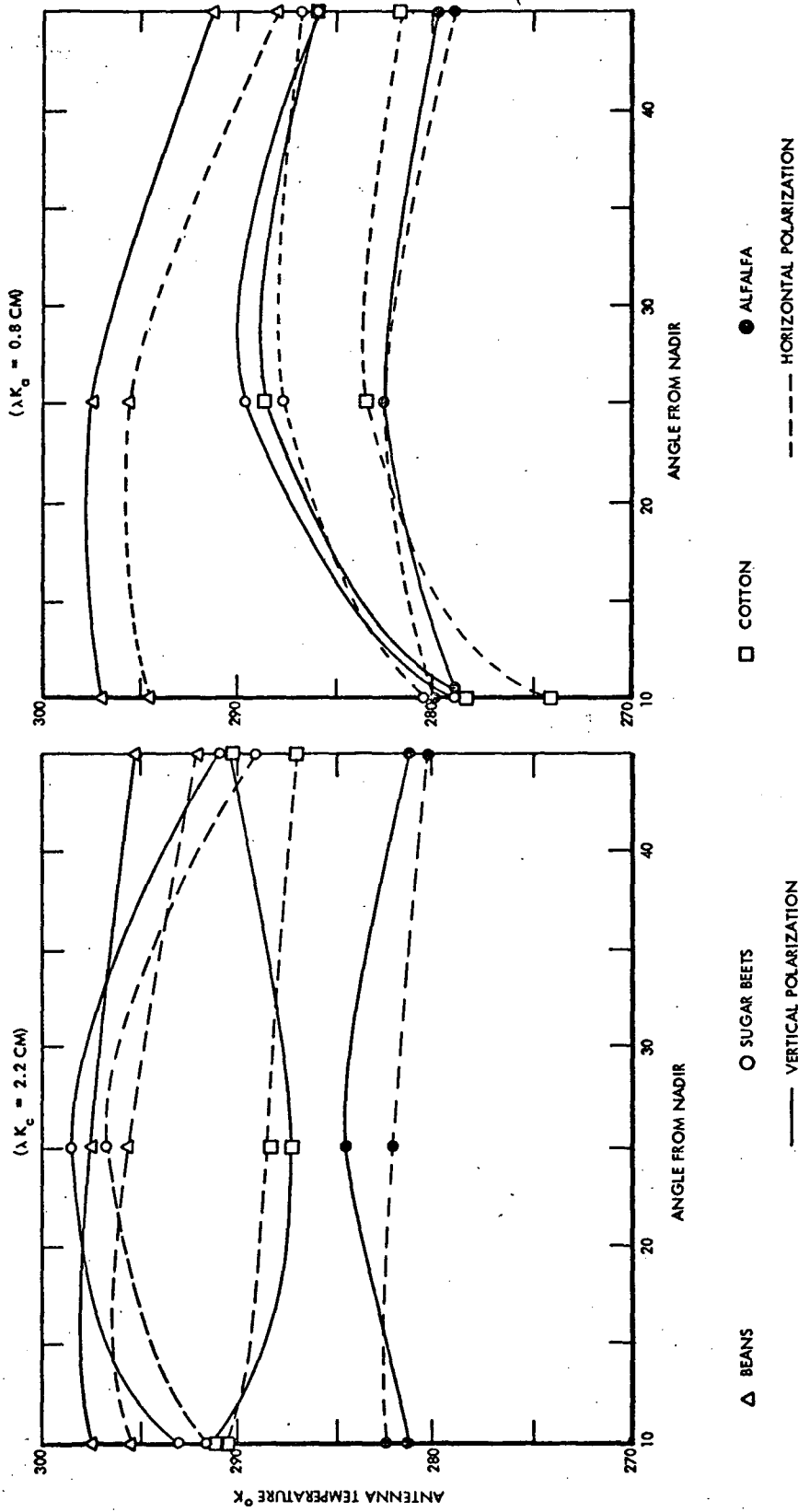


Figure 7. Crop Comparisons

scattering by vegetal surfaces. Scattering tends to obscure microwave emission characteristics of the underlying soil surface in much the same manner as visible light is scattered by fog. Other related factors which affect microwave determination of soil moisture include the percentage of ground obscured by vegetation, the height of the foliage, and the water equivalent of the vegetal column.

Studies conducted on Site 18 illustrate how dense vegetal cover adversely affects soil moisture determination. This encompassed a partially-cut alfalfa field, a portion of which was under irrigation. The cut portion of the field had approximately 50-percent vegetal cover, consisting of mowed alfalfa and stubble. The uncut portion contained dense alfalfa standing one-foot high. Soil moisture was moderately high throughout the field, and part of the uncut crop was under irrigation with water standing on the ground surface beneath the alfalfa. The air temperature was 25°C.

A microwave traverse was taken along the edge of the field using an antenna viewing angle of 50°. The traverse began in the mowed portion of the field and progressed across the uncut crop, going from an unirrigated portion to a portion that was partially flooded. The cut alfalfa exhibited only small polarization differences at all wavelengths (0.8 cm, 2.2 cm, and 21 cm), and antenna temperatures were characteristically high (Figure 7). The transition from mowed to uncut alfalfa occurs on data frame 50 and is conspicuous on the 0.8-cm and 2.2-cm data where all polarization differences ( $T_v - T_h$ ) abruptly diminish. The polarization differences measured by 21-cm antenna also declined slightly. Data frames 62 through 79 correspond to flooded alfalfa, and data frames 79 through 84 correspond to a portion of the field where there were barren spots with standing water. The microwave data taken at all three wavelengths exhibit no appreciable change in response to the flooded portions of alfalfa. Near the end of the traverse (frames 79 through 84), the instruments all respond to the unobscured standing water.

Site 18 represents an extreme situation in which the soil was entirely obscured by vegetation. The alfalfa data was cited to illustrate the importance of vegetal cover. In a majority of the agricultural fields investigated, the vegetal cover was less dense, and the radiometric signatures do bear a consistent relationship with soil moisture.

### 2.3 Geologic Investigations

Two microwave traverses across the San Andreas Fault at different localities and a traverse across a series of steeply dipping Tertiary lacustrine deposits constituted the microwave measurements of geologic structures.

#### 2.3.1 San Andreas Fault Traverses

The microwave response of the structurally complex area associated with the San Andreas Fault was measured on 6 June 1968. These measurements are designated as Sites 14 and 15. A detailed discussion of the geology and radiometric temperatures measured along the traverse are presented in Appendix B.

Greater variation in radiometric temperature associated with areas of increased moisture are noted for the longer wavelength (21 cm) radiometer. The shorter wavelength sensors also have decreasing temperatures with increasing moisture but are more readily affected by surface texture. Roughness and textural difference along the traverse line tend to mask radiometric temperatures directly associated with soil moisture.

An interesting anomaly in the 21-cm brightness temperatures occurs between stations 16 and 18 (see Figure B-20, Appendix B). The antenna brightness temperature increases with increased moisture content. This increase in temperature is associated with the increased salinity of the rising ground water. The surface is characterized by a brittle crust bonded by salt crystals. This relationship between saline concentration and increased brightness temperature for the 21-cm radiometer was first noted during microwave measurements on Harper Lake, California

in June, 1968 under a program sponsored by the Office of Naval Research. Geyer (1968) investigated the microwave emission characteristics of sea water as a function of salinity.<sup>3</sup> The results of these investigations indicate that low frequency radiometers are sensitive to changes in salinity, whereas higher frequency (shorter wavelength) systems are not affected by salinity variations from 30,000 to 35,000 ppm.

### 2.3.2 Inclined Sediments

A microwave traverse across steeply dipping mudstones and sandstones east of the Salton Sea was performed to evaluate the utility of microwave radiometry for mapping geologic structures. The results were inconclusive but indicate that the 21-cm radiometer may be more suitable for geologic studies because of its greater depth of penetration and immunity to surface roughness effects. A more detailed discussion of the radiometric response of geologic structures is presented in Appendix B under the Site 16 discussion.

---

<sup>3</sup> Geyer, R. A., Oceanography of the Gulf of Mexico, Progress Report, Texas A & M University, Project 286, 1968.

### Section 3

#### AIRBORNE MICROWAVE MEASUREMENTS

During the week of 20 May 1968 a series of airborne multi-frequency microwave measurements were taken in the Salton Sea area, using the NASA CV-240 aircraft with MR62 and MR64 microwave radiometers. These radiometers operate at wavelengths of 0.88 cm, 1.35 cm, 1.9 cm and 3.2 cm (frequencies of 34 GHz, 22.2 GHz, 15.8 GHz and 9.3 GHz, respectively). The 3.2-cm radiometer was inoperative during the mission. Data were acquired along several flight lines, as outlined in a document titled "USGS/NASA Southern California Remote Sensing Program," published for the U. S. Geological Survey during May 1968.

Microwave data acquired along Flight Lines 2<sup>1</sup>, 5a and 5b have been examined in the course of this study. These measurements were taken at an aircraft altitude of 1000 ft using a one-second integration time. Overflights of Flight Line 2<sup>1</sup>, along the west side of Jackson Street (Indio), were intended to test the feasibility of using airborne microwave radiometry for remotely determining the amount of moisture in the upper several inches of soil. During this overflight upwards of 50 people acquired ground truth information, and a number of well-instrumented ground stations were occupied along the flight line. Regretably, the microwave data acquired during the overflight were not recorded, apparently due to a malfunction in the data logging system.

During the week of 3 June 1968 additional overflights of the Salton Sea area were conducted using the NASA Convair 990. The primary purpose of these overflights was to acquire microwave imagery by means of the NASA/Goddard 1.55-cm (19.35 GHz) microwave imager. Imagery was acquired for both the Coachella and Imperial Valley farmland areas, the San Andreas Fault on the eastern side of the Salton Sea, the Salton Sea proper, and also of the Los Angeles area. Imagery was acquired at altitudes ranging from 40,000 ft down to 10,000 ft.

### 3.1 Airborne Multifrequency Measurements

The NASA CV-240A aircraft with three microwave radiometers was used to examine the small towns and agricultural areas in the Coachella and Imperial Valleys near the Salton Sea. Measurements were conducted to determine the microwave radiometric characteristics of rural agricultural areas. Interpretation of the microwave radiometric data was confined to that of USGS Flight Lines 2<sup>1</sup>, 5a and 5b. Figure 8 is a map showing the location of these flight lines.

#### 3.1.1 USGS Flight Line 2<sup>1</sup>

Flight Line 2<sup>1</sup> is parallel to, and one mile west of Jackson Street, near Indio, California. The line encompasses a variety of crops and fields. The overflight was configured as a soil moisture experiment. Consequently, antennas were oriented with vertical polarization and a viewing angle of 10° above nadir. This configuration was used to minimize radiometric temperature variations associated with surface roughness. Figure 9 shows antenna temperatures measured along the flight line plotted as a function of time. All three radiometers responded similarly. Desert terrain, dry fields and dense crops were radiometrically warm, and the recently irrigated moist fields were radiometrically cooler. The 1.4-cm (22.2 GHz) sensor is 10°K warmer than the other channels because of the increased atmospheric water vapor absorption at this wavelength. Anomalous portions of Figure 9 are annotated.

The rather lengthy one-second integration time of the radiometers tends to smooth the data so that boundaries between moist and dry fields are indistinct. The range of measured brightness temperatures for any given sensor was only 23°K.

Ground truth information was not available for the flight line, and the foregoing interpretation is based on correlation of the microwave data with aerial photography acquired during the overflight.



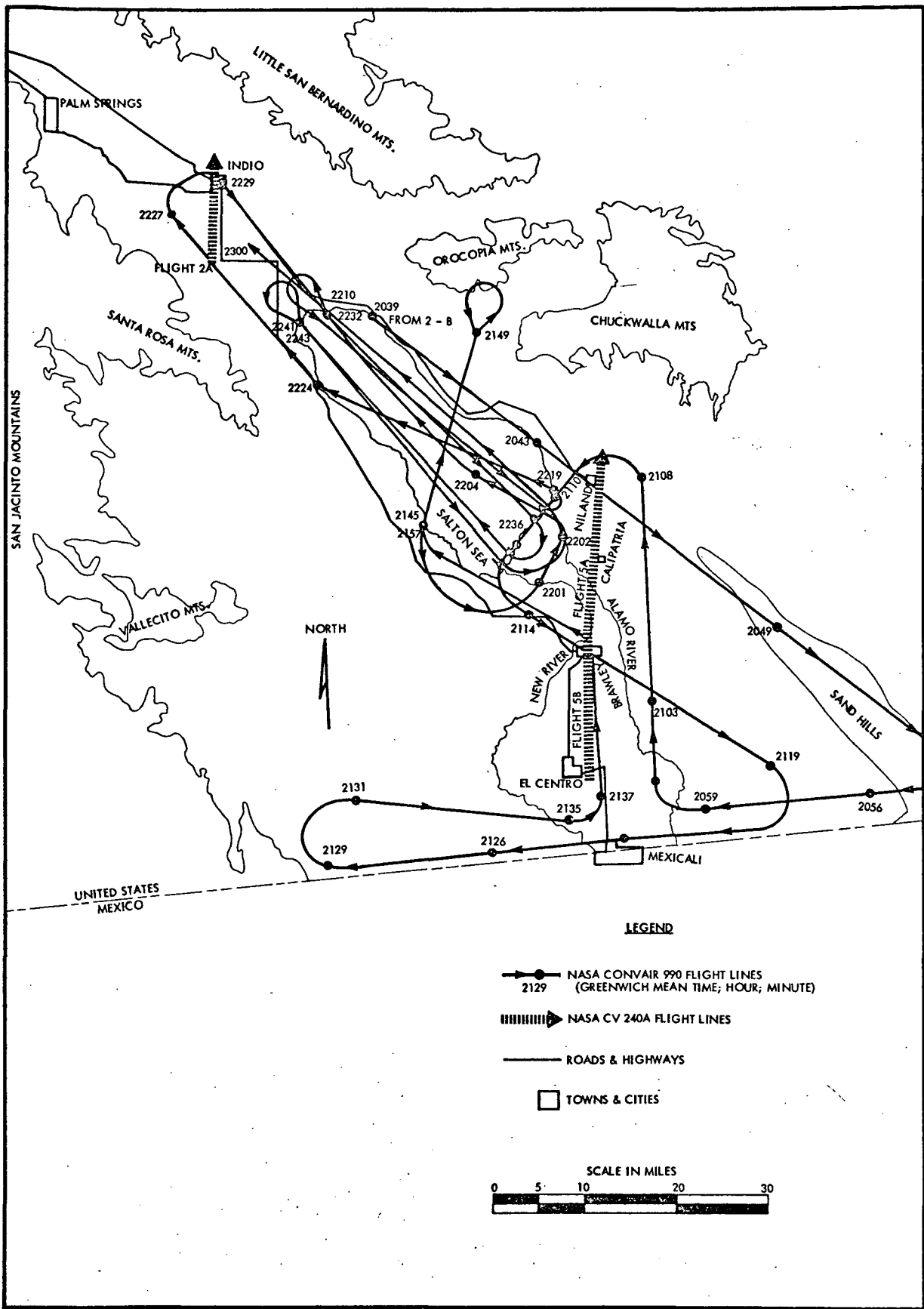


Figure 8. Salton Sea and Vicinity Showing Location of NASA Convair 990 Aircraft Flight Line (7 June 1968) and Flight Lines 2<sup>1</sup>, 5a, and 5b of NASA Convair 240A Aircraft (21 May 1968)

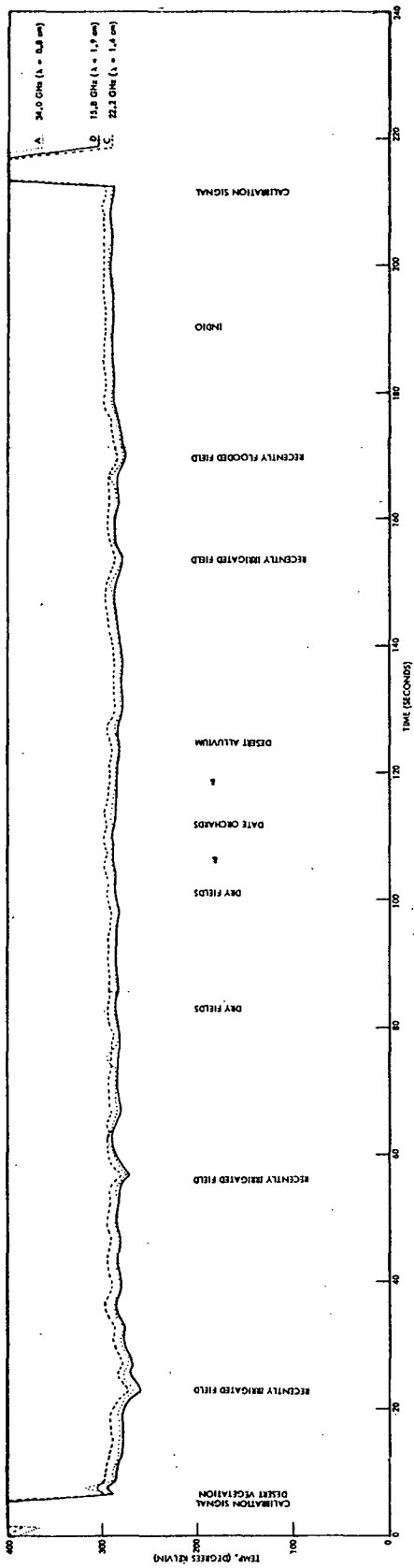


Figure 9. Microwave Radiometric Temperatures Along USGS Flight Line 2<sup>1</sup>

### 3.1.2 USGS Flight Lines 5a and 5b

USGS Flight Lines 5a and 5b encompass agricultural and rural areas of the Imperial Valley south and east of the Salton Sea. Overflights were conducted on 21 May 1968. Line 5a extends from Brawley to Niland and was flown in a north-northeasterly direction. The line traverses farmland under various stages of irrigation, barren fields, and undeveloped desert terrain. The predominant crops were alfalfa and cotton. Line 5b was flown in a north-south direction between Brawley and El Centro. The flight line is similar to line 5a, except that the dominant crop along 5b was sugar beets. Figure 10 shows 0.8 cm, 1.4 cm and 2.0 cm antenna brightness temperatures measured along the flight lines. These data were correlated with vertical aerial photography acquired during the overflights, and Figure 10 has been annotated to reflect the reasons for the various microwave anomalies.

Antenna brightness temperatures along Line 5a exhibit moderate fluctuations, on the order of  $10^{\circ}\text{K}$ . These generally correspond with land utilization. The dry barren fields and dense crops are radiometrically warm, and the more moist fields exhibit lower antenna temperatures. The 0.8 cm sensor exhibits anomalous antenna temperatures at points corresponding to 40 seconds and 160 seconds. These data points are ascribed to instrument malfunctions. Antenna temperatures observed along Line 5b were similar to those of Line 5a. An exact correlation between the microwave data and the aerial photography could not be accomplished. The radiometers were forward-looking with a viewing angle of  $10^{\circ}$  above nadir in contrast with the vertical photography. There was no common timing for the two systems, and the data-taking intervals were significantly different for the two sensor systems.

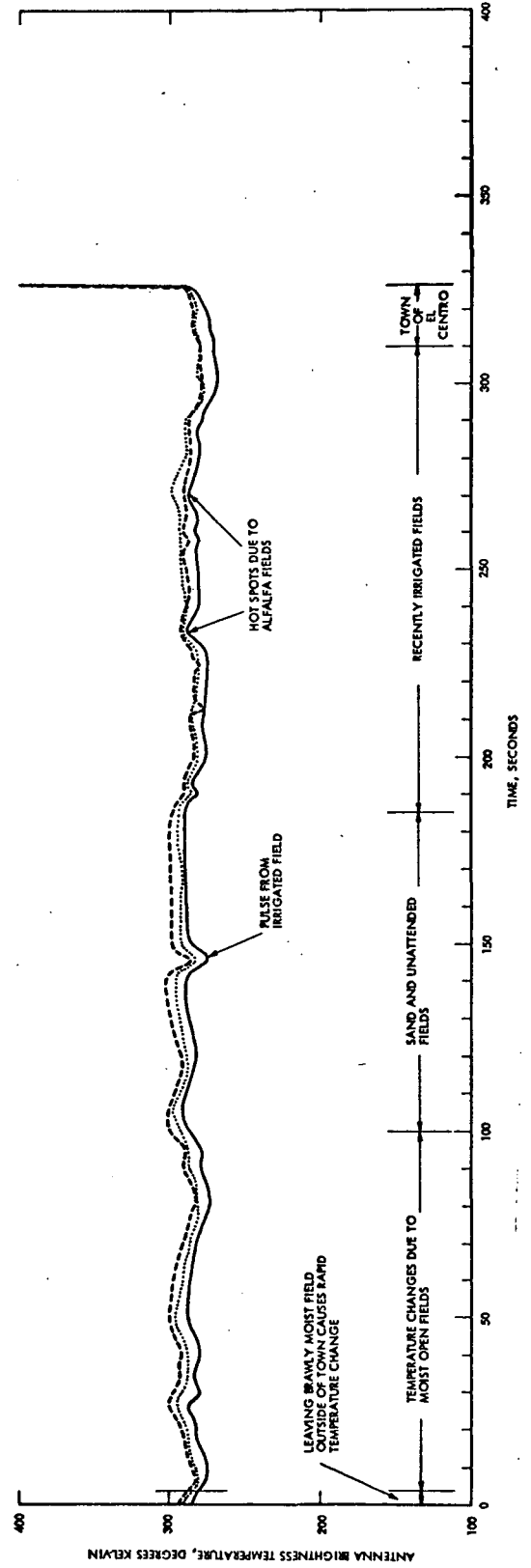
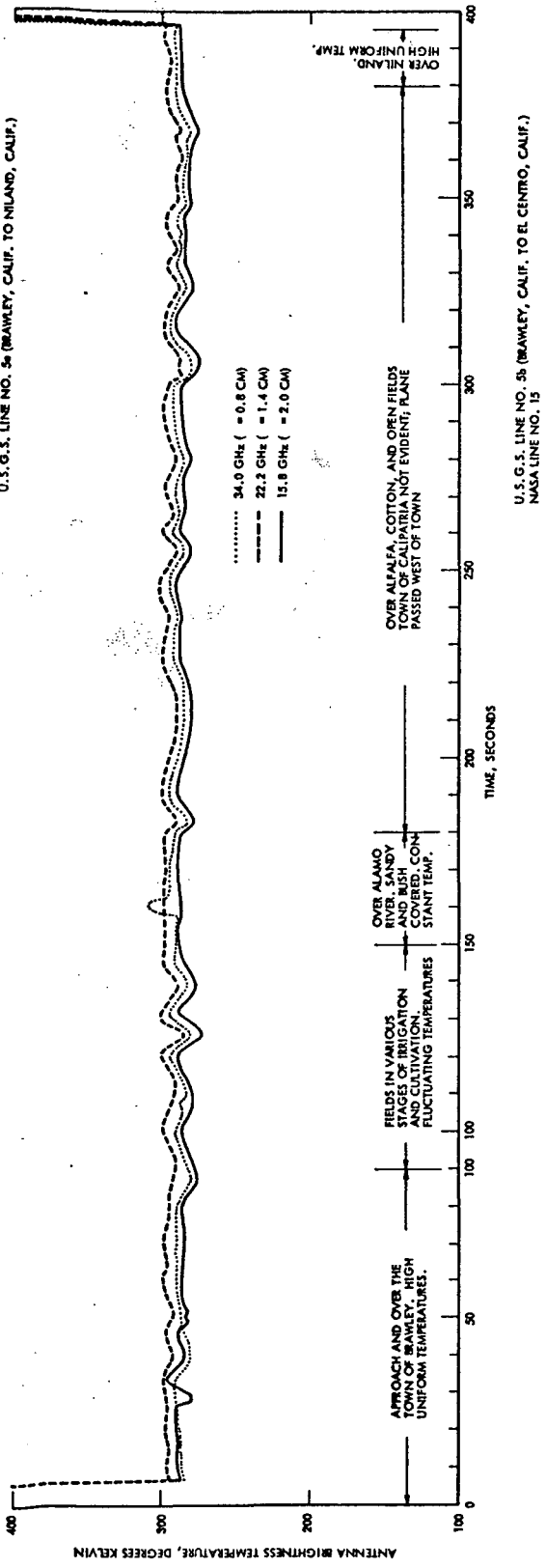


Figure 10. Antenna Brightness Temperatures Measured Along USGS Flight Lines 5a and 5b

### 3.2 1.55-cm (19.35 GHz) Microwave Imagery

Imagery of the Salton Basin was acquired with NASA-Goddard's 1.55-cm (19.35 GHz) Microwave Imager installed on the NASA Convair 990. Flights were conducted on the 5th and 7th of June 1968 over a variety of terrains including the Salton Sea, agricultural areas, desert terrain, and urban areas. The 7 June 1968 flight lines are shown on Figure 8. These overflights, designated Flight 2, provided quality data for evaluating microwave imagery as a tool for land use studies. Imagery of the Eastern Imperial Valley, desert terrain, the Mexico-Calexico Area, and the Salton Sea will be discussed in the following sections.

#### 3.2.1 Instrumentation and Data Processing

The sensor used to obtain the image is a completely passive device that senses thermal emission in the band 19.25, 19.45 GHz (15.3, 15.6 mm). The sensor is a Dicke radiometer using an all solid-state superheterodyne receiver. Calibration is provided by means of a liquid nitrogen load. The antenna is a phased array using edge-slotted waveguides. The antenna is electronically scanned in the cross-track direction through an angle of  $102^\circ$ , centered on nadir. The scan consists of 39 discrete steps, with a beamwidth of  $2.8^\circ$  at the center of the scan. The forward movement of the aircraft provides the scanning in the orthogonal (along the ground track) direction.

The antenna is sensitive only to radiation whose electric vector is parallel to the direction of flight. Thus, when the beam is scanned away from nadir, the antenna receives only horizontally-polarized emission. (At nadir, all emission is horizontally polarized since electromagnetic waves are always transverse. In the nadir position, the antenna receives that portion of the horizontally-polarized emission whose electric vector is parallel to the direction of flight.)

A period of 1 or 2 sec was required for each scan line, giving an integration time per beam position of about 25 and 50 msec, respectively. With the 2-sec integration time, the rms system noise level was about 1 to  $2^\circ\text{K}$ .

The image is obtained from a digital tape. The tape is played back on a computer and a specified portion of the dynamic range of the data is selected. The data is then recorded on another digital tape, which is used to drive a CRT plotting system to produce an image. The geometrical distortions caused by the antenna scan were corrected at this point so that the CRT system would produce an image that was a true linear map of the ground (assuming straight and level flight). Because of the nature of the CRT system, the continuous data from the radiometer was broken up into a series of frames, each consisting of 128 scan lines.

The imagery derived from the CRT is photographed and presented in time sequences. Higher radiometric temperatures appear as lighter colors, with white being the warmest. There are 50 color steps not including white and black. Each temperature is represented by a color which may be varied by the use of different slope and offset combinations.

Numbers on the right side of each frame represent the time, day of the year, slope and offset for the particular frame. Below is a representation showing the position of each number and its designation.

	22	
	33	Greenwich mean time at center of frame
	12	22 hrs 33 min. 12 sec.
	1	Day and Year
	5 6	159th Day (7 June) 1968
	9 8	
	1 2	
	0 5	Slope and offset
	0 0	1.00 = slope, -250 = offset counts

Due to an error in the computer program, even number minutes were printed out as odd numbers. The time between center points of each frame is 72 seconds. It is only necessary to be aware of this time problem when locating imagery on the map of flight lines.

The slope and offset are used to determine the radiometric temperature represented by each color. Since slope and offset are varied to optimize the imagery it is necessary to calculate the temperature of white and black and divide the difference by 50, which gives the radiometric temperature per color step.

By substituting in the following equations, the slope and offset used for a particular sequence will give the radiometric temperature of white when  $x_n = 0$  and for black when  $x_n = 104$

$$N = \frac{x_n}{m} + b$$

where:

$N$  = counts

$x_n$  = counts/color; 0 = white, 104 = black

$b$  = offset

$m$  = slope

Using the counts ( $N$ ) calculated from the above equation and substituting it into the radiometric temperature equation, the radiometric temperature at the antenna can be calculated:

$$T_R = 338 - \frac{338 - 116}{N_c} N$$

where;

$T_R$  = radiometric temperature in  $^{\circ}K$   
(uncorrected for instrument loss)

$N_c$  = calibrate counts (assumed = 485)

The corrected radiometric temperature measured at the antenna is calculated by:

$$T_A = T_R L - (L - 1) t_A$$

where:  $T_A$  = radiometric temperature of antenna  
 $L$  = loss factor = 2db = 1.59  
 $t_A$  = ambient temperature of antenna  
(assume = 273°K)

Therefore, a slope and offset of 1.00 and -250, respectively, yield white  $\geq 195^\circ\text{K}$ , black  $\leq 119^\circ\text{K}$ . Dividing the difference ( $76^\circ\text{K}$ ) by 50 (50 colors) a value of  $1.5^\circ\text{K}$  per color step is obtained.

Temperatures derived from the previous equations are not the true radiometric temperature of the target material, but are the temperatures measured at the antenna without correction for atmospheric attenuation, which is altitude dependent. Therefore, the radiometric temperatures can only be used in a qualitative sense in comparing variations of different terrains.

### 3.2.2 Agricultural and Desert Terrain

Imagery obtained from 21:15:00 to 21:19:36 corresponds to an agricultural area east of Brawley and to desert terrain east of the East Highline Canal and is presented on the following page. The aircraft altitude was 10,000 feet and the speed was 269 knots. The agricultural area was described by an observer in the aircraft as being broken farm land with 30-percent vegetation and 20-percent dry vegetation.

Of interest in this sequence of imagery is the marked difference in radiometric temperatures measured over the farmland and those measured over desert terrain. In frames 21:17:24 and 21:17:48 a diagonal line with colder radiometric temperatures represents the East Highline Canal. The area in the upper portion of these frames is desert terrain. The desert area appears radiometrically colder than agricultural areas below the canal. From ground truth measurements it was found that desert terrain had a higher thermometric temperature than areas under cultivation. However, crops appear radiometrically warmer due to the high degree of scattering associated with vegetation. Some areas within the agricultural area have radiometric temperatures that are on the order of

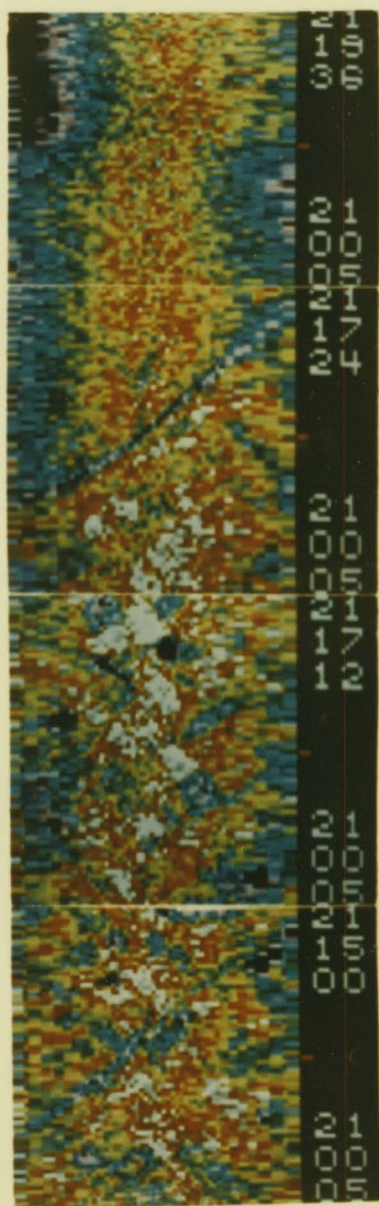




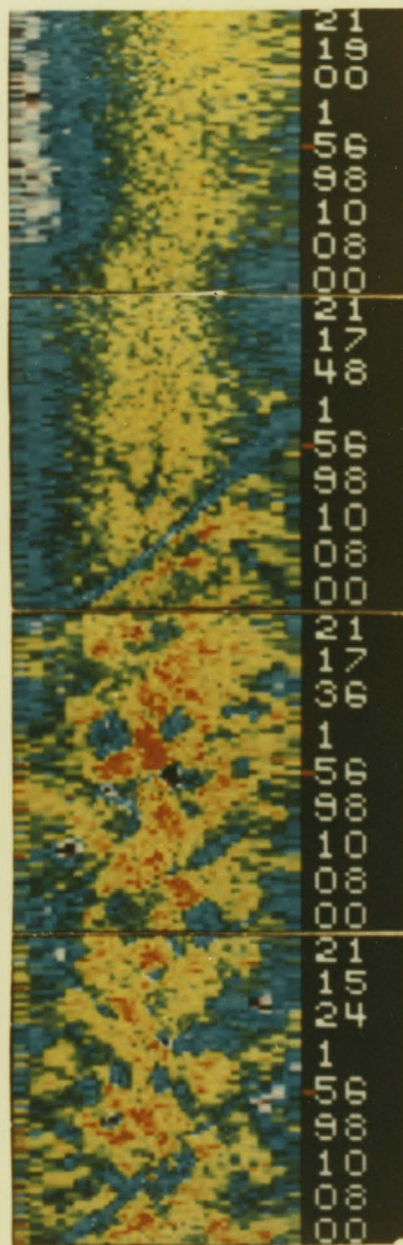
WHITE = HOTTEST



BLACK = COLDEST



WHITE  $\geq 300^{\circ}\text{K}$   
 BLACK  $\leq 262^{\circ}\text{K}$   
 $^{\circ}\text{K}/\text{COLOR} = 0.8$



WHITE  $\geq 317^{\circ}\text{K}$   
 BLACK  $\leq 243^{\circ}\text{K}$   
 $^{\circ}\text{K}/\text{COLOR} = 1.5$

Reproduced from  
 best available copy.

RADIOMETRICALLY COOLER DIAGONAL LINE IN FRAME 21:17:24 CORRESPONDS TO THE EAST HIGHLINE CANAL WHICH SEPARATES CULTIVATED AREA (BELOW) AND DESERT AREA (ABOVE)

AGRICULTURAL AND DESERT TERRAIN EASTERN IMPERIAL VALLEY

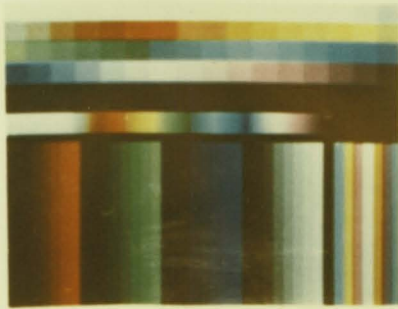
those measured over desert and very likely represent barren fields.

In frame 21:17:12, a few areas appear black in both sequences. These areas are fields under irrigation or recently irrigated fields with high moisture content near the surface. The radiometric temperature represented by black in the sequence with a slope of 1.00 and an offset of -080 is  $\leq 243^{\circ}\text{K}$ . Such low radiometric temperatures are indicative of water at or near the surface.

### 3.2.3 Mexicali-Calexico Area

Imagery acquired at time 21:23:24 (see following page) shows the All American Canal and flooded fields east of Calexico. It was obtained flying east to west along the international border at an altitude of 10,900 feet and an air speed of 265 knots. The next frame (21:23:36) is interesting in that the town of Mexicali and the commercial district of Calexico appear significantly colder than the surrounding cultivated area and residential areas of Calexico. This relationship is displayed using a slope of 2.00 and an offset of -130. With this combination, white is equal to or greater than  $281^{\circ}\text{K}$ . The agricultural areas and residential area of Calexico have radiometric antenna temperatures greater than or equal to  $281^{\circ}\text{K}$ , as opposed to radiometric temperatures in the realm of  $263^{\circ}\text{K}$  for the town of Mexicali. A range in temperature from less than  $245^{\circ}\text{K}$  to greater than  $281^{\circ}\text{K}$  is apparent within the town of Mexicali. The course of the All American Canal is evident as in the bifurcation of the East Highline Canal in frame 21:23:36. Radiometrically colder areas north and west of Calexico are assumed to be recently irrigated fields.

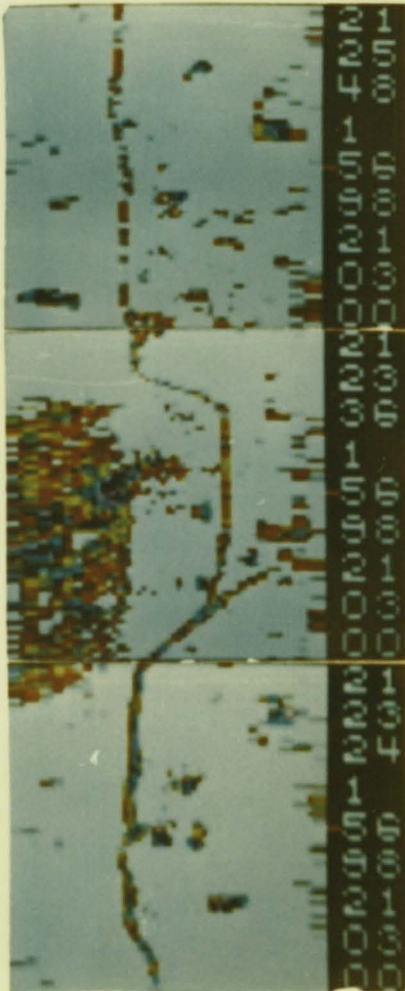
The radiometric temperature anomaly between Mexicali and residential Calexico is believed to be the result of vegetation such as trees, shrubs and lawns. In Mexicali there is a lack of such vegetation except in parks, which may account for warm (white) areas within the city. This temperature anomaly is evident on false-color infrared photography of the International Border in the Calexico-Mexicali area where infrared photography shows an increase in the amount of vegetation in residential



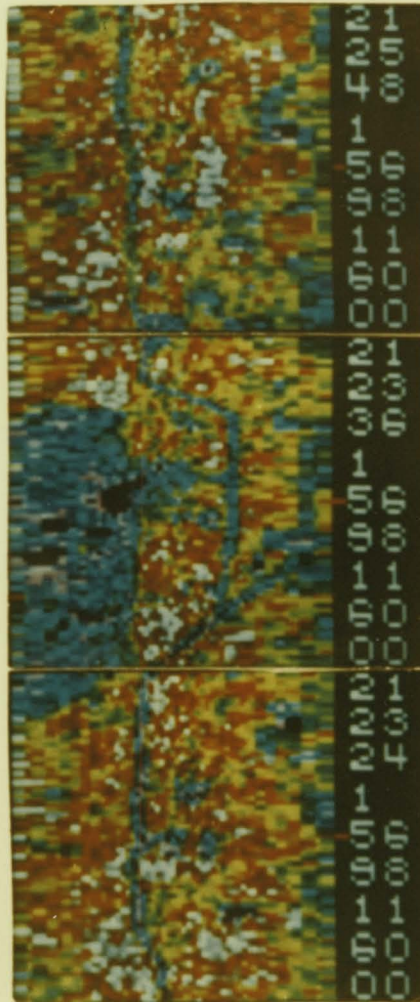
WHITE = HOTTEST



BLACK = COLDEST

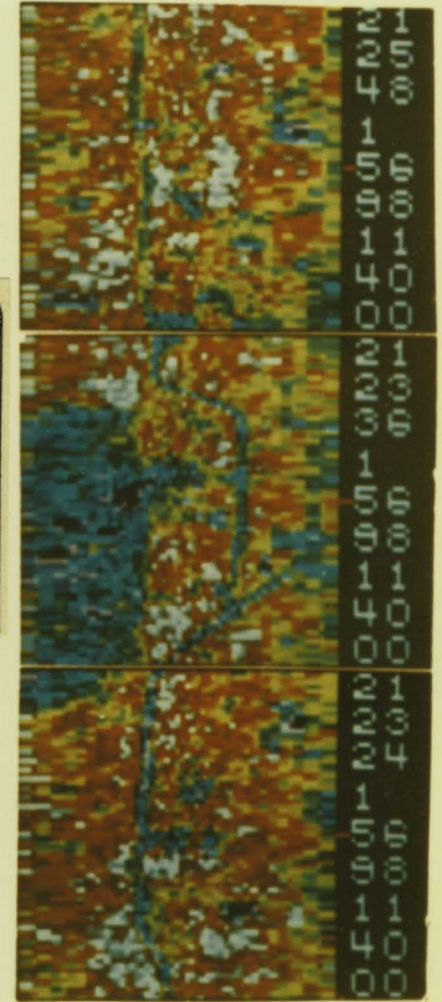


WHITE  $\geq 281^{\circ}\text{K}$   
 BLACK  $\leq 245^{\circ}\text{K}$   
 $^{\circ}\text{K}/\text{COLOR} = 0.7$



WHITE  $\geq 304^{\circ}\text{K}$   
 BLACK  $\leq 256^{\circ}\text{K}$   
 $^{\circ}\text{K}/\text{COLOR} = 1.0$

Reproduced from  
 best available copy.



WHITE  $\geq 304^{\circ}\text{K}$   
 BLACK  $\leq 249^{\circ}\text{K}$   
 $^{\circ}\text{K}/\text{COLOR} = 1.1$

RADIOMETRICALLY COOLER AREA IN FRAME 21:23:36 CORRESPONDS TO THE CITY OF MEXICALLI, MEXICO. CALEXICO, CALIFORNIA LIES BETWEEN MEXICALLI AND THE CURVE IN THE ALL AMERICAN CANAL. CALEXICO APPEARS RADIOMETRICALLY WARMER THAN ITS SISTER CITY IN MEXICO.

ALL AMERICAN CANAL ALONG THE UNITED STATES-MEXICO BORDER

areas of Calexico. The commercial district is devoid of vegetation and appears colder. Also, the more specular surfaces such as streets, parking lots and roof tops would tend to be cooler than surrounding agricultural and residential areas.

#### 3.2.4 Salton Sea

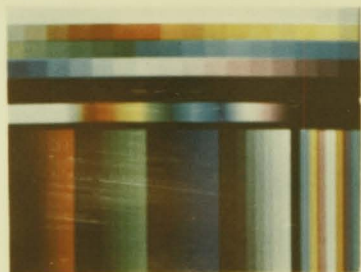
Overflights of the afternoon of 7 June 1968 (day 159) covered portions of the Salton Sea. Imagery during that part of the overflight from 22:33:12 to 22:35:48 (see following page) is presented to show variations in microwave temperature as a function of surface roughness (sea state). Flight direction for this time period was from north to south; therefore, the south end of the Sea is at the top of the sequence.

A marked difference in radiometric temperature of the Salton Sea surface occurs in frames 22:33:12 and 22:35:36. The temperature difference as measured at the antenna is approximately  $15^{\circ}\text{K}$  for the lower portion of Frame 22:33:12. Each color step in this frame represents a change in radiometric temperature of  $4.7^{\circ}\text{K}$ . For the sequence of photographs (right-hand column) with a slope 1.00 and an offset of 250, each color step represents a change in temperature of  $1.5^{\circ}\text{K}$ . The change in color from blue to green in the lower portion of frame 22:35:36 is predominant and represents an increase in sea state, resulting from high winds blowing across the southern portion of the sea. Average wind velocity measured at the USGS Headquarters of the Salton Sea test base during the overflights was 20 miles per hour between 13:00 and 14:00 hours and 23 miles per hour between 14:00 and 15:00 hours. The wind direction was west/southwest.

The large difference in radiometric temperature of approximately  $20^{\circ}\text{K}$  in frame 22:35:36 is due to increased sea state. Theoretically, an increase in horizontally polarized radiation between the two areas should be approximately  $15^{\circ}\text{K}$  for a 19.4 GHz radiometer at an incidence angle of  $50^{\circ}$ . However recent studies of the sea surface have shown that

---

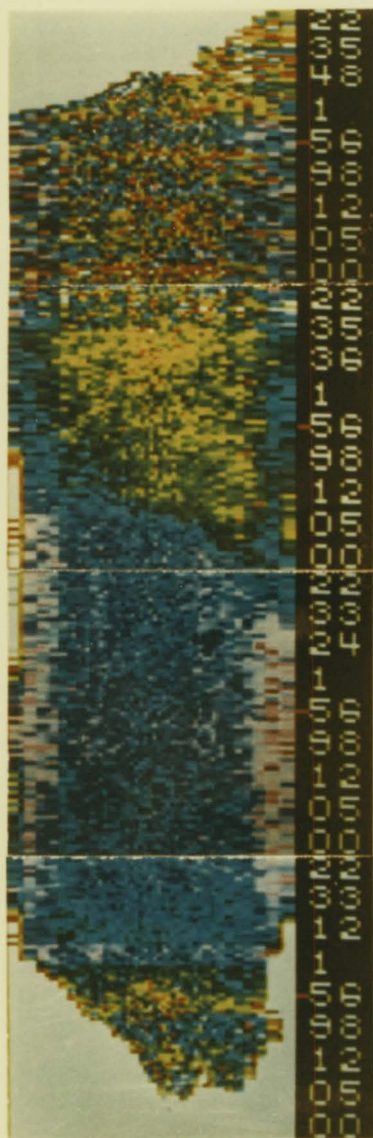
4. A. Stogryn, "Apparent Temperatures of the Sea at Microwave Frequencies," IEEE Transactions on Antennas and Propagation, Vol. AP-15, No. 2, March 1967.



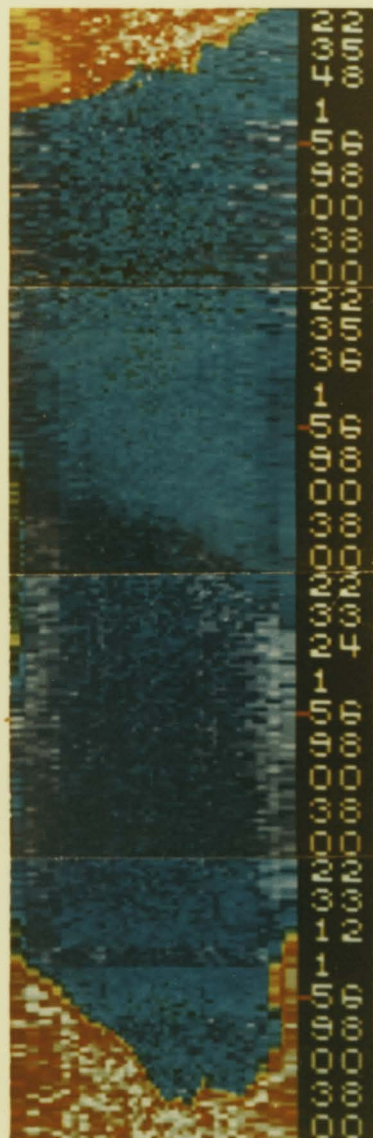
WHITE = HOTTEST



BLACK = COLDEST



WHITE  $\geq 317^{\circ}\text{K}$   
 BLACK  $\leq 67^{\circ}\text{K}$   
 $^{\circ}\text{K}/\text{COLOR} = 4.7$



WHITE  $\geq 195^{\circ}\text{K}$   
 BLACK  $\leq 119^{\circ}\text{K}$   
 $^{\circ}\text{K}/\text{COLOR} = 1.5$

FLIGHT DIRECTION WAS FROM NORTH TO SOUTH, THEREFORE THE SOUTHERN END OF THE SEA IS AT THE TOP OF THE SEQUENCE. FRAME 22:35:36 SHOWS A MARKED DIFFERENCE IN RADIOMETRIC TEMPERATURE OF THE SEA SURFACE WHICH CORRESPONDS TO HIGHER SEA STATE IN THE SOUTHERN HALF OF THE SEA.

SEA STATE CONDITIONS OF THE SALTON SEA (7 JUNE 1968)

the presence of foam and spray tend to increase the radiometric temperature of the sea surface. During the time of overflights the southern end of the Salton Sea was partially covered with white caps and 2-3 foot waves were breaking on the eastern shore.

Radiometrically warmer temperatures are also apparent in the northern portion of the Sea in frame 22:33:12. No records are available for wind conditions in this area. However, radiometrically warmer temperatures tend to indicate a higher sea state existed over the northern portion of the Sea during overflights than for the central portion where radiometric temperatures are colder. Warmer radiometric temperatures in the northern portion may also be due, in part, to the sidelobes of the antenna recording the radiometrically warmer ground surface in this frame.

For a more thorough discussion of the Salton Sea imagery see "Sea State Observations from Aircraft by Means of Measuring Emitted Microwave Radiation," W. Nordberg, J. Conoway and P. Thaddeus.

## Section 4

### CONCLUSIONS

A primary purpose of the microwave study of the Southern California Test Site was to establish the feasibility of using microwave radiometry for soil moisture determination. Toward this end, ground-based and airborne microwave measurements were collected over a variety of agricultural areas covering a range of moisture conditions.

The ground-based measurements, discussed in Section 2 of this report, show good correlation between soil moisture content and measured brightness temperatures. Measured brightness temperatures decrease with increasing amounts of soil moisture. The relationship is consistent for barren fields and fields with modest vegetal cover, and can be used to obtain a qualitative estimate of soil moisture content. In areas of dense vegetal cover, the unique signatures associated with soil moisture variations are obscured. This is due to intensive scattering of the microwave energy by the foliage. The moisture content-microwave signature relationship can be developed to the point of being at least semi-quantitative by combining an infrared sensor with the radiometer system. This would provide the needed physical temperature data so that microwave data could be evaluated strictly on the basis of emissivity variations.

A noteworthy exception to the soil moisture-microwave signature relationship occurs at longer wavelengths where the presence of significant amounts of dissolved salts in soil moisture overshadows the fundamental moisture relationship. This is evidenced in the 21-cm data gathered on Sites 14 and 15.

The airborne data were inconclusive in terms of soil moisture determination. The data acquired by the Convair 240 aircraft show a general correlation with moisture conditions, but the excessive integration time of the radiometer systems precluded good spacial resolution. Consequently, the microwave data is very difficult to relate with the

soil moisture information of a particular field. The imagery obtained by the Convair 990 aircraft also shows a general correlation with moisture conditions. However, the spatial resolution provided by the imagery was again insufficient for resolving individual fields, and quantitative comparisons could not be made.

Airborne and ground-based data acquired for the various crops show that vegetation exhibits characteristically high emissivity due to intensive scattering of microwave energy. Thus, the microwave brightness temperatures of vegetation tend to be very warm and unpolarized.

Imagery obtained from the radiometer aboard the Convair 990 aircraft indicates the usefulness of microwave radiometry as a tool for mapping terrain differences on the basis of microwave emission characteristics. Areas under cultivation are distinct from desert terrain. Indications of the soil moisture content of barren fields may be inferred by comparing radiometric temperatures. Cultural landmarks such as canals and cities are a prominent feature of the imagery.

The imagery also shows that surface conditions of large areas of open water such as lakes and seas can be determined. Microwave brightness temperatures increase with increasing sea state (surface roughness) as a function of the steeper slope of the waves. White caps (foam) and spray tend to make the radiometric temperature higher than temperatures calculated by analytical models.

Some difficulties were encountered in relating the small area ground measurements with the larger area airborne data. The airborne sensors, with their much larger field of view, can potentially provide statistically more meaningful data on the average characteristics (e.g., soil moisture) of areas viewed. The difficulty in relating ground measurements to the airborne data was partially overcome by acquiring statistical ground data along traverse lines. It was unfortunate that the resolution cells of the airborne sensors encompassed more than one field at a time. In future experiments, this can be avoided by using shorter integration intervals.



The single beam radiometers are useful for exploring the feasibility of applying microwave radiometry to land use studies and geographic investigations. However, imaging radiometer systems promise to be of much greater value for these studies. Imaging systems are more costly, and therefore, it is practical to conduct initial feasibility studies with the available single beam systems. These studies will provide a sound data base for defining appropriate sensor characteristics (e.g., wavelength, polarization, etc.) of imaging systems.

Microwave sensors are low resolution devices and as such, are useful for aircraft studies but would seem to have little value for detailed land use studies conducted at satellite altitudes. For satellite applications, these sensors are best suited to regional problems such as meteorological, hydrological, and oceanographic surveillance.

The research reported herein was funded at a very modest level. Consequently, the investigators were unable to devote enough time for a thorough analysis of all the airborne data. Some of these data do warrant further analysis.

## APPENDIX A

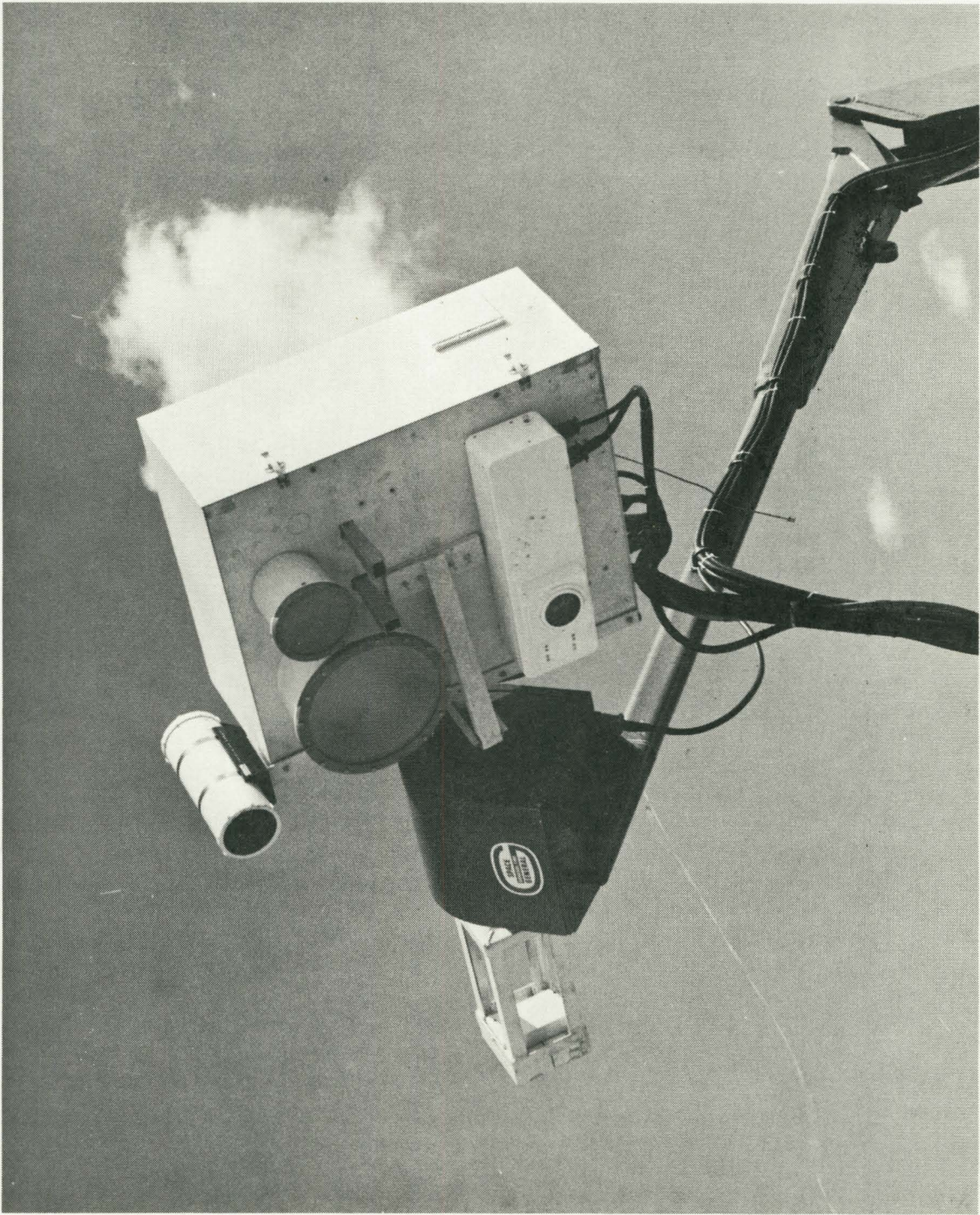
### MULTIFREQUENCY MICROWAVE LABORATORY AND GROUND TRUTH SYSTEM

The microwave radiometer system used for field measurements consists of the Aerojet-General multifrequency microwave field laboratory, and the Aerojet-General ellipsometer.

The microwave radiometer field unit consists of a four-frequency, dual-polarization, radiometric sensor equipped with an automatic digital data recording and control system. The instrumentation is housed in a 16-foot mobile laboratory and a 1-1/2 ton flat bed truck. The trailer houses the monitoring, recording and control equipment associated with the radiometric sensors as well as geological, geophysical and meteorological instruments. The truck serves as the mounting platform for the diesel power generator and the radiometer mounting boom. The boom is a 16-foot long, hydraulically-operated crane, controlled from a position near the cab of the truck. A remote control head, mounted on the end of the boom, allows the radiometer to be scanned in the elevation plane through an angle of  $180^{\circ}$ . The programming of this head is controlled by a digital data acquisition system in the trailer. The end points of terrain scans are adjusted to coincide with the local gravity vector, scanning from nadir to zenith. Scan steps have been set at  $5^{\circ}$ , but other values, including unequal steps, can be obtained as desired.

The microwave radiometers and accessory equipment are mounted on a common plate, attached to the movable boom head, as shown in Figure A-1. They contain the switch which selects the three input configurations, horizontal polarization, vertical polarization, and a calibration load. The basic specifications of the radiometer units are as follows:

<u>Parameters</u>	<u>Radiometers</u>			
Center Frequency	1.4 GHz	13.4 GHz	37 GHz	94 GHz
Bandwidth	80 MHz	300 MHz	300 MHz	300 MHz
Sensitivity	$0.3^{\circ}\text{K/sec}$	$0.5^{\circ}\text{K/sec}$	$0.5^{\circ}\text{K/sec}$	$2.0^{\circ}\text{K/sec}$



829/191

Figure A-1. Close-up View of Radiometer

<u>Parameters</u>		<u>Radiometers</u>		
Antenna Beamwidth	15°	5°	5°	6°
Antenna Types	Long periodic with 3 ft parabolic reflector	Lens-Horn	Lens-Horn	Two Tapered Horns
Calibration Capability	±1°K	±1°K	±1°K	±1°K
Integration period	0.4 to 10.0 seconds (all radiometers)			

The data acquisition system installed in the laboratory is a completely automatic digital system that records directly on computer-compatible magnetic tape. This system provides the basic timing for the entire measurement sequence and generates all the commands necessary to operate all of the radiometric and positioning equipment. The data acquisition system integrates the output of the radiometers, the integration time constants being selectable.

The data acquisition system also records the identification labeling and the non-radiometric data inputs, such as relative humidity, barometric pressure, and temperature. Extra channel space is available for recording analog data when special additional instrumentation is required.

The data recording sequence is continued through all of the steps of the mount position that are pre-set and records horizontal, vertical and calibration radiometric temperature at each step position. At the completion of the desired sequence, indicated by an "end of travel" switch closure, the mount is returned to the initial position, and the acquisition system either stops or continues on automatically, depending on the selected mode of operation. Other operational modes are available, including fixed angle measurements and continuous line surveys wherein the entire unit is driven along a prescribed route obtaining measurements for any desired viewing angle.

A digital-to-analog converter parallels the digital data recording system. The analog outputs are fed to separate chart recorders to allow real-time evaluation of the complete data system and to allow

on-site determination of the data quality and information values.

The accessory equipment included in the field laboratory includes a 35-mm robot camera, TV system, meteorological instrumentation, and associated geophysical and hydrological instruments. The 35-mm camera and the TV camera are boresighted with the radiometer antennas and remote controlled from the laboratory unit. In this manner, real-time photographs and visual information are continuously acquired for data comparison purposes. The meteorological instruments include the following: 8 movable thermistors for monitoring temperatures, a barometer, a relative humidity meter, and wind speed and direction indicator. All instrument outputs are recorded directly on digital tape. The geophysical and hydrological instruments include equipment for measuring moisture content, particle size, bearing strength, density, etc.

The digital tape produced by the data acquisition system is formatted for direct computer entry. The values obtained from the tape are processed by the computer using a data reduction program. This program produces a tabular printout of all the values obtained throughout the run, corrected and reduced to radiometric temperatures. The program, at the same time, produces an output tape. This output tape is re-submitted to the computer. The computer then produces a second output tape using a plotter program. This tape is formatted to run a CalComp incremental plotter. The plotter then is used to produce graphs of the radiometric temperatures versus the mount position. A flow chart for the complete data reduction process is shown in Figure A-2.

The reduction of radiometric data from the digitized output of the data acquisition system (DAS) to radiometric brightness temperatures in tabular form and graphs is a three-step process.

STEP 1 - COPYING - The purpose of this processing is to copy the digitized data from a DAS output tape onto a computer compatible tape. The data is copied exactly as it exists but all tape parity and check character errors are removed. This eliminates time-consuming tape error correction processing in Step 2.

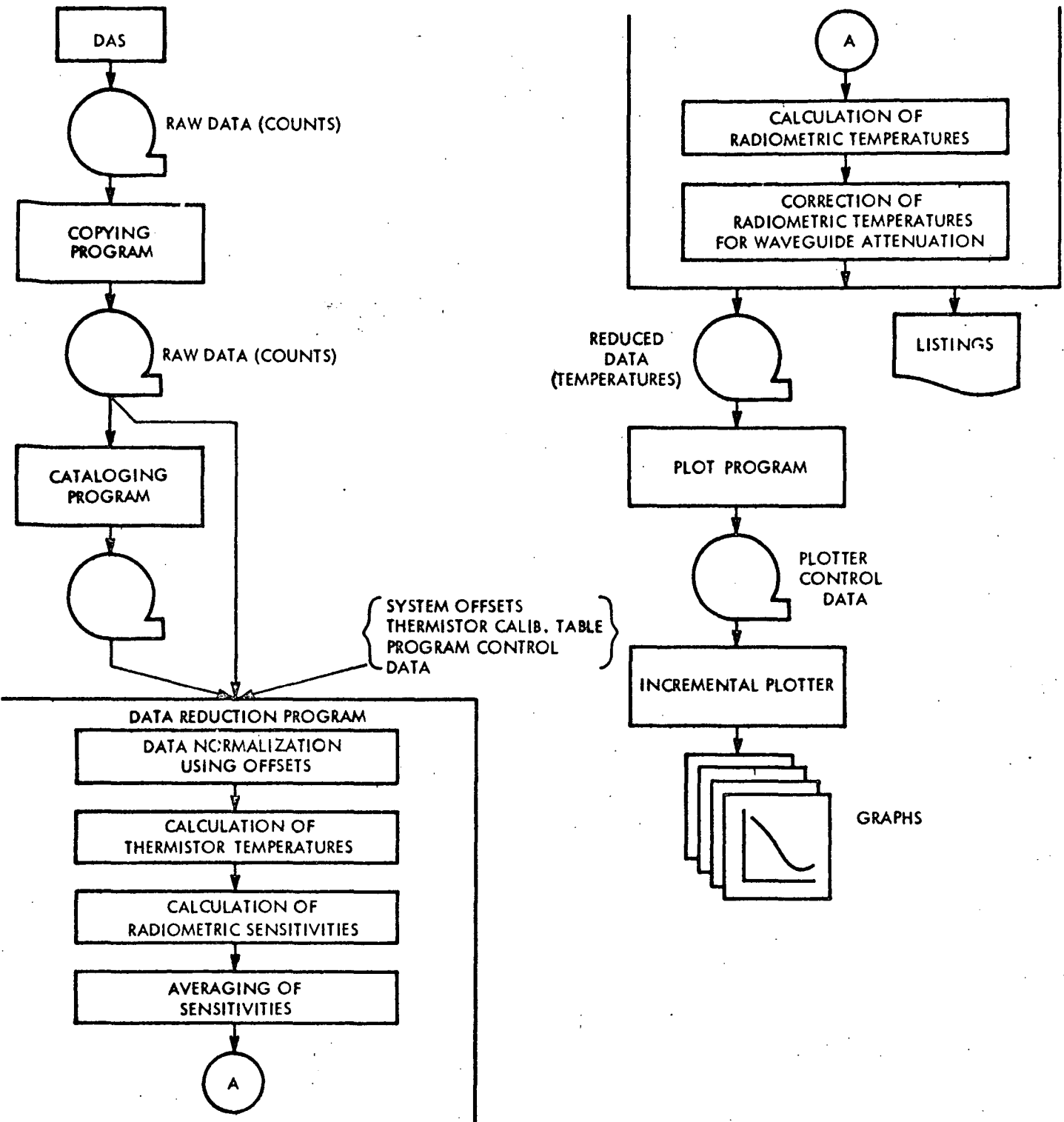


Figure A-2. Data Processing Flow Chart

STEP 2 - REDUCTION - In the reduction step, radiometric brightness temperatures are calculated; the results are listed in tabular form on computer printout sheets; and an output tape is created which is used in the plotting operation, Step 3. The basic calculation of radiometric temperatures consists of the following:

- (1) The elimination of definable system errors.
- (2) The calculation of the sensitivity of each radiometer.
- (3) The calculation of radiometric brightness temperatures.
- (4) The correction of antenna brightness temperatures to system attenuation.

STEP 3 - PLOTTING - The production of graphs of radiometric temperatures versus angle from nadir consists of the following:

- (1) The output tape of the reduction step is processed to produce a tape which will control an incremental plotting device.
- (2) This data is used to control a CalComp plotter.

## APPENDIX B

### DETAILED DESCRIPTION OF GROUND SITES INCLUDING PERTINENT GEOPHYSICAL AND MICROWAVE DATA

#### SITE 1 (21 MAY 1968)

Site 1 was located in a barren field along Jackson Street and 61st, near Indio, California. The field is comprised of recently-tilled fine, sandy loam as shown on Figure B-1. Soil temperatures ranged from 53°C on the surface to 26°C at a depth of 24 inches. Microwave measurements were initiated at 11.6 hrs. PDT and the air temperature was 34.5°C. Soil moisture content ranged from 0 to 1/2 percent near the surface and from 4 to 9 percent at a depth of 6 inches. Geophysical data collected on Site 1 are presented on Figure 3 in the main body of this report.

On this site a series of three detailed elevation scans were taken wherein microwave temperatures were measured as a function of antenna viewing angle. Figures B-2a, B-2b, and B-2c are typical of these measurements. Vertically-polarized antenna temperatures at low viewing angles are on the order of 300°K for the 0.8 and 2.2-cm radiometers compared with approximately 270°K at 21-cm wavelength. Microwave data are discussed in Section 2.1.1 of this report.

#### SITE 2 (21 MAY 1968)

Site 2 was located in a recently irrigated barren field on the southeast corner of Jackson and 58th Streets near Indio, California. The site is shown in Figure B-3. Two elevation scans were taken on this location at 15.5 hrs. PDT. Thermometric temperature of the soil spanned only 9°C from the surface (35°C) to a depth of 24 inches (26°C). This slight change in physical temperature is a reflection of the moderately-high moisture content of the soil. Moisture content ranged from 8.9 percent to 12.4 percent near the surface and from 12 to 14.5 percent at a depth of 6 inches. Although the percent moisture is higher at Site 2, bearing strength values approximate those measured at Site 1. Geophysical data collected on this site are treated in Section 2.1.2 of this report.





3425/059

  
Reproduced from  
best available copy.

Figure B-1. Site 1

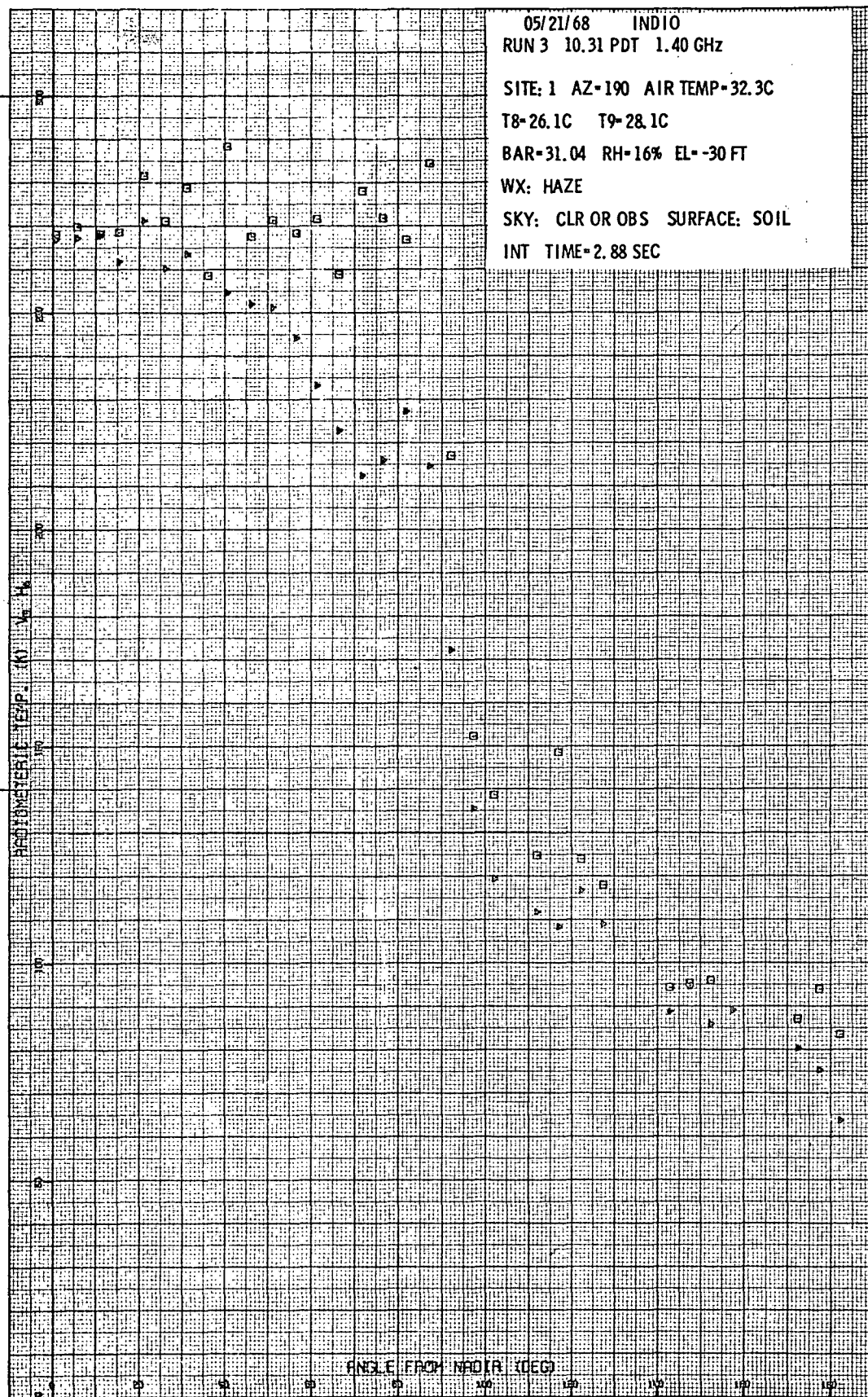


Figure B-2a. Site 1 - Radiometric Brightness Temperature Measured at 21-cm Wavelength

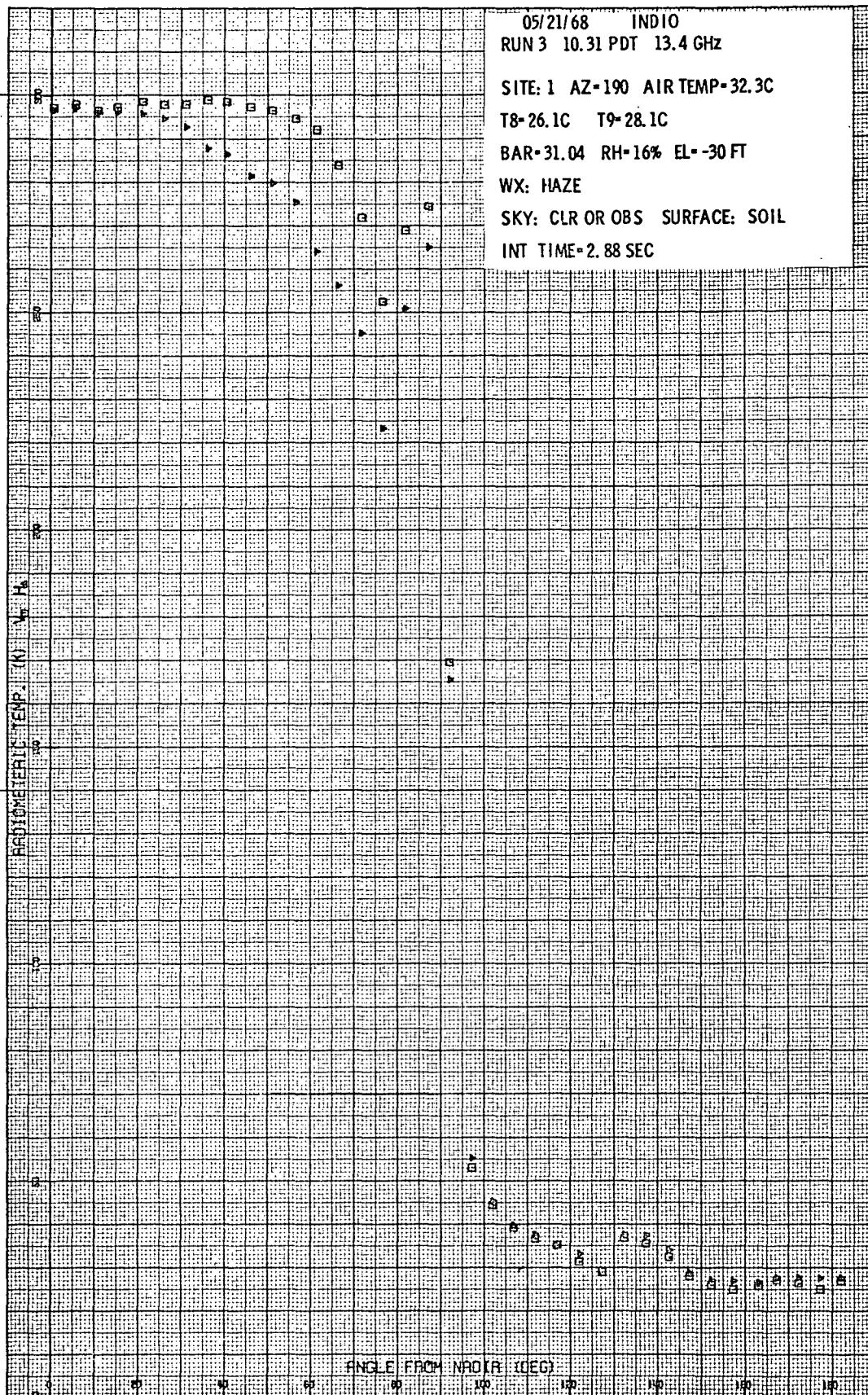


Figure B-2b. Site 1 - Radiometric Brightness Temperature Measured at 2.2-cm Wavelength

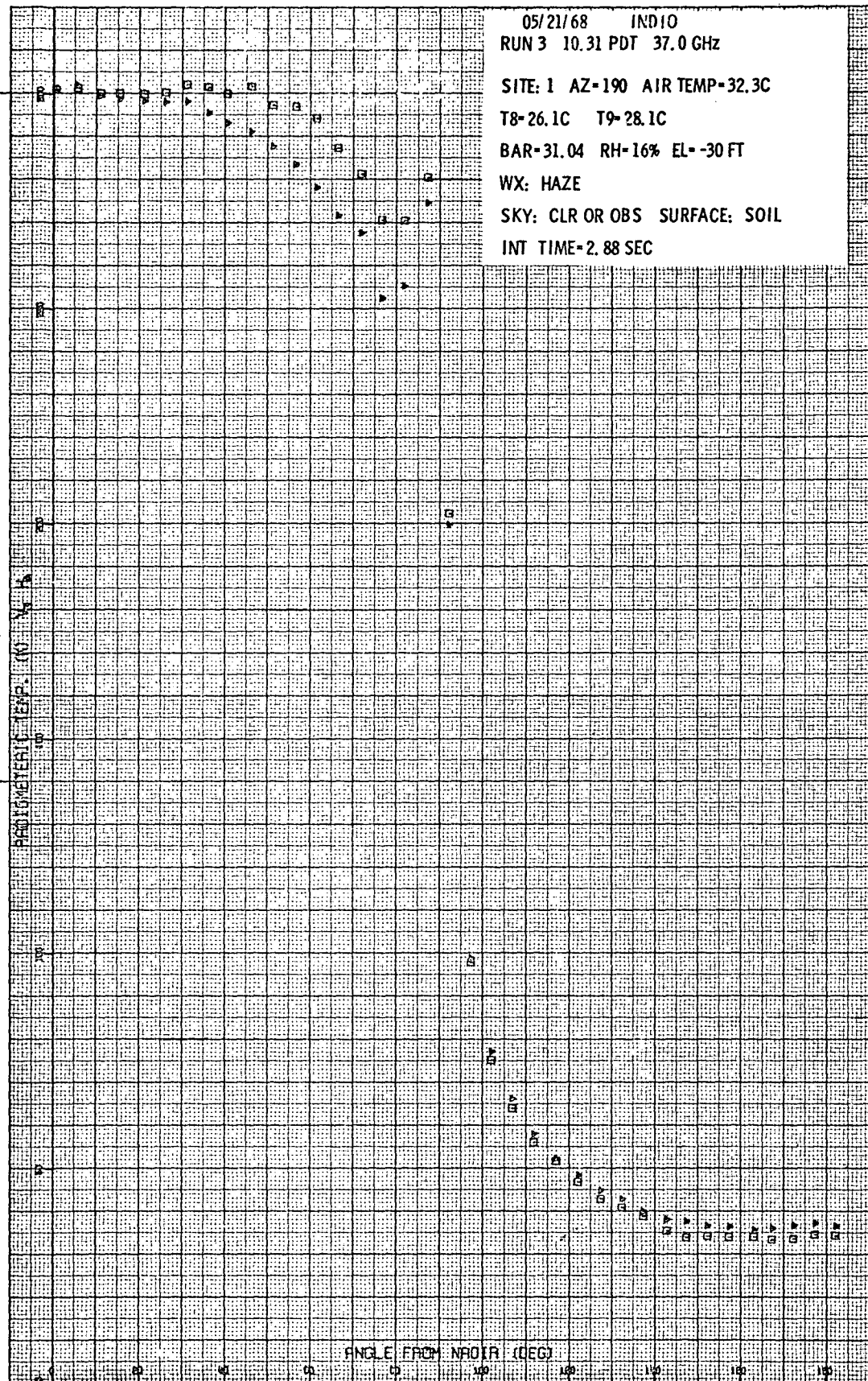
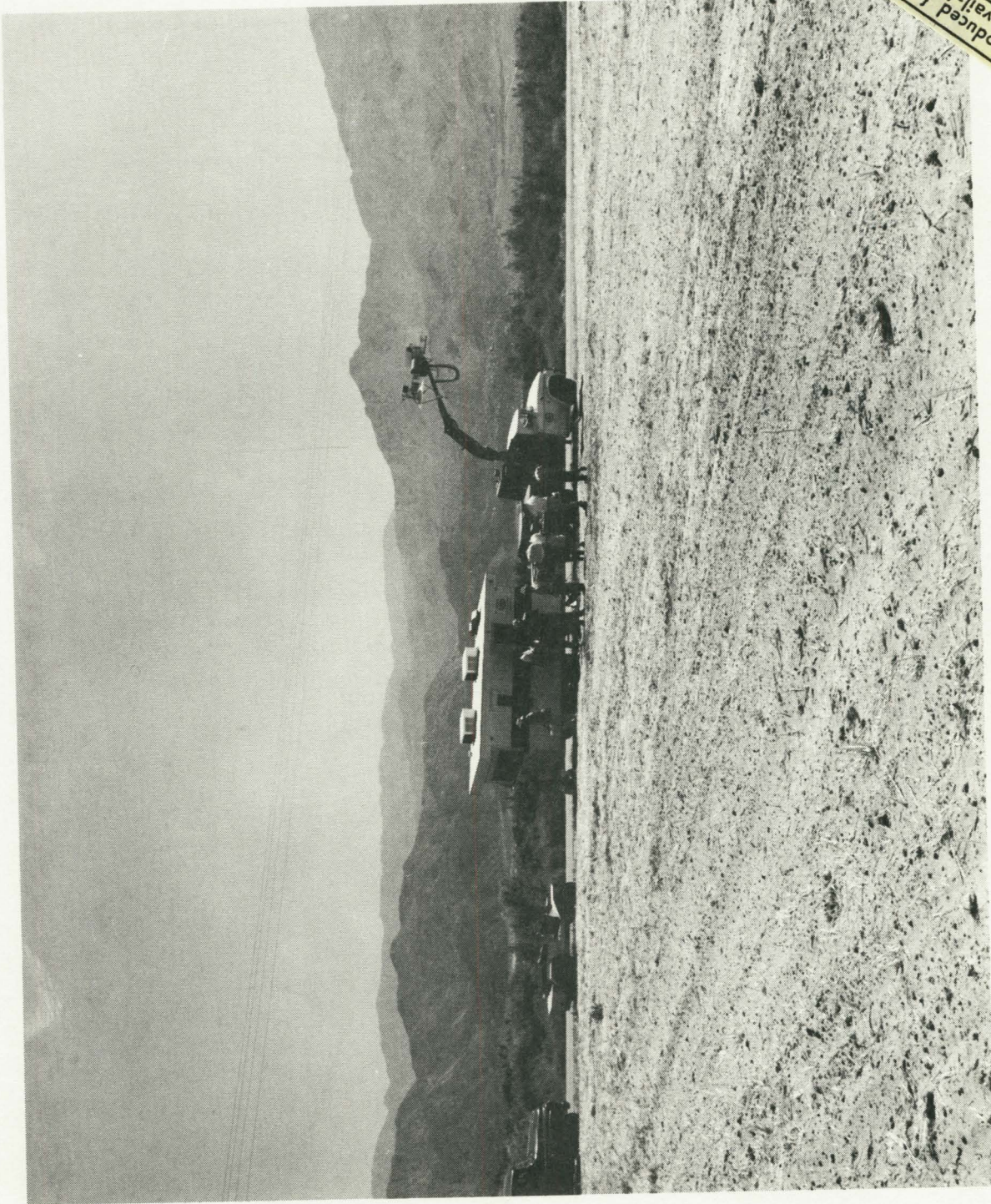


Figure B-2c. Site 1 - Radiometric Brightness Temperature Measured at 0.8-cm Wavelength

20



3425/067

Reproduced from  
best available copy.

Figure B-3. Site 2

Radiometric temperatures at this site were low for all viewing angles. Antenna temperatures at selected viewing angles and polarization temperature differences ( $T_V - T_H$ ) are tabulated in Table B-1.

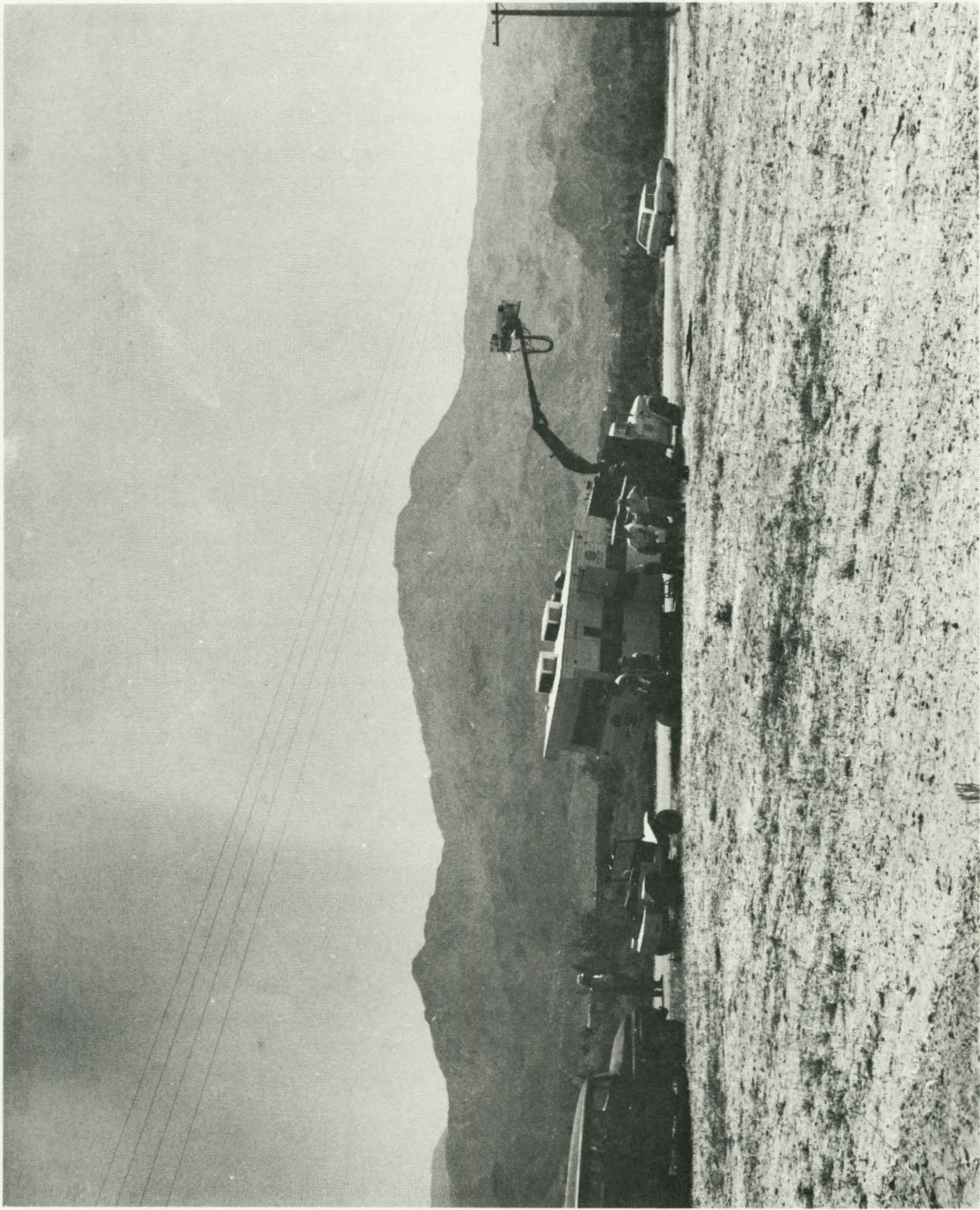
TABLE B-1

Angle from Nadir	21-cm			2.2-cm			0.8-cm		
	$T_V, ^\circ K$	$T_H, ^\circ K$	$T_V - T_H, K^\circ$	$T_V, ^\circ K$	$T_H, ^\circ K$	$T_V - T_H, K^\circ$	$T_V, ^\circ K$	$T_H, ^\circ K$	$T_V - T_H, K^\circ$
10°	242	242	0	263	260	3	267	267	0
25°	240	226	14	268	256	11	278	267	10
45°	186	153	34	263	231	32	274	252	21
10°	238	236	2	262	259	3	270	270	0
25°	232	225	6	267	254	13	280	269	11
45°	235	200	35	262	232	32	277	256	21

Polarization temperature differences are large for all radiometers at viewing angles greater than 20° from nadir. The difference in polarization temperatures is characteristic of relatively smooth soils with moderate to high moisture contents. Typically, the antenna temperature for moist soils will be lower than dry soils and polarization differences are large for wet soils.

SITE 3 (21 MAY 1968)

Site 3 was located in a drier portion of the Site 2 field, Figure B-4. Moisture content near the surface ranged from 0 to 4½ percent, while at depth, the moisture content ranged as high as 13 percent along the scan path. Thermometric temperature on the surface was 49°C, decreasing to 25.4°C at a depth of 2 feet. Bearing strength values were similar to those



3425/064

Figure B-4. Site 3

measured at Site 2, although slightly higher values were recorded at a depth of 12 inches.

A series of three elevation angle scans were taken on Site 3 commencing at 14.12 hrs. Figures B-5a, B-5b, and B-5c are typical elevation scans. Antenna temperatures measured with the long wavelength 21-cm radiometer were some 40 to 50°K colder than the 0.8 and 2.2-cm temperatures. This is attributed to the greater penetration of the long wavelength radiometer along with substantially higher moisture values and cooler thermometric temperatures in the soil at depth. The radiometric scans are generally quite smooth or specular in character, except for the first 20° of the scan where the radiometers viewed dry, matted foliage adjacent to the access road.

#### SITE 4 (21 MAY 1968)

Site 4 was used to designate a microwave traverse taken around the perimeter of the field containing Sites 2 and 3. Measurements were taken at wavelengths of 0.8 cm and 2.2 cm with an antenna viewing angle of 60°. Continuous measurements were taken around the perimeter of the field to determine the variability of microwave temperatures within a large, recently-irrigated field and to determine the significance of relating small-area ground measurements in a field to large-area airborne measurements of the same field. The range of measured temperatures was quite large, as shown in Table B-2.

TABLE B-2  
BRIGHTNESS TEMPERATURE VARIATIONS OBSERVED AROUND PERIMETER OF RECENTLY  
IRRIGATED FIELD

	<u>Wavelength</u>	
	<u>0.8-cm</u>	<u>2.2-cm</u>
Vertical Polarization	270°K - 305°K	265°K - 305°K
Horizontal Polarization	200°K - 280°K	180°K - 275°K



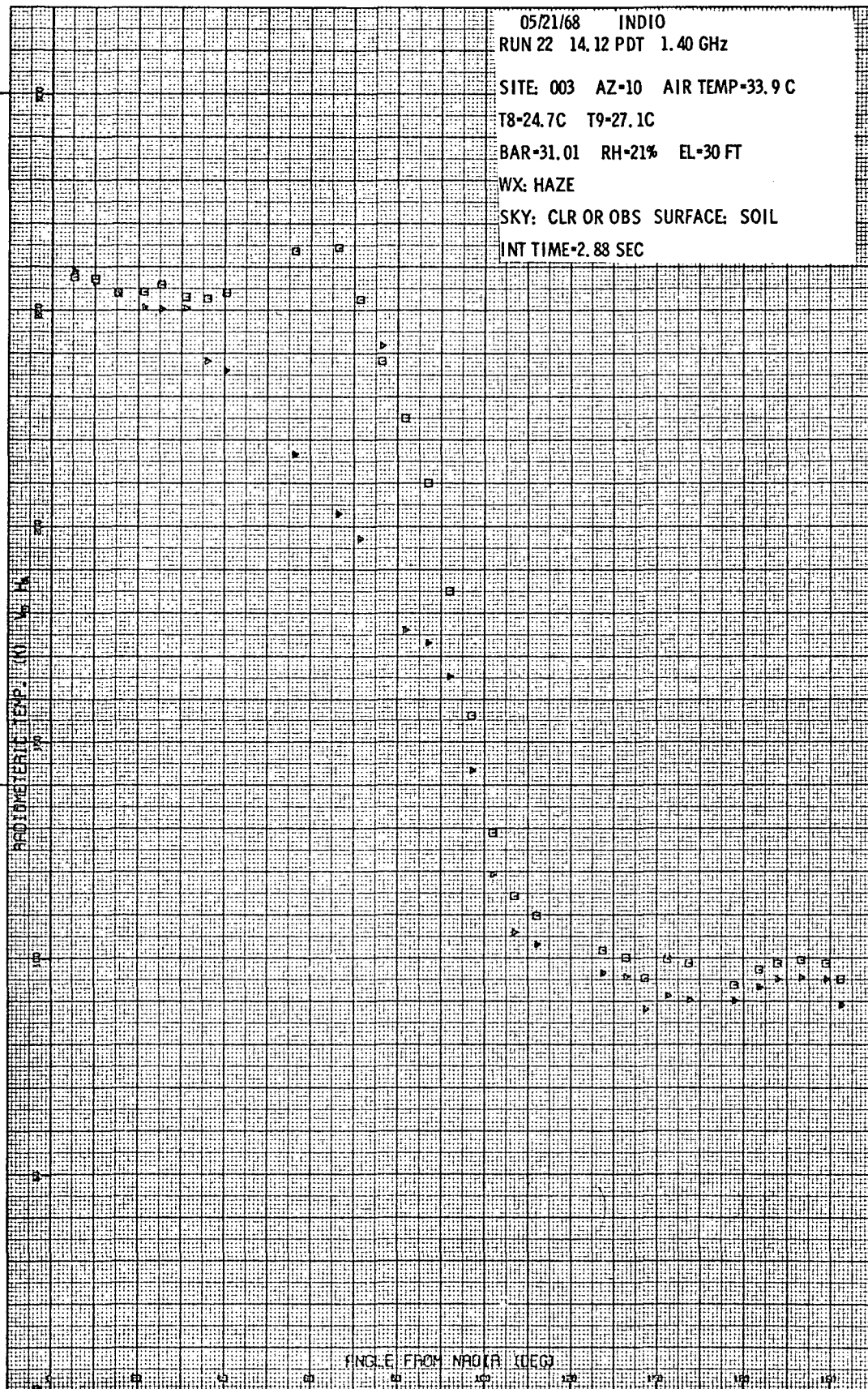


Figure B-5a. Site 3 - Radiometric Brightness Temperature at 21-cm Wavelength

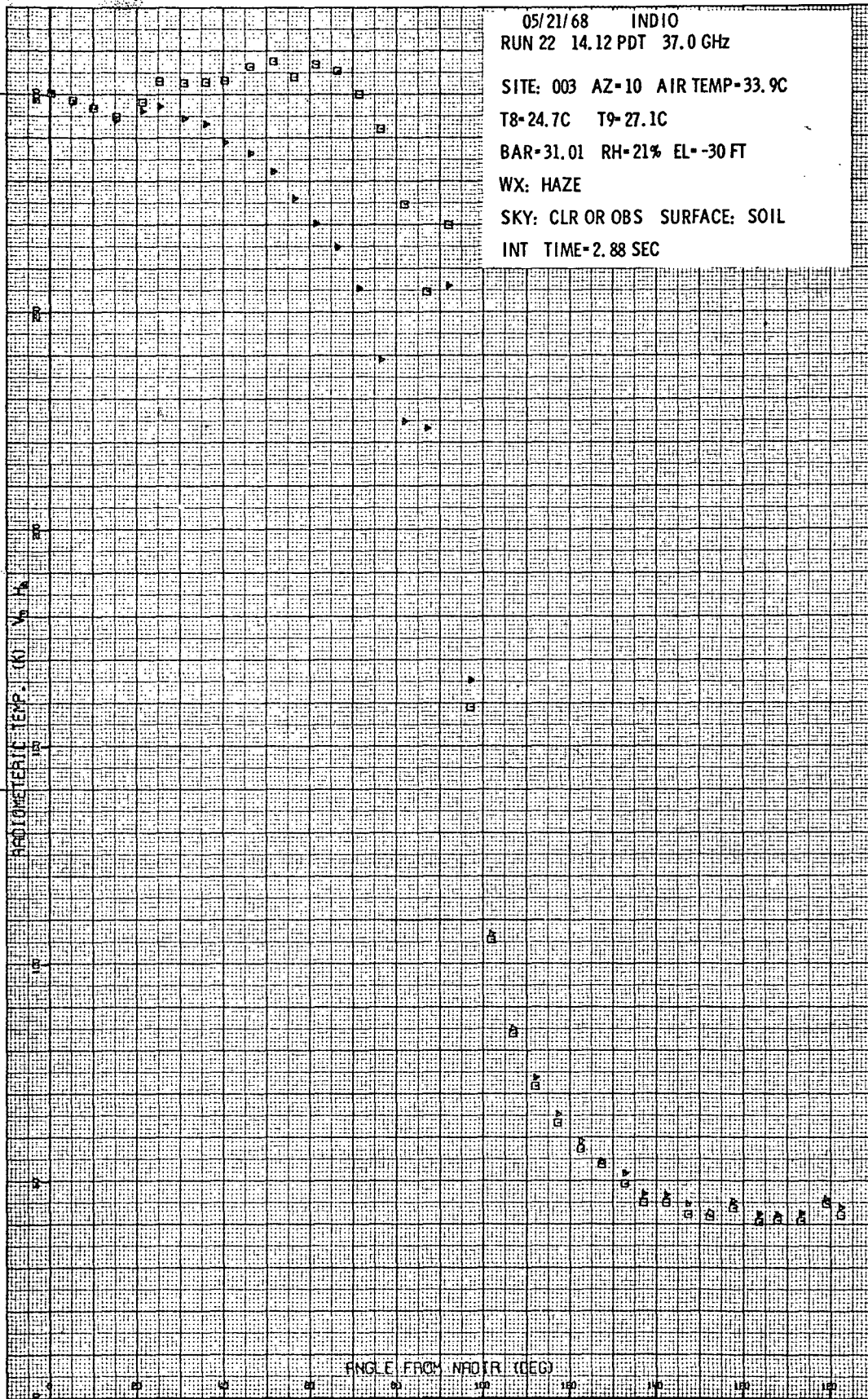


Figure 5b. Site 3 - Radiometric Brightness Temperature Measured at 0.8-cm Wavelength

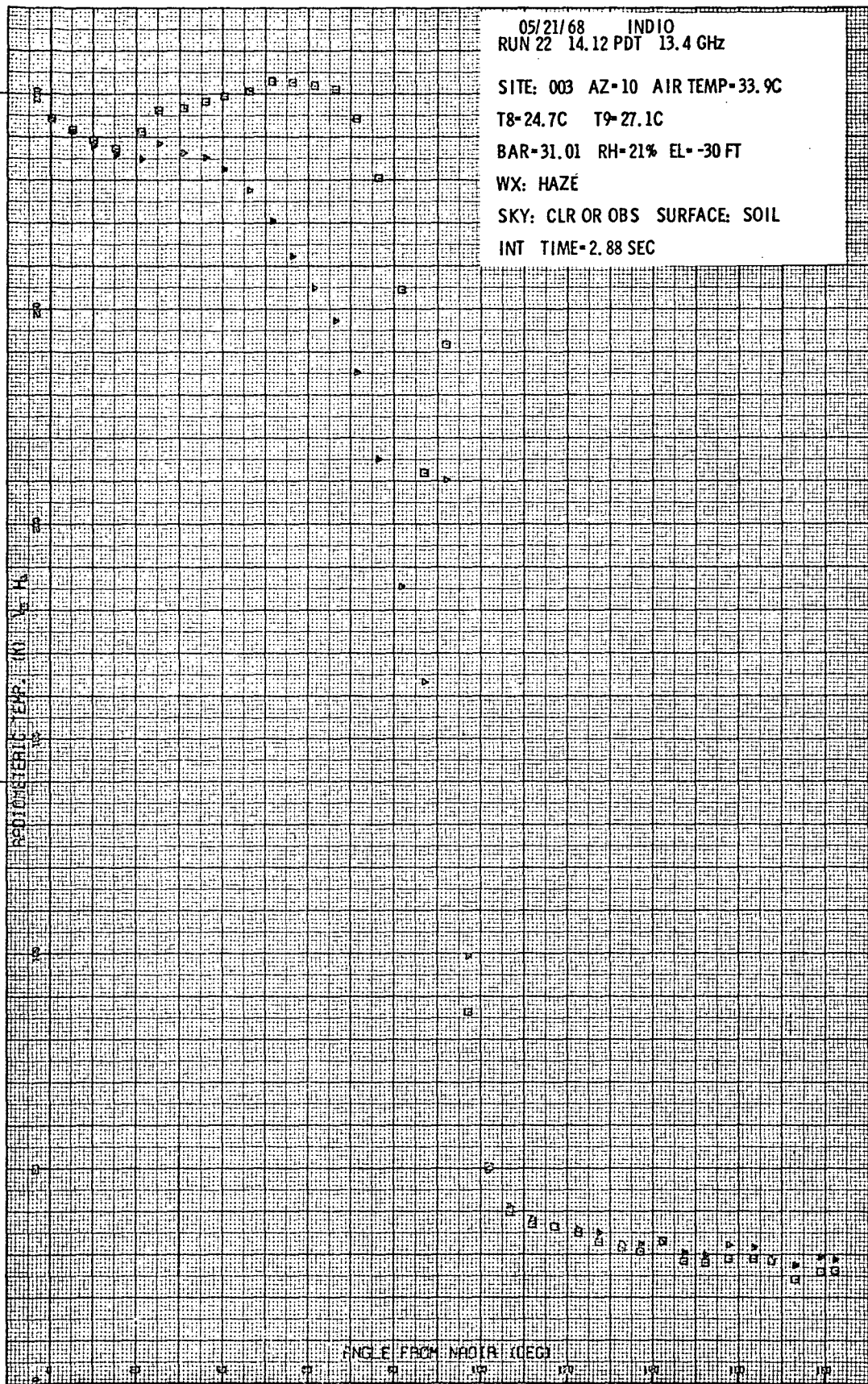


Figure 5c. Site 3 - Radiometric Brightness Temperature Measured at 2.2-cm Wavelength

These variations were associated with irregular distribution of irrigation waters. Both the horizontal and vertical components are sensitive to moisture variations. The horizontally polarized component is also influenced by surface roughness variations and exhibits a wider range of brightness temperatures. The magnitude of the variations makes it very difficult to establish a meaningful relationship between the small area ground measurements and large area airborne microwave data. This is particularly true for fields free of vegetal cover where nonuniform irrigation shows pronounced influence on the measured brightness temperatures. Similar data collected in fields containing crops show less-pronounced variations.

#### SITE 5 (22 MAY 1968)

A bean field adjacent to the flooded field at which Sites 2, 3 and 4 were located was designated as Site 5, Figure B-6. Soil thermometric temperature ranged from  $39^{\circ}\text{C}$  at the surface to  $22.5^{\circ}\text{C}$  at a depth of 2 feet. The percent moisture was as high as 3.5 percent at the surface and 14.2 percent at a depth of 12 inches. Bearing strength values are appreciably lower at this site, and in some cases, values at a depth of 12 inches are 50 percent lower than comparable uncultivated fields.

Antenna temperatures from Site 5 are shown as a function of the incidence angle in Figures B-7a, B-7b and B-7c. Temperatures are higher than those at Site 2 for all wavelengths at the angles of  $10^{\circ}$ ,  $25^{\circ}$ , and  $45^{\circ}$ . Antenna temperatures are comparable for the shorter wavelengths at Site 3; however, at 1.4 GHz ( $\lambda = 21$  cm) the temperatures are lower at angles approaching  $45^{\circ}$  from nadir. An important factor to note is the polarization temperature difference of Site 5 as compared with Sites 2 and 3. Site 5 has very small polarization temperature differences as shown by the separation of the curves. Small polarization temperature differences are characteristic of areas with vegetal cover.

#### SITE 6 (22 MAY 1968)

An area of desert terrain east of the Salton Sea in the vicinity of the San Andreas Fault was measured as Site 6. The purpose of the



3425/057

Figure B-6. Site 5

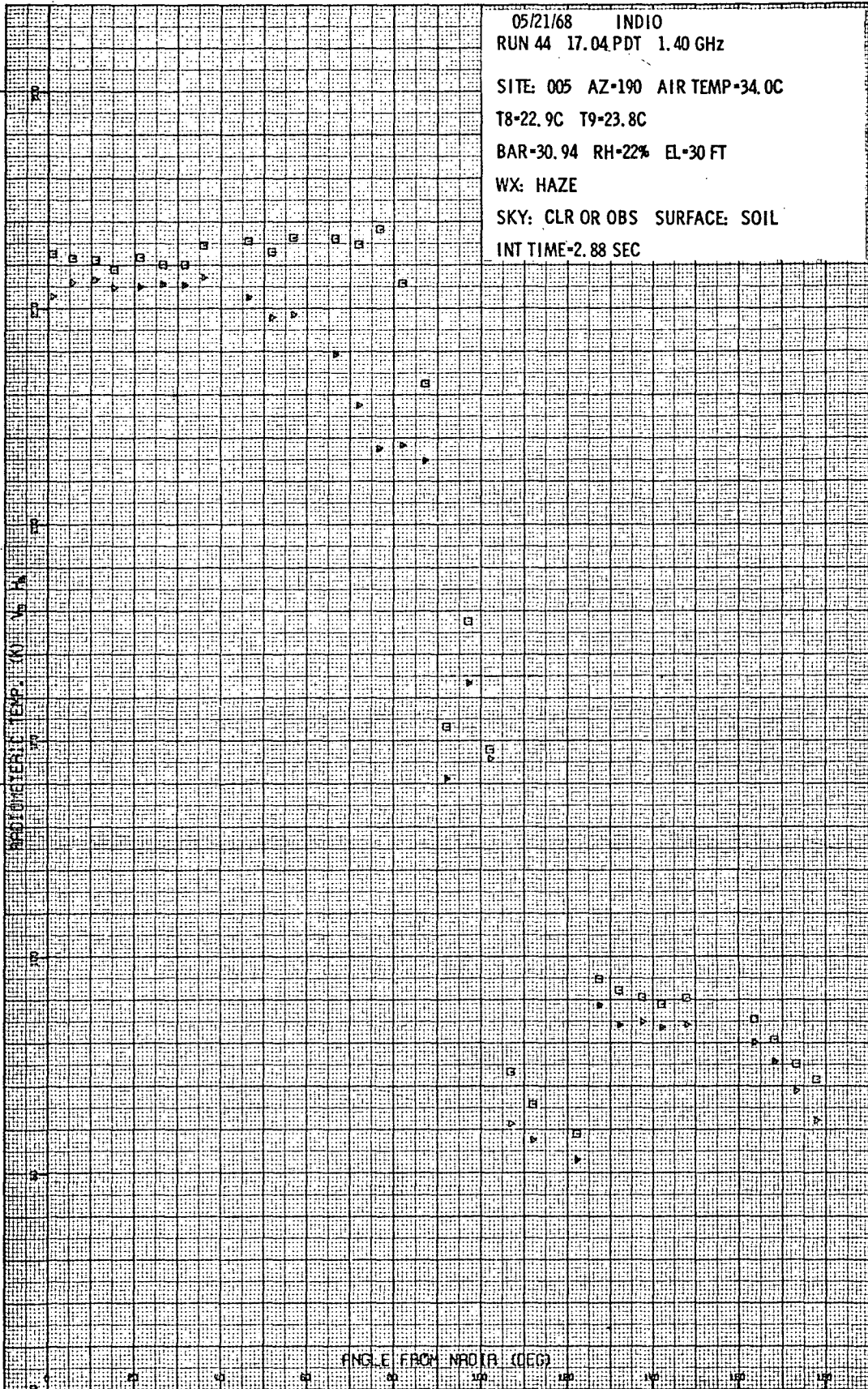


Figure B-7a. Site 5 - Radiometric Brightness Temperature Measured at 21-cm Wavelength

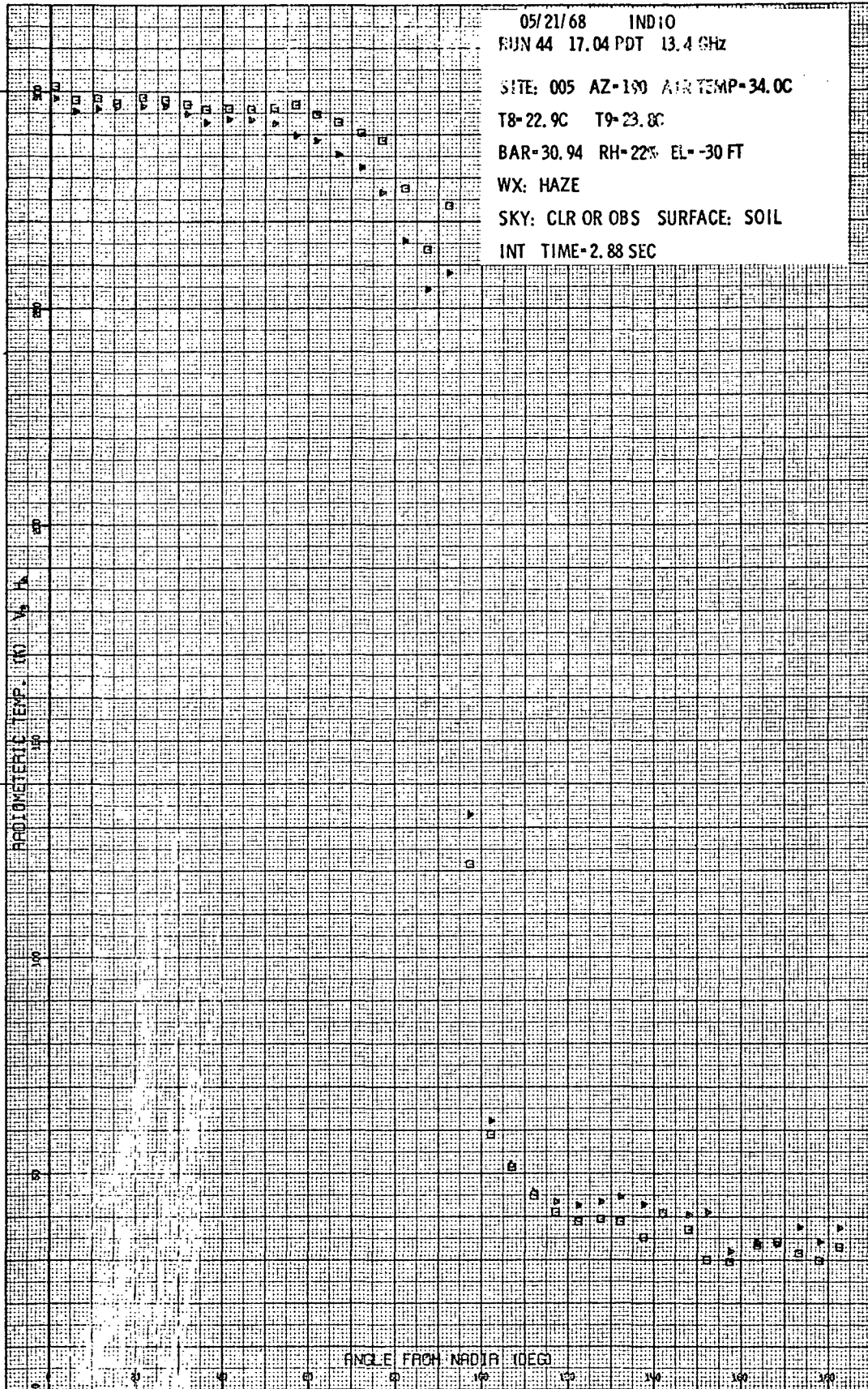


Figure B-7b. Site 5 - Radiometric Brightness Temperature Measured at 2.2-cm Wavelength

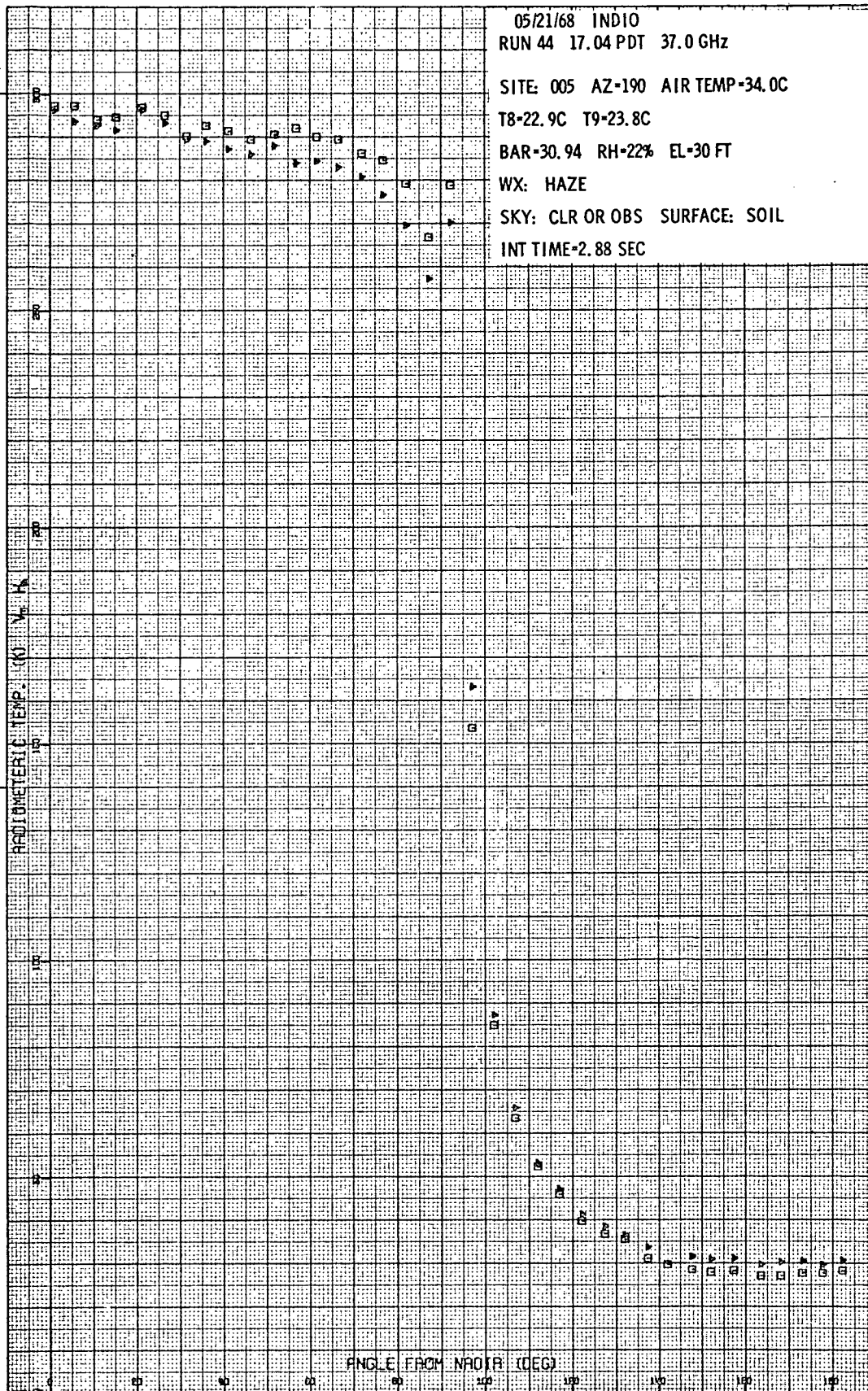


Figure B-7c. Site 5 - Radiometric Brightness Temperature Measured at 0.8-cm Wavelength



measurements was to determine if radiometric temperature anomalies could be detected near the fault zone. However, the data tape was destroyed while a copy tape was being made, and the data was lost. Another attempt to make measurements across the fault was successful and is discussed in connection with Sites 14 and 15.

#### SITE 7 (22 & 23 MAY 1968)

Site 7 comprises both a barren field and a bean field. Measurements consisted of a series of elevation angle scans taken at 1890 hours on 22 May 1968, and 0600 hours on 23 May 1968. Physical parameters of the barren field are plotted on Figure B-8. Moisture content of the barren field was moderately high, averaging approximately 10 percent (dry weight) along the scan path at a depth of 12 inches. Bearing strengths on the surface were constant with values less than 10 lbs/in<sup>2</sup>. At depths of 6 and 12 inches bearing strengths ranged from 30 to 160 lbs/in<sup>2</sup>.

Antenna brightness temperatures varied considerably from evening to morning. Typically, temperatures were 287 and 285<sup>o</sup>K for the 2.2-cm radiometer at vertical and horizontal polarizations, respectively, for a viewing angle of 10<sup>o</sup>, Figures B-9a and B-9b. Temperatures for the 0.8-cm radiometer were 279<sup>o</sup>K for both polarizations at the same viewing angle. Soil temperatures ranged from 22<sup>o</sup>C to 28<sup>o</sup>C during these measurements.

Measurements during the morning hours of 23 May were of the barren field, Figures B-10a and B-10b. Antenna temperatures were slightly lower, ranging from 280<sup>o</sup>K and 278<sup>o</sup>K respectively, for the 2.2-cm vertical and horizontal polarizations for a 10<sup>o</sup> antenna viewing angle. The vertical and horizontal polarization temperatures were 277<sup>o</sup>K and 276<sup>o</sup>K for the same viewing angle as measured with the 0.8-cm radiometer. The lower temperatures are associated with lower soil temperatures which ranged from 17 to 24<sup>o</sup>C during the early morning hours.

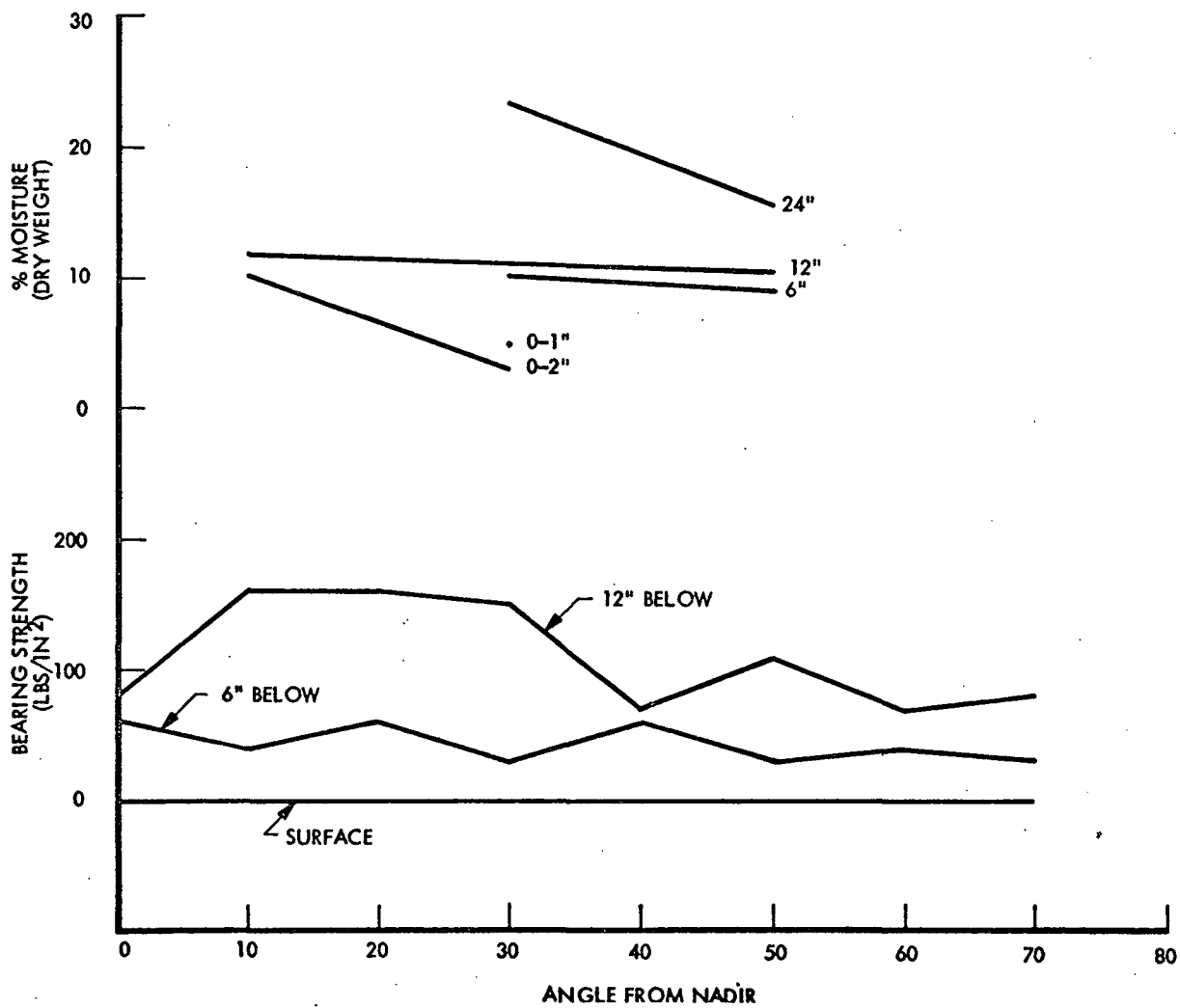
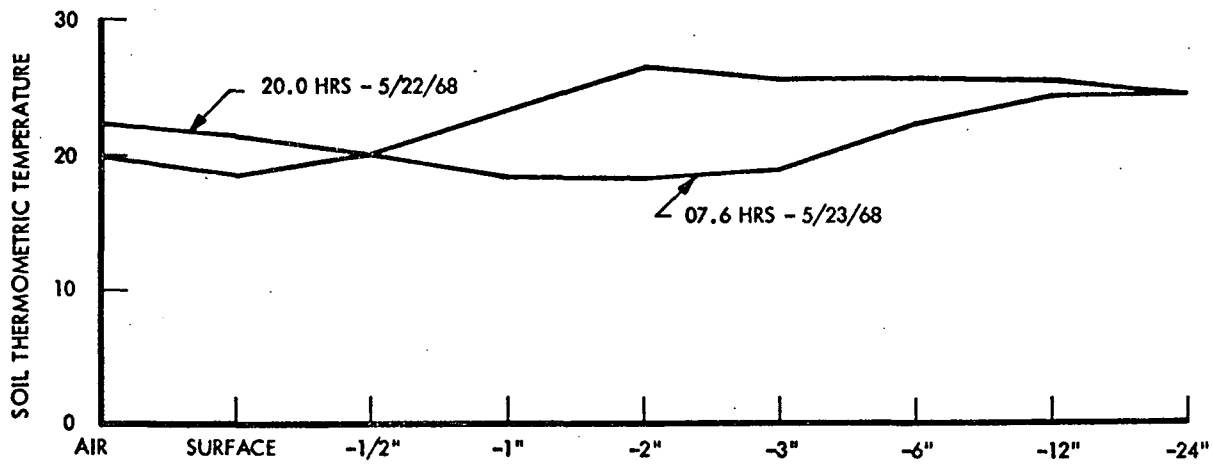


Figure B-8. Physical Parameters of Site 7

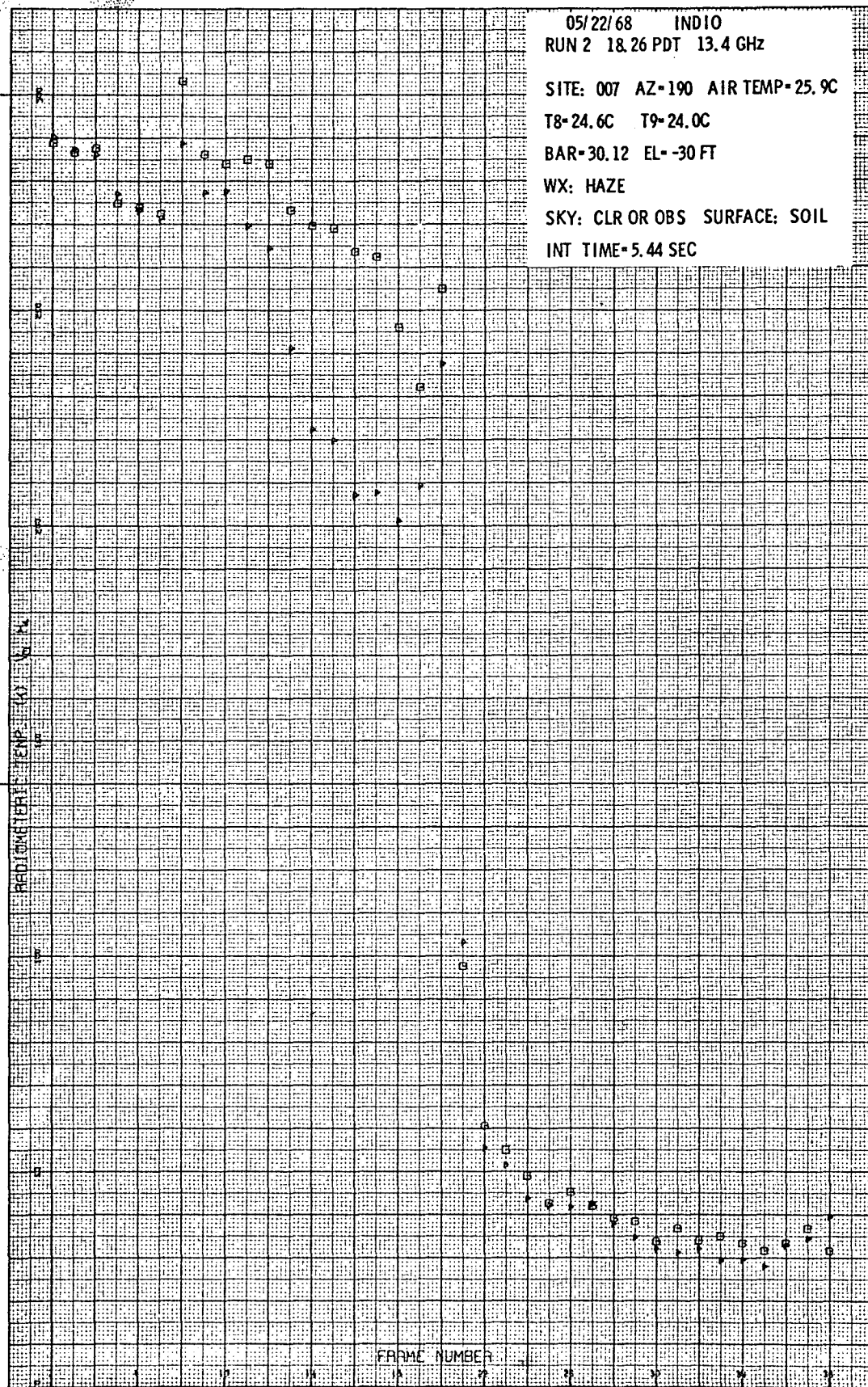


Figure B-9a. Site 7 - Radiometric Brightness Temperature Measured at 2.2-cm Wavelength (Run 2)

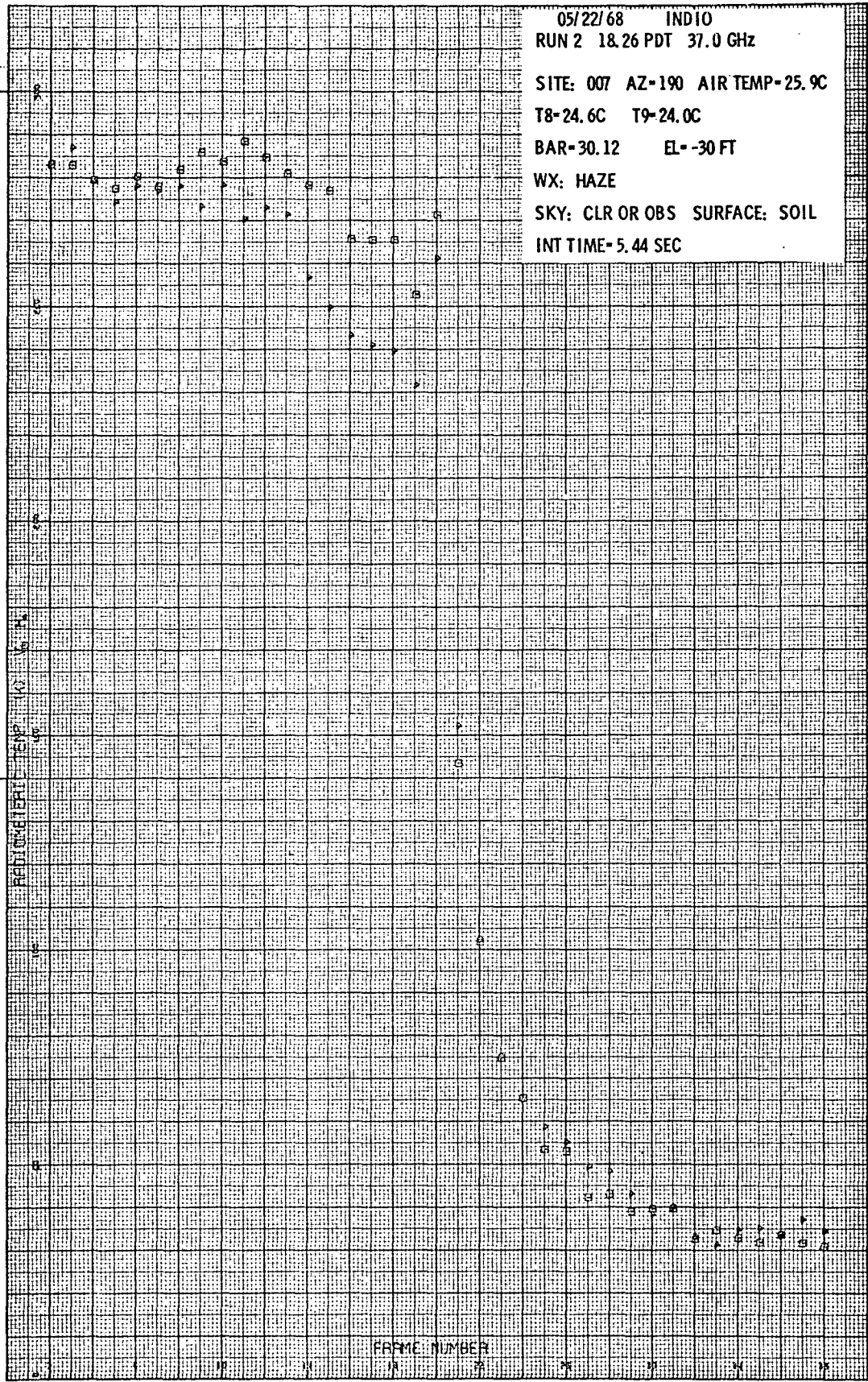


Figure B-9b. Site 7 - Radiometric Brightness Temperature Measured at 0.8-cm Wavelength (Run 2)

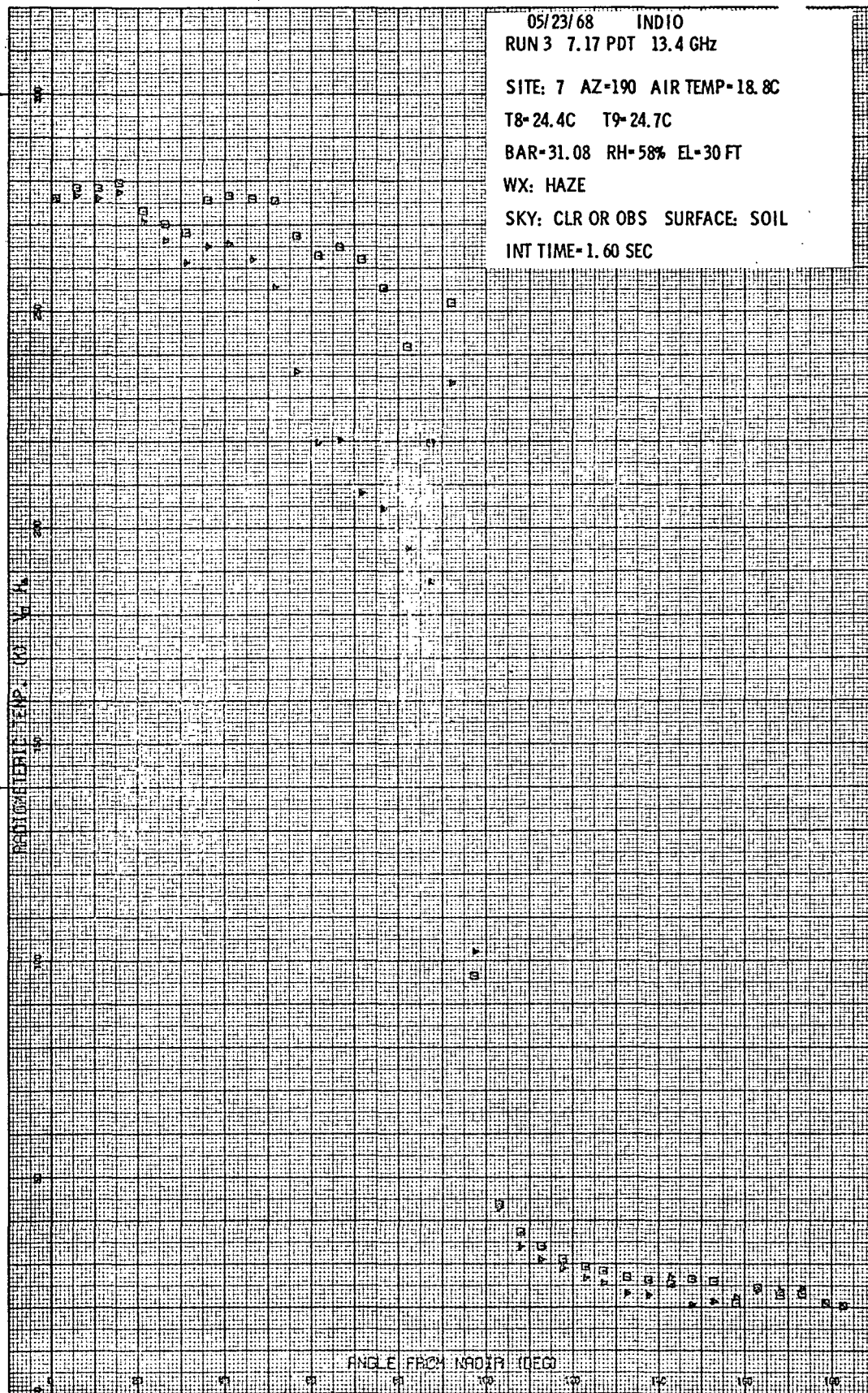


Figure B-10a. Site 7 - Radiometric Brightness Temperature Measured at 2.2-cm Wavelength (Run 3)

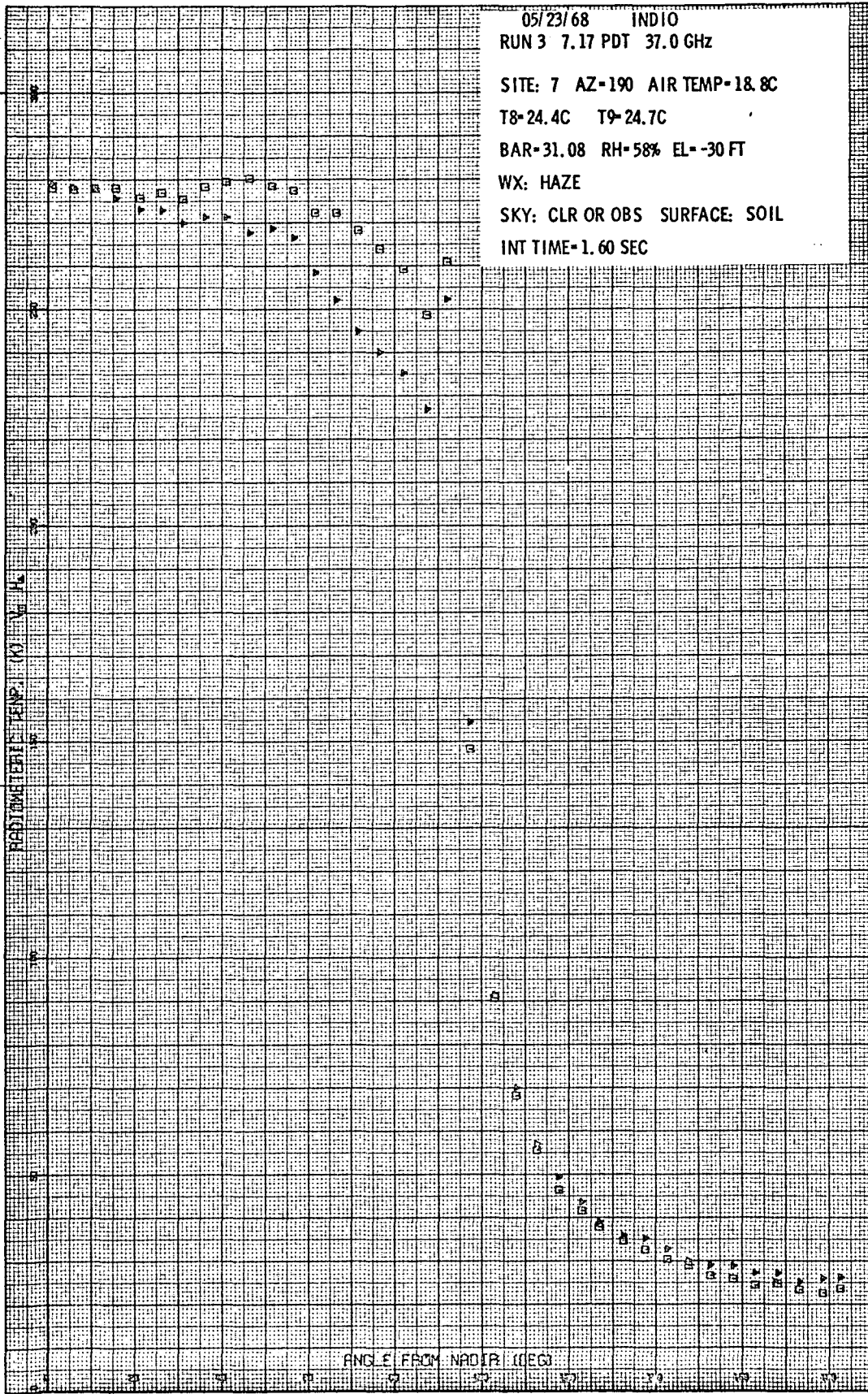


Figure B-10b. Site 7 - Radiometric Brightness Temperature Measured at 0.8-cm Wavelength (Run 3)

SITE 8 (23 MAY 1968)

Site 8 was located on the causeway of the Calipatria Boat Ramp where measurements were taken of the Salton Sea in conjunction with overflights by the NASA C240. Measurements were taken at 2100 hours on 23 May. The water surface contained waves having a wavelength of approximately 8 feet and an amplitude of 6-9 inches. The wind was to the southeast at a velocity of 20 to 30 miles per hour and the water temperature was 21.2°C.

Measurements consisted of a series of three elevation scans. The scan azimuth was 180°, oblique to the direction of wave propagation, Figure B-11.

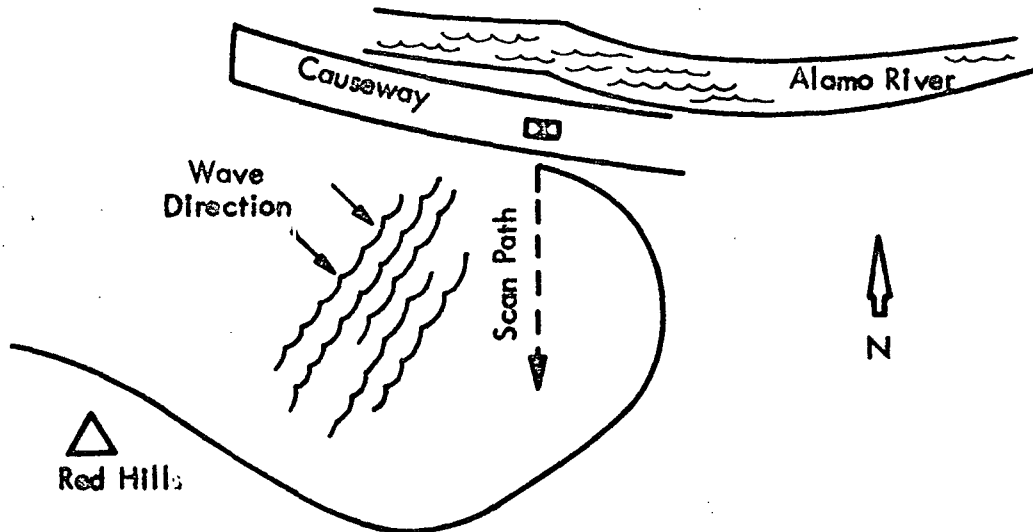


Figure B-11. Sketch Map of Site 8

Antenna brightness temperatures of the water surface are shown on Figures B-12a and B-12b. Measurements of the water were taken so that ground-based and airborne microwave data could be compared. Hopefully, the ground data could be used as a calibration reference for the aircraft radiometers.

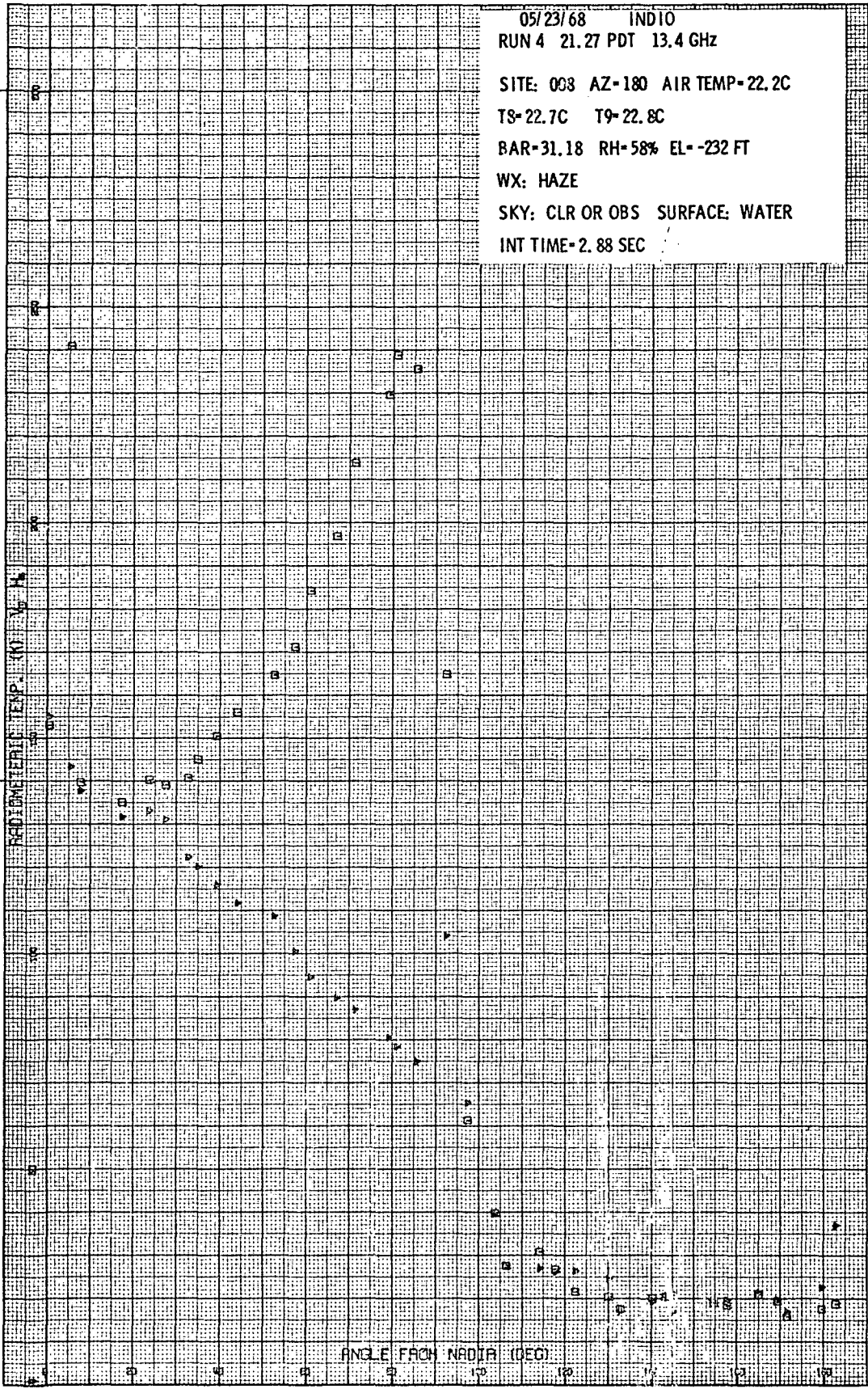


Figure B-12a. Site 8 - Radiometric Brightness Temperature Measured at 2.2-cm Wavelength



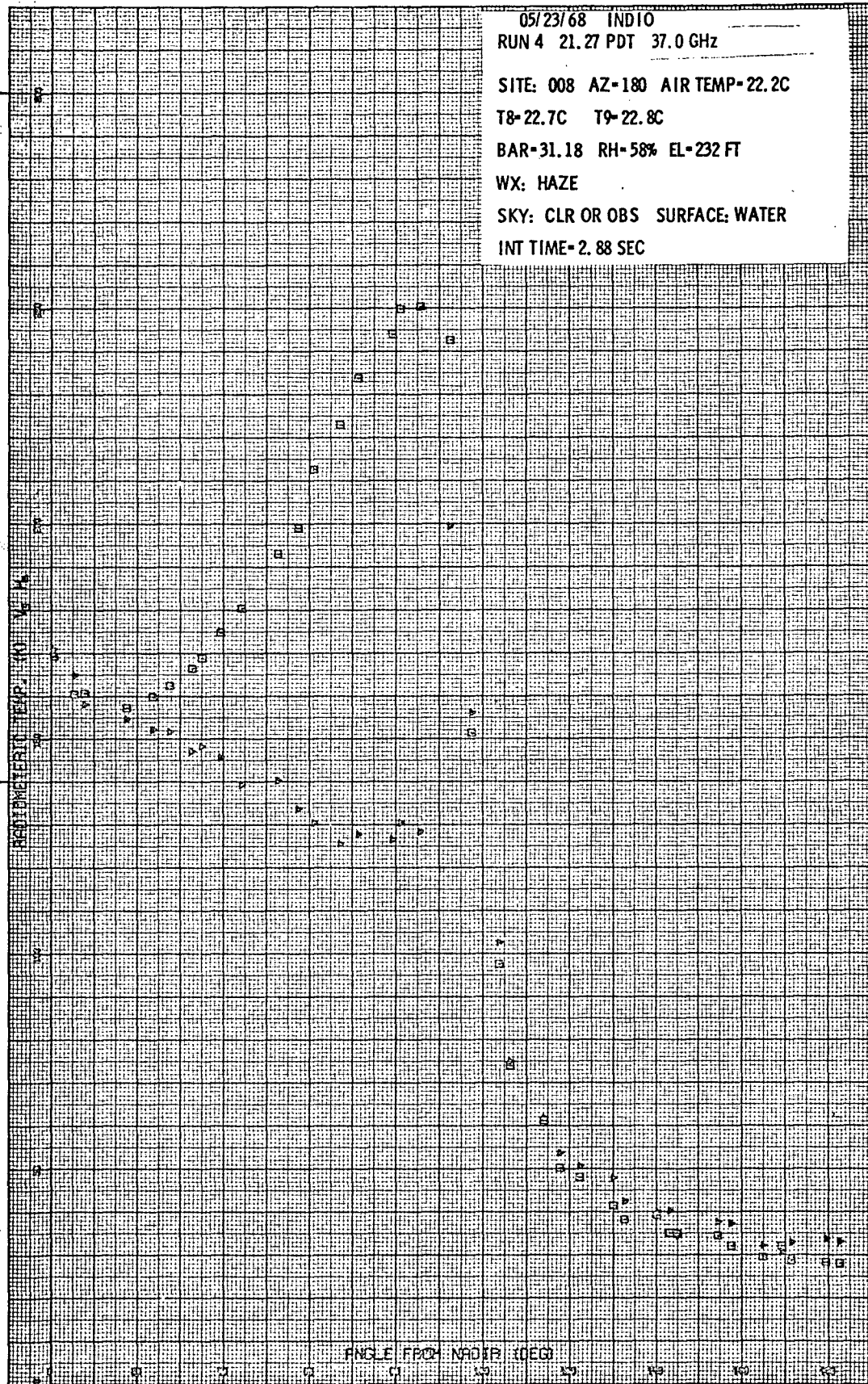


Figure B-12b. Site 8 - Radiometric Brightness Temperature Measured at 0.8-cm Wavelength

### SITE 9 (23 MAY 1968)

Site 9 was a saturated silt loam field located along Sinclair Road, just south of the Salton Sea. The barren field was being leached to remove saline constituents. Moisture content of the soil was very high (in excess of 50 percent by weight, dry basis) and somewhat variable. The field contained leach basins which in places contained standing water, separated by earthen dikes. Thermometric temperature of the soil ranged only  $8^{\circ}\text{C}$  from the surface to a depth of 18 inches. The small range in soil thermometric temperature reflects the saturated condition of the soil.

Three elevation scans and a fixed angle traverse at a viewing angle of  $45^{\circ}$  were made of the field. Antenna temperatures for the scans were appreciably lower than other barren fields measured during this study. Maximum antenna temperature measured with the 2.2-cm sensor was  $245^{\circ}\text{K}$  and  $227^{\circ}\text{K}$  respectively for vertical and horizontal polarizations. The 0.8-cm temperature maxima were  $263^{\circ}\text{K}$  and  $255^{\circ}\text{K}$  for the vertical and horizontal polarizations respectively. The maximum temperatures were measured at a viewing angle of  $55^{\circ}$  for both radiometers. Figure 1, in the main body of the report, compares the brightness temperatures of Site 9 with that of drier fields.

Antenna temperatures recorded during the fixed angle traverse at  $45^{\circ}$  indicate a large variation in the moisture content for different portions of the field. During the mid-portion of the traverse, 2.2-cm temperatures ranged as low as  $180^{\circ}\text{K}$  for the vertical polarization and  $127^{\circ}\text{K}$  for the horizontal polarization. Such low temperatures are indicative of standing water on the surface.

### SITE 10 (24 MAY 1968)

An alfalfa field near the intersection of Walker and McKinney Roads was designated as Site 10. The mature alfalfa crop was chosen to represent a hot, unpolarized body. The alfalfa was 9-inches high and covered 90 percent of the ground surface. Soil moisture conditions ranged from 2.3 to 3.1 percent at the surface along the scan path. The

moisture content increased to 10 percent at a depth of 12 inches. Thermometric temperature of the soil had a range of only 3°C (18.5°C at the surface to 22.5°C at a depth of 12 inches). The air temperature was 20.4°C at the initiation of the measurements.

Radiometric measurements consisted of two elevation scans and a traverse with a viewing angle of 50°. Antenna temperatures as a function of incidence angle for the 0.8-cm and 2.2-cm radiometers are plotted in Figures B-13a and B-13b. A significant feature of the plots is the small polarization difference ( $\Delta T = T_v - T_h$ ) for both radiometers. Small polarization differences are indicative of diffuse surfaces, and the mature alfalfa represents such a surface.

Average antenna temperatures (0.8-cm and 2.2-cm) measured along the traverse line were 282°K and 281°K for vertical and horizontal polarizations. Maximum polarization differences ( $T_v - T_h$ ) were 3.9°K and 3.8°K for the 2.2-cm and 0.8-cm radiometers, respectively. Polarization differences are expected to be slightly larger for traverses than for elevation scans because each antenna port is viewed sequentially and the field of view for each polarization is slightly different due to movement of the field laboratory along the traverse line.

#### SITE 11 (5 JUNE 1968)

Site 11 was a cotton field on the west side of Highway 111, 2.5-miles north of the intersection of Highway 111 and Highway 115. The crop was immature with individual plants having an average height of 18 inches. Plant spacing along crowns between furrows was 3 feet, and the direction of the furrows was east-west, Figure B-14. Every other furrow was irrigated, and alternating unirrigated furrows contained dessication polygons on the order of 5 inches in diameter.

Soil moisture content ranged from 0 percent at the surface to 24 percent at a depth of 12 inches. A penetrometer survey was conducted in both the irrigated and non-irrigated furrows. Results of these surveys are tabulated in Table B-3.

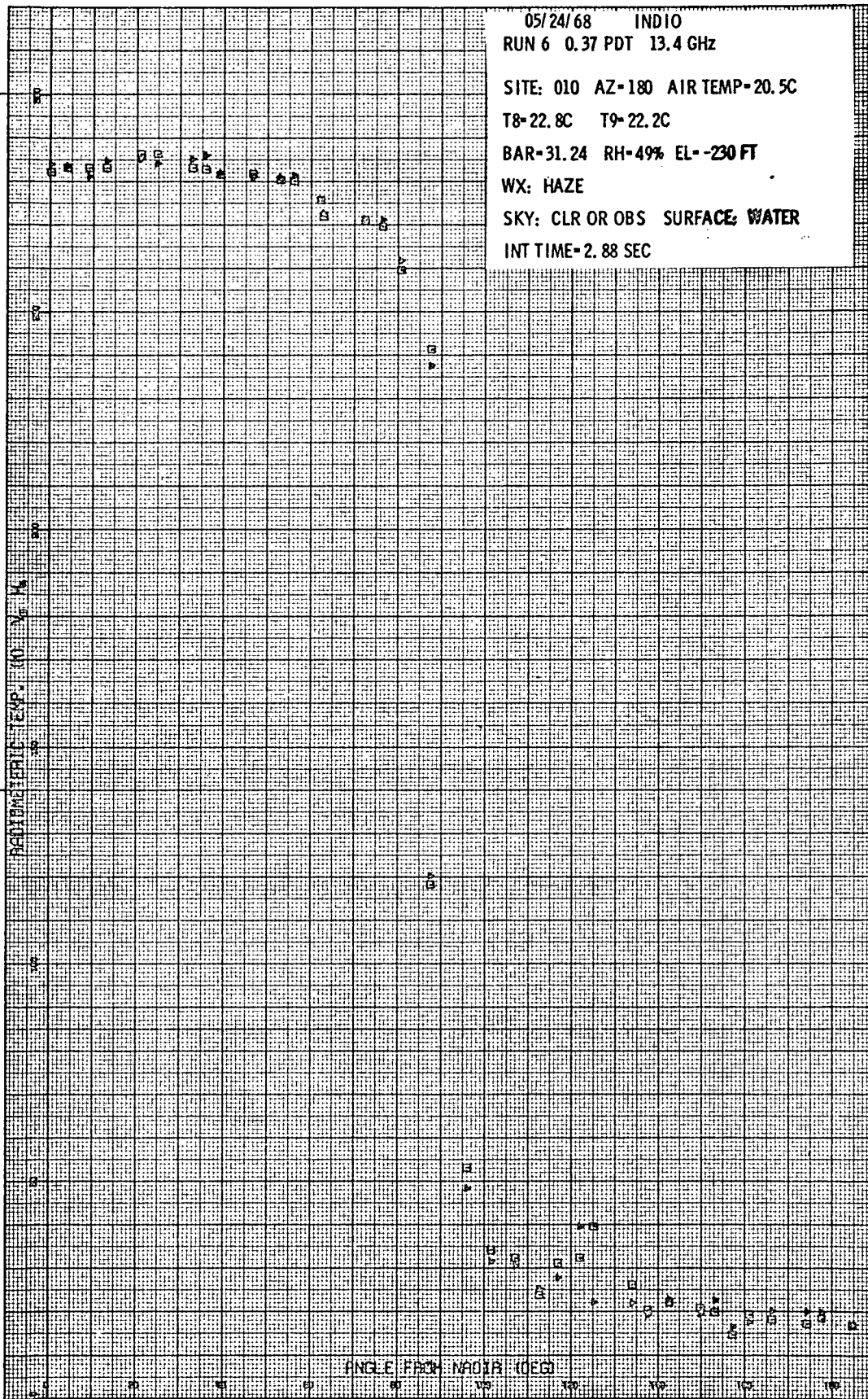


Figure B-13a. Site 10 - Radiometric Brightness Temperature Measured at 2.2-cm Wavelength

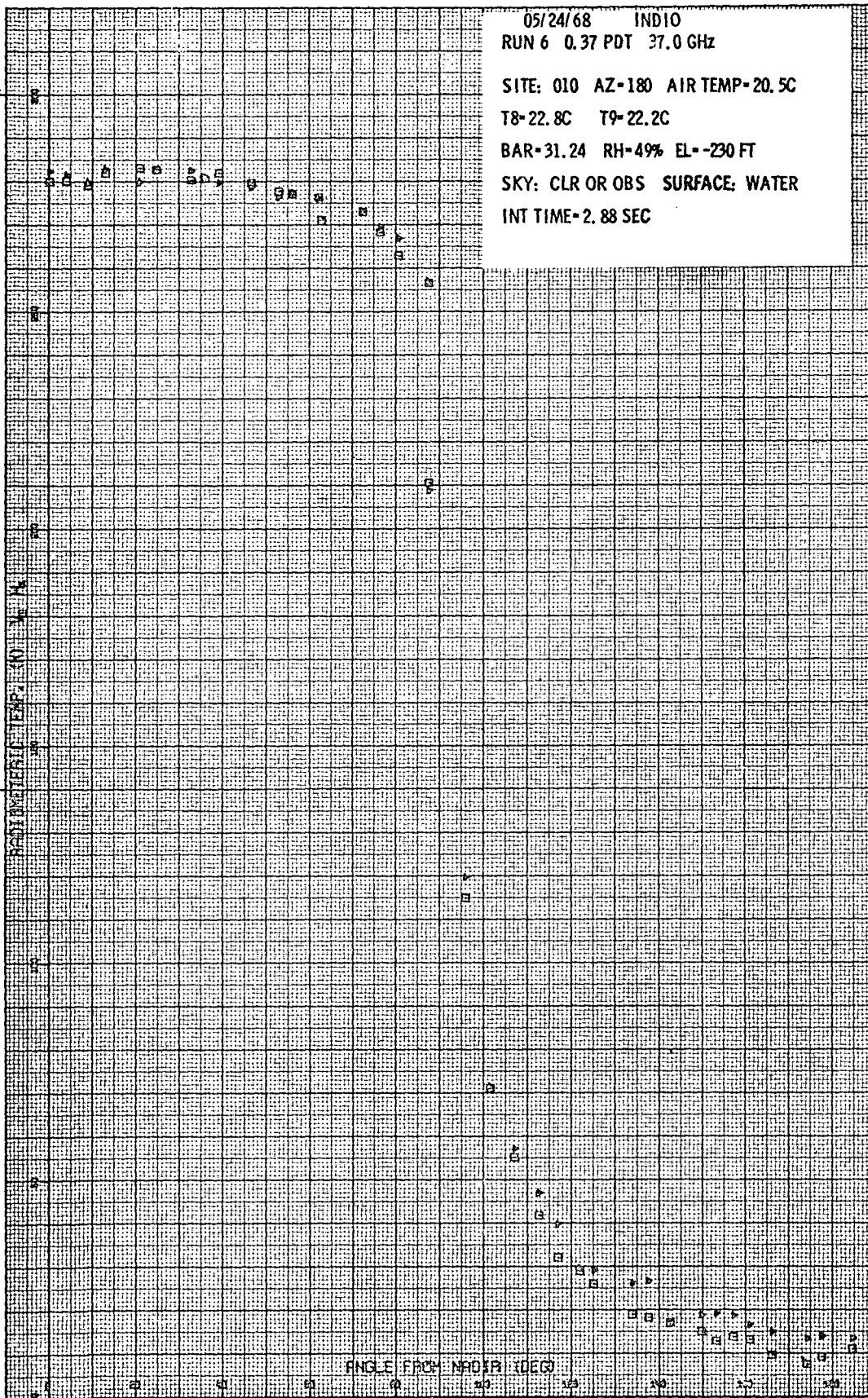


Figure B-13b. Site 10 - Radiometric Brightness Temperature Measured at 0.8-cm Wavelength

Reproduced from  
best available copy.



3425/576

Figure B-14. Site 11

TABLE B-3

PENETROMETER SURVEY SITE 11

<u>Depth Below Surface in Inches</u>	<u>Bearing Strength in Pounds Per Square Inch</u>	
	<u>Irrigated Furrow</u>	<u>Non-Irrigated Furrow</u>
0	10	0
3	40	15
6	40	30
9	40	20
12	40	10

Thermometric temperature of the soil at the surface was 45°C, decreasing to 34°C, 1-inch below the surface. The temperature decreased slowly with depth to 26°C at 12 inches. The thermometric temperature of the cotton plants was 31°C, while the air temperature was 30°C. Throughout this study, a close relationship has been noted between the air and plant temperatures. Since this relationship exists, it is reasonable to assume a plant temperature equal to the air temperature for crops which are not measured directly. An approximation of the emissivity of cotton can be calculated by using this assumption. The basic radiometric equation,  $T_A = \epsilon T_g + (1 - \epsilon) T_s$ , can be simplified to

$$\epsilon = \frac{T_A - T_s}{T_g - T_s}$$

where  $T_A$  is the antenna brightness temperature in °K,  $\epsilon$  is the emissivity,  $T_g$  is the thermometric temperature of the target material in °K, and  $T_s$  is the radiometric sky temperature in °K.  $T_s$  is small compared to  $T_A$  and  $T_g$ , and can be disregarded, further simplifying the equation to:

$$\epsilon = \frac{T_A}{T_g}$$

A first order approximation of the emissivity can be made using the above simplified form. Calculated emissivities for the cotton crop are presented in Table B-4 for viewing angles of 25° and 45°. At this particular site it is justifiable to use only antenna temperatures measured at viewing angles greater than 20°, because of the 3-foot spacing of the crowns between furrows.

TABLE B-4  
CALCULATED EMISSIVITIES OF COTTON ON SITE 11  
(25° AND 45° VIEWING ANGLES)

<u>Viewing Angle, deg</u>	<u>21-cm Sensor</u>		<u>2.2-cm Sensor</u>		<u>0.8-cm Sensor</u>	
	<u>Vert. Plzn.</u>	<u>Horiz. Plzn.</u>	<u>Vert. Plzn.</u>	<u>Horiz. Plzn.</u>	<u>Vert. Plzn.</u>	<u>Horiz. Plzn.</u>
25	0.82	0.81	0.95	0.95	0.95	0.93
45	0.82	0.81	0.96	0.95	0.94	0.89

As shown in Figures B-15a, B-15b and B-15c, antenna temperatures have small polarization differences. The high values at Frame 3 for the 2.2-cm and the 0.8-cm sensors result from the field of view being partially filled by soil in the furrows between the rows of cotton.

SITE 12 (5 JUNE 1968)

Site 12 is located 1.5 miles north of Calipatria on the west side of Highway 111, on a dry field free of vegetal cover; Figure B-16. Soil moisture was low with less than 1-percent moisture on the surface and only 10 percent at a depth of 18 inches. Thermometric temperature also reflects the dry nature of the field. Surface thermometric temperature at nadir position was 43°C and decreased gradually with depth to a minimum of 29°C, 18 inches below the surface.

Radiometric measurements on Site 12 consisted of two elevation scans. Typical antenna temperatures at 21 cm are presented in Figure B-17. Site 12 is relatively smooth, and the radiometric scans exhibit conspicuous Brewster angles, characteristic of specular surfaces.



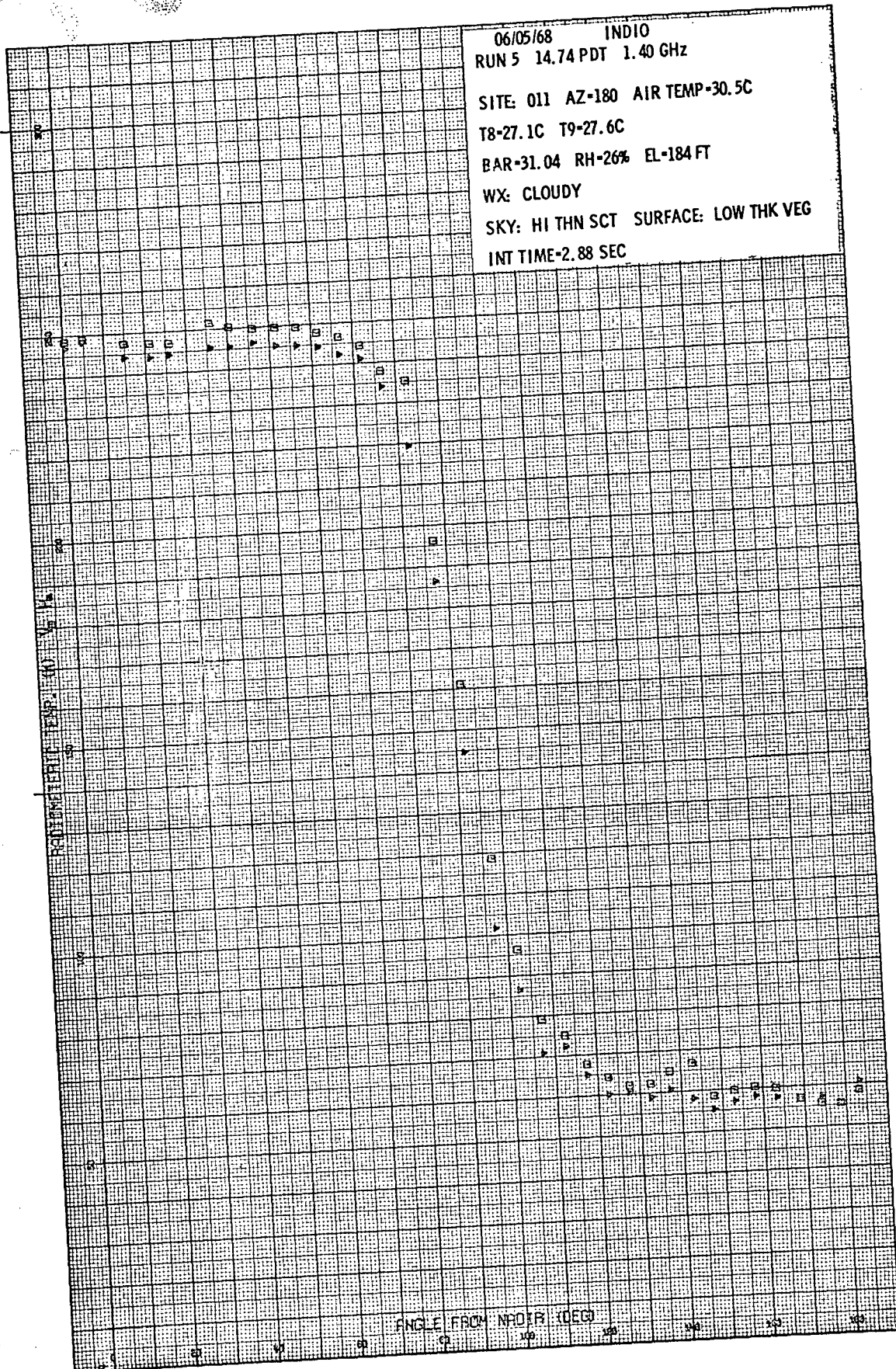


Figure B-15a. Site 11 - Radiometric Brightness Temperature Measured at 21-cm Wavelength

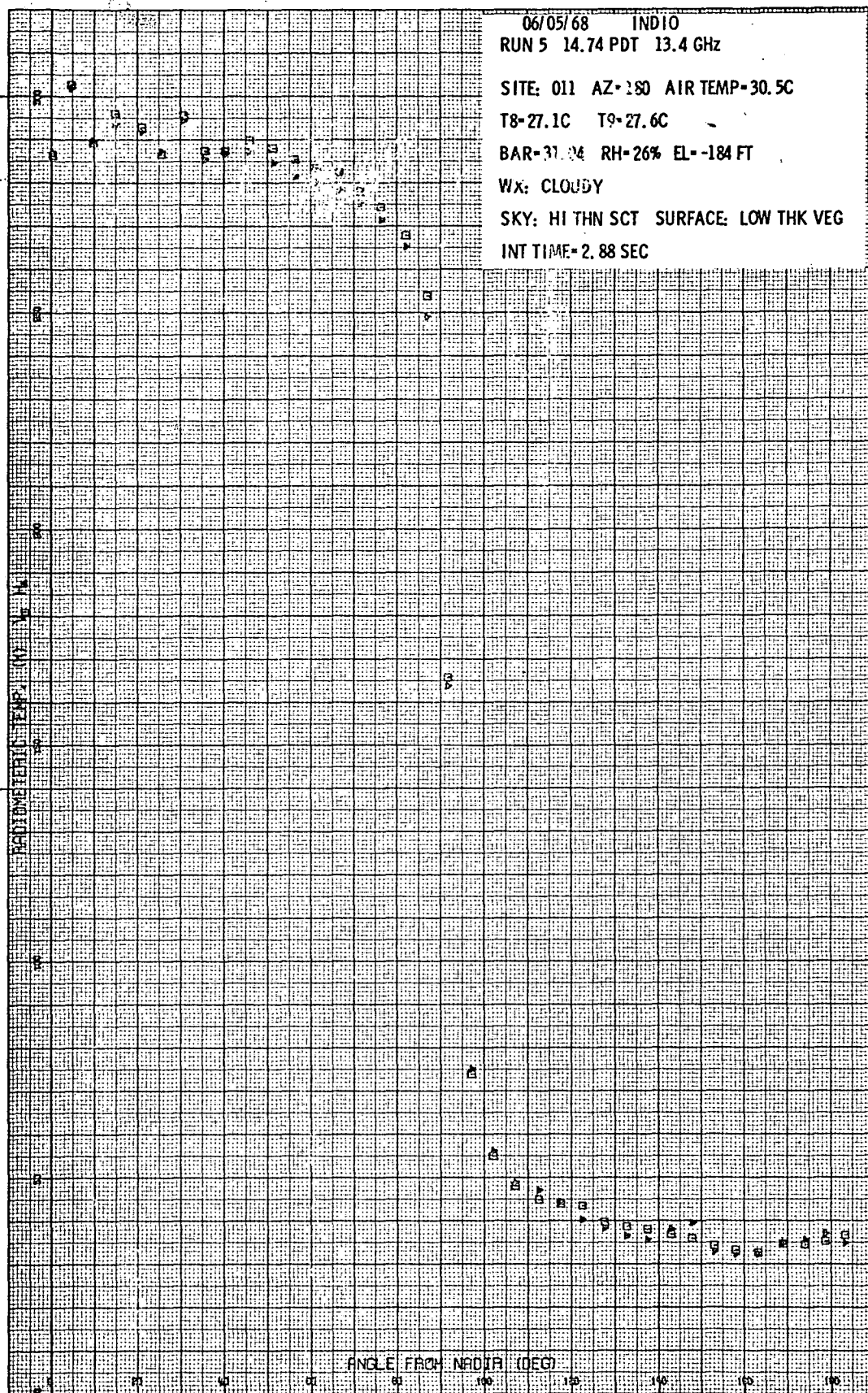


Figure B-15b. Site 11 - Radiometric Brightness Temperature Measured at 2.2-cm Wavelength

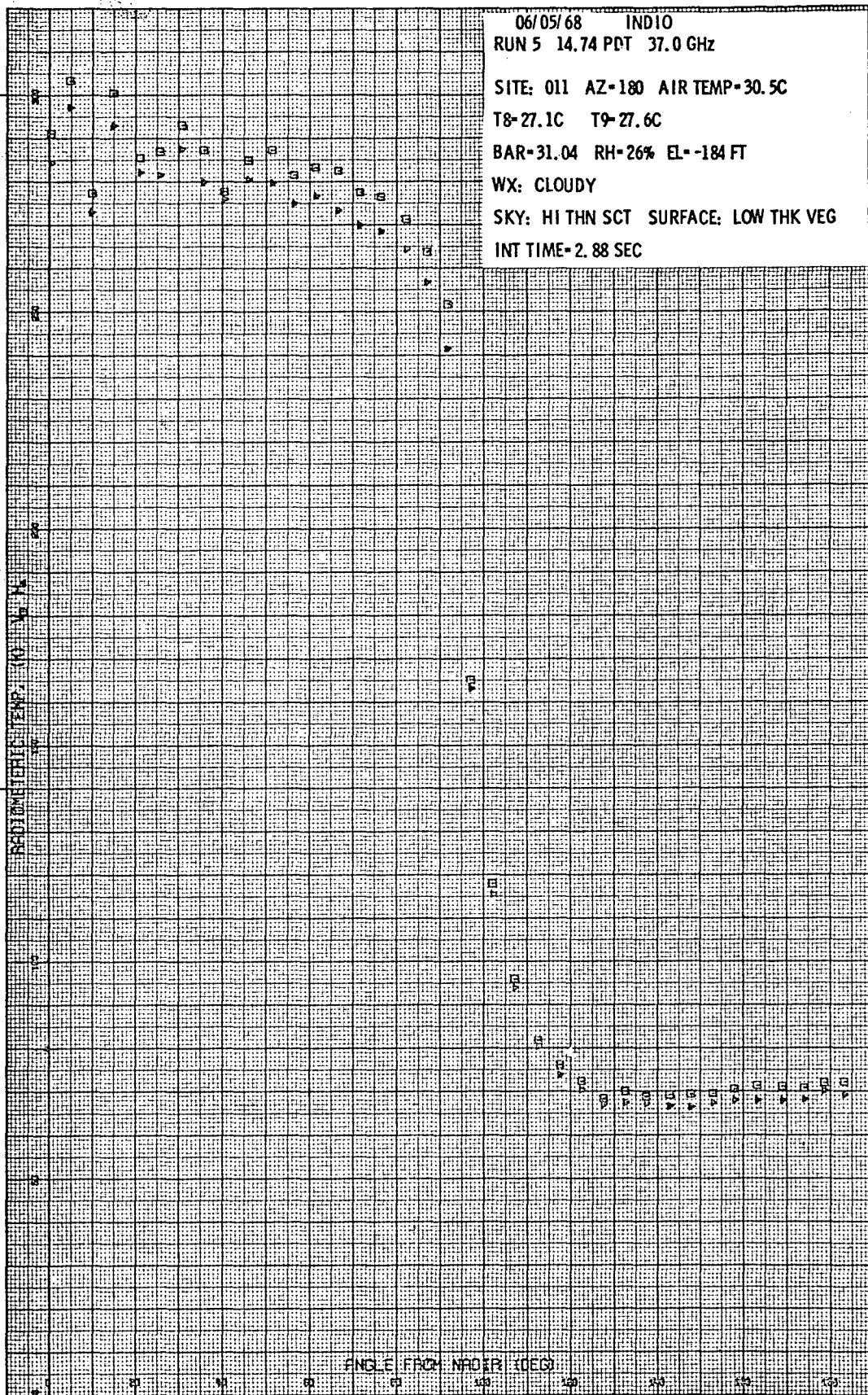
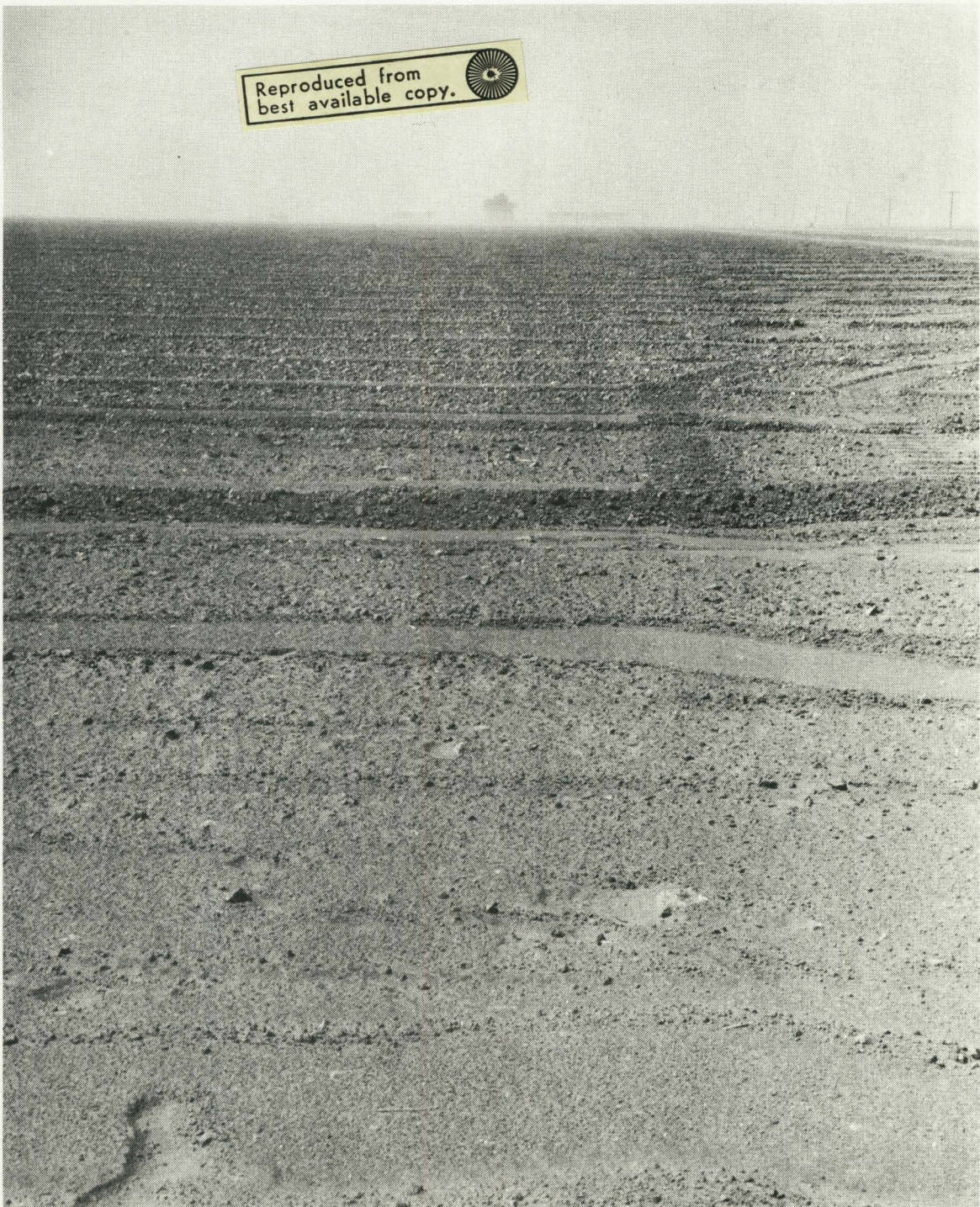


Figure B-15c. Site 11 - Radiometric Brightness Temperature Measured at 0.8-cm Wavelength



3425/072

Figure B-16. Site 12

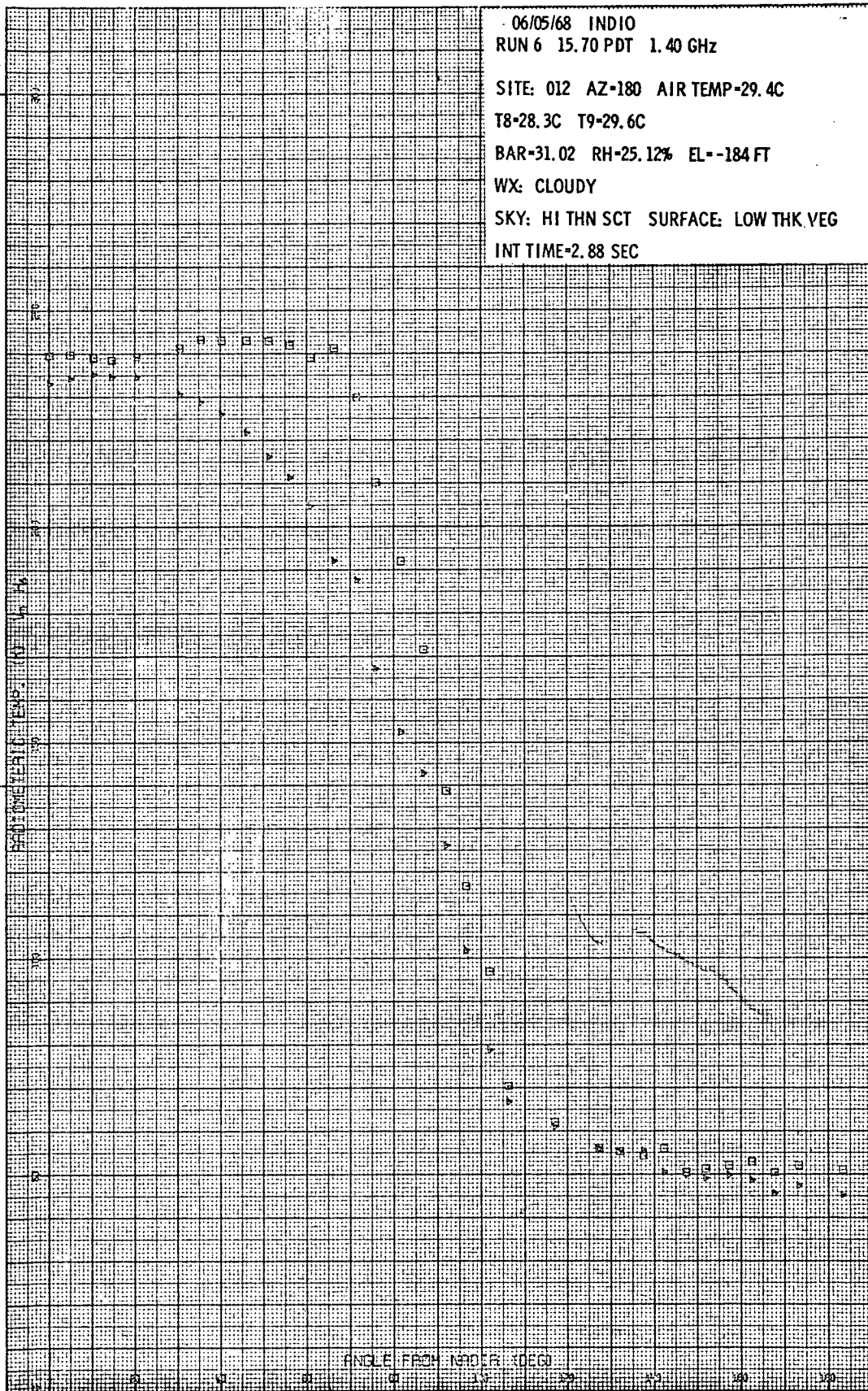


Figure B-17. Site 12 - Radiometric Brightness Temperature Measured at 21-cm Wavelength

SITE 13 (5 JUNE 1968)

A recently plowed barren field 1.3 miles south of Calipatria was designated Site 13. The surface was moderately rough with dirt clods up to 6 inches in diameter, Figure B-18. The thermometric temperature of the soil ranged from 36°C at the surface to 26°C at a depth of 18 inches. Soil moisture conditions were slightly higher than Site 12 with the surface at 1.6 percent and a very moist 24 percent at a depth of 6 inches. Only 2.2-cm antenna temperatures were measured at this site. Other radiometers were inoperative. Site 13 affords a diffuse surface to the 2.2-cm sensor. Consequently, apparent temperatures are quite warm and unpolarized. Polarization differences for sites 12 and 13 are compared in Table B-5.

TABLE B-5

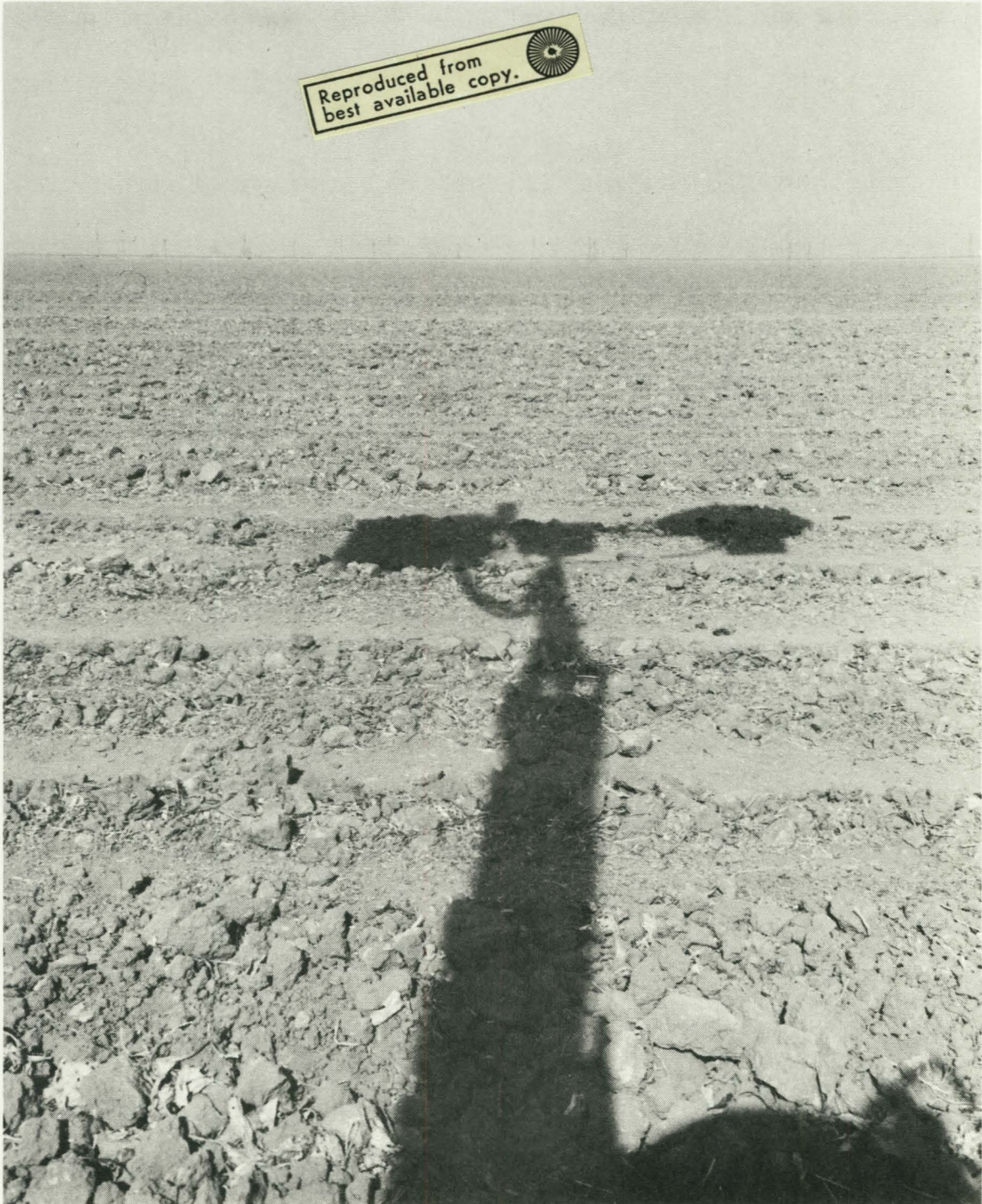
POLARIZATION DIFFERENCE FOR 2.2-CM SENSOR

<u>Viewing Angle, deg</u>	<u>Site 12</u>	<u>Site 13</u>
10	0.9	0.4
25	6.5	2.5
45	23.8	5.7

SITES 14 AND 15 (6 JUNE 1968)

In an area east of the Salton Sea near Salton Parkside, a microwave traverse was taken across the trace of the San Andreas Fault. In this area, as with many areas along the fault, rising ground water occurs, increasing the moisture content near the surface. The fault zone acts as a barrier to the normal migration of ground water in recent alluvial sediments, and can be distinguished by this increase in soil moisture. Typical terrain characteristics of the site can be noted in Figure B-19. The traverse was 8,000-foot long, and measurements were taken with a viewing angle of 50° from nadir.

Reproduced from  
best available copy.



3425/075

Figure B-18. Site 13



3425/069

Figure B-19. Sites 14 and 15



The soil thermometric temperature was measured at the start of the traverse. Temperatures were high, ranging from 57.5°C at the surface to 31.0°C at a depth of two feet. The moisture content of the soil was sampled every 400 feet along the traverse. The samples were integrated to give the moisture content for depth intervals from the surface to three inches, from the surface to six inches, and for the surface to twelve inches.

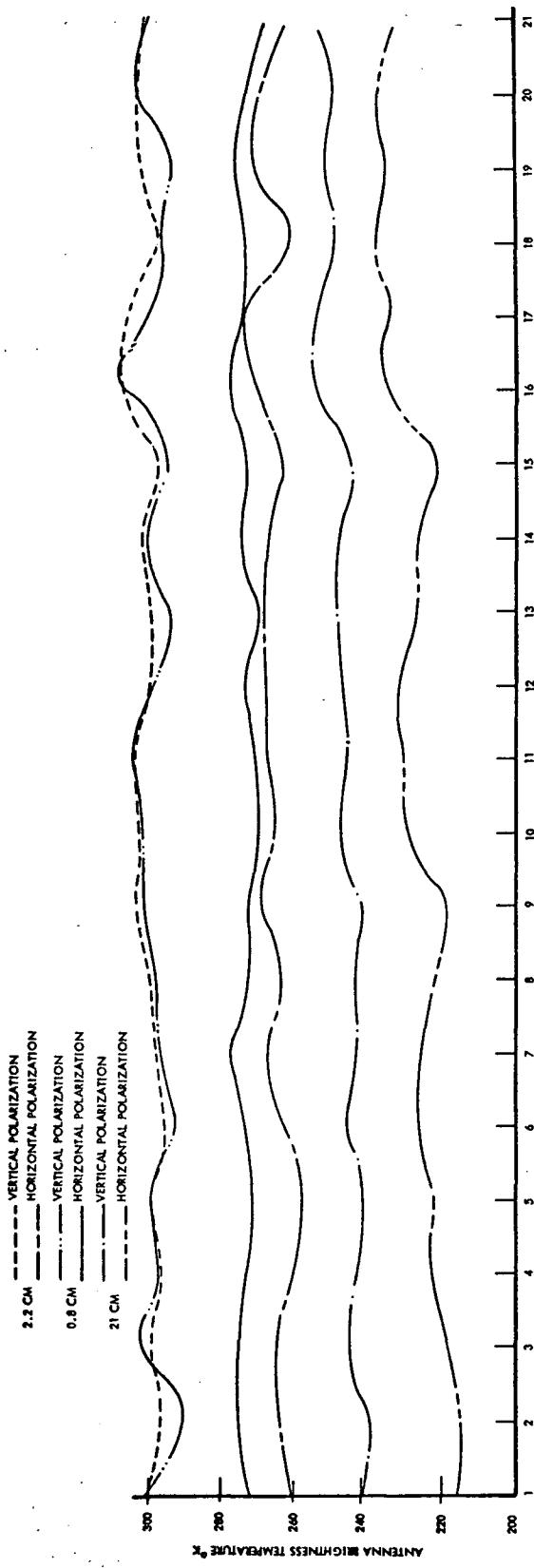
Antenna temperatures and the percent moisture for each 400-foot interval of the traverse are plotted on Figure B-20. The 0.8-cm and 2.2-cm antenna temperatures along the traverse varied by only 18°K. The 21-cm temperatures exhibited a maximum range of 15°K for vertical polarization and 33°K for horizontal polarization. High saline concentrations near stations 16-18 cause an increase in antenna temperature for the 21-cm radiometer. Polarization differences for all the radiometers decreased in areas where soil moisture was higher.

Measurements designated Site 15 are along the same track as Site 14 and consist of a traverse across the portion of the fault from Station 21 to 10 using an antenna viewing angle of 30°. The 0.8-cm and 2.2-cm vertically-polarized antenna temperatures were lower by approximately 10°K for most of the traverse, except at stations 15, 17, and 19 where temperatures were equal to those measured at a viewing angle of 50°.

#### SITE 16 (6 JUNE 1968)

Located in the same general area as Sites 14 and 15, this site consisted of a traverse along the road leading from Salton Parkside to Highway 111. The principal objective of the traverse was to determine the value of microwave radiometry as a tool for mapping geologic structures.

Geologically, the area contains a sequence of steeply dipping sedimentary rocks of Tertiary Age. The predominant rock type is mudstone; however, sandstone is present in moderate quantities. The rocks dip steeply to the west and strike perpendicular to the direction of traverse.



B-43

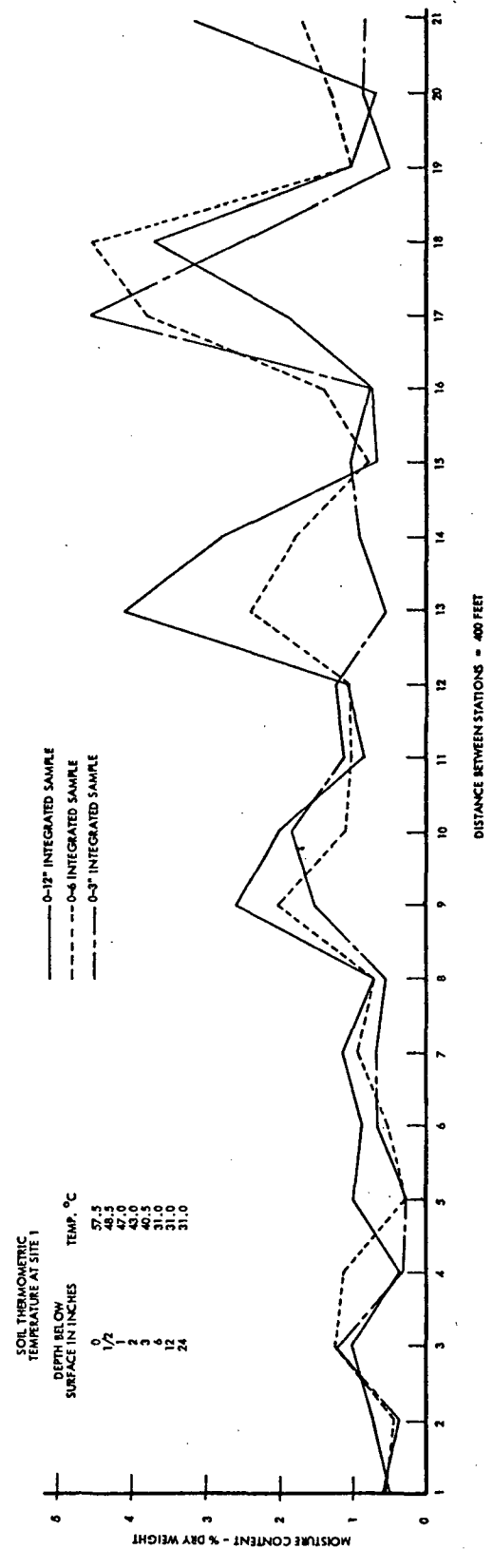


Figure B-20. San Andreas Fault Traverse

Antenna temperatures have been plotted, but correlation with structures in the area is difficult. The shorter wavelength radiometers are not suited for this type of application, since surface texture, such as roughness, particle size and particle shape, are the influencing factors on the measured temperatures. The long wavelength (21-cm) radiometer temperatures appear to be influenced by changes in attitude and rock type.

SITE 17 (7 JUNE 1968)

Site 17 is located north of Brawley on the west side of highway 111, on a barley-stubble field. The cut barley stalks cover 80 percent of the ground surface forming a mat of intertwined dry vegetation. Figure B-21. Although the field had not been irrigated for 45 days prior to radiometric measurements, soil moisture was moderately high. This condition is undoubtedly related to the mat of cut barley which shelters the soil from solar radiation. The percent moisture at the surface was 8.5 percent and increased to 23 percent at a depth of six inches. Air temperature at the time of measurement was 24°C.

A traverse was taken in a north-south direction using a viewing angle of 45°. Average antenna temperatures are shown on Table B-6.

TABLE B-6

AVERAGE ANTENNA TEMPERATURES FOR CUT BARLEY ON SITE 17  
(45° Viewing Angle)

	Radiometer		
	<u>21 cm</u>	<u>2.2 cm</u>	<u>0.8 cm</u>
Vertical Polarization	255°K	290°K	289°K
Horizontal Polarization	240°K	281°K	284°K

Low average antenna temperatures for the 21-cm radiometer reflect the increased moisture at depth. The moderately large (15°K) polarization difference can be attributed to increased moisture. Antenna temperatures for the 2.2-cm and 0.8-cm radiometers are high, characteristic

Reproduced from  
best available copy. 



3425/074

Figure B-21. Site 17

of soils with low moisture.

Emissivities calculated from average antenna temperatures are presented in Table B-7.

TABLE B-7

CALCULATED EMISSIVITIES FOR CUT BARLEY ON SITE 17  
(45° Viewing Angle)

	<u>Radiometer</u>		
	<u>21 cm</u>	<u>2.2 cm</u>	<u>0.8 cm</u>
Vertical Polarization	0.86	0.98	0.97
Horizontal Polarization	0.81	0.95	0.96

SITE 18 (7 JUNE 1968)

Site 18 encompassed a partially cut alfalfa field. The cut portion of the field had 50 percent vegetal cover; the vegetation being the cut alfalfa and stubble. The uncut alfalfa stood one-foot tall and presented a nearly diffuse surface.

Soil moisture was generally high. Portions of the field were under irrigation and contained standing water on the surface. Air temperature at the time of the measurements was 25°C.

A microwave traverse was conducted using a viewing angle of 50°, Figure B-22. The difference in temperature ( $T_v - T_h$ ) for the cut alfalfa did not differ appreciably from that of the uncut crop. The transition from cut to uncut alfalfa occurred on data frame number 50. Antenna temperatures for the 21-cm radiometer remain approximately the same throughout the traverse until frame number 78, where antenna temperatures for all radiometers decrease due to the presence of standing water.

Calculated emissivities for the alfalfa crop are presented in Table B-8.

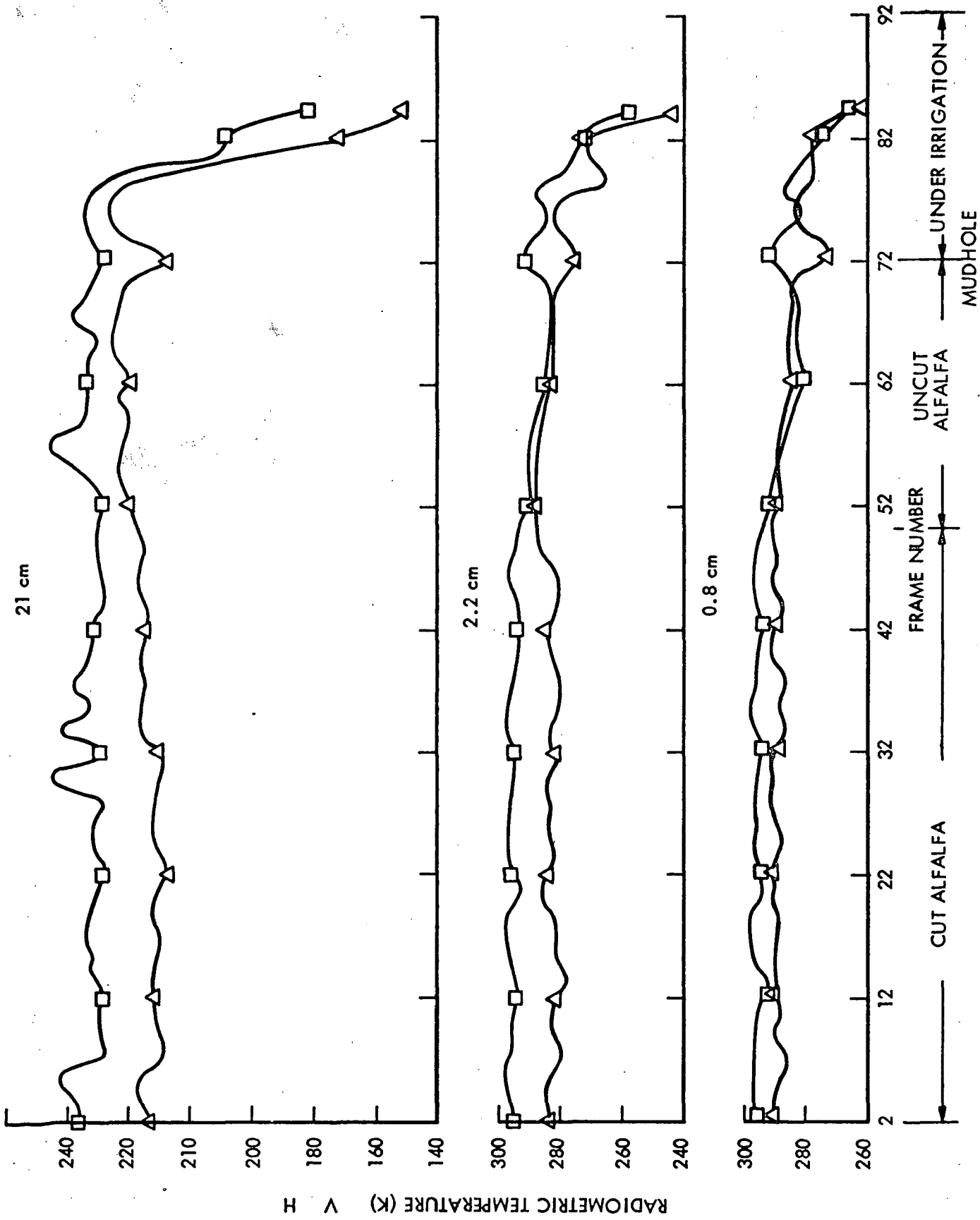


Figure B-22. Microwave Brightness Temperatures at Three Wavelengths Taken During Traverse of Site 18

TABLE B-8

CALCULATED EMISSIVITIES FOR ALFALFA ON SITE 18  
(50° Viewing Angle)

	<u>21-cm Sensor</u>		<u>2.2-cm Sensor</u>		<u>0.8-cm Sensor</u>	
	<u>Vert.</u> <u>Plzn.</u>	<u>Horiz.</u> <u>Plzn.</u>	<u>Vert.</u> <u>Plzn.</u>	<u>Horiz.</u> <u>Plzn.</u>	<u>Vert.</u> <u>Plzn.</u>	<u>Horiz.</u> <u>Plzn.</u>
Cut Alfalfa	0.85	0.78	0.99	0.95	0.99	0.97
Mature Alfalfa	0.83	0.79	0.99	0.95	0.99	0.98
Alfalfa & Water	0.70	0.58	0.90	0.84	0.91	0.87

The low emissivities calculated from the 21-cm data for the area under irrigation indicate the presence of the standing water on the ground surface. Water having a low emissivity (~ 0.45) causes a lower emissivity for the combined alfalfa-water system. Slightly lower emissivities for shorter wavelength radiometers have also been calculated for the same area.

SITE 19 (7 JUNE 1968)

Site 19 is located on the southwest corner of the intersection of Rutherford Road and Highway 111, between Brawley and Calipatria. This site contains a mature sugar beet crop. The individual sugar beet plants were 1-foot high with 3-inch wide leaves. The leaves were crenulated and turned due to the high alkali content of the soil.

Soil moisture conditions ranged from dry at the surface to 19 percent just below the surface and 21 percent at a depth of 12 inches. Thermometric soil temperature at the time of the measurements was 41°C on the surface, decreasing to 22°C at depth of 18 inches. A temperature of 28°C was measured for the beets by placing a button thermistor on the underside of the leaf.

The radiometric measurements consisted of two elevation scans and a traverse with a viewing angle of  $45^{\circ}$ . One scan was taken in a direction parallel to the furrows, Figure B-23. The second scan was made in a direction perpendicular to the furrows. Antenna temperatures were slightly higher for the second scan and indicate that a larger portion of the field of view was covered with plants. Polarization temperature differences were small for all angles of view. In some cases, horizontal polarization temperatures were warmer than vertically polarized temperatures. In the horizontally polarized sense, a larger portion of the energy is contributed by the plant.

The average antenna temperatures measured during the traverse ( $45^{\circ}$  antenna viewing angle) were consistent with temperatures observed during the elevation scans. The traverse was taken around two sides of the field. During the first portion of the traverse, the radiometers were looking parallel to the furrows, and during the latter portion the field of view was perpendicular to the furrow direction. Slightly lower antenna temperatures were measured during the latter portion of the traverse.

Emissivities calculated from average temperatures recorded during the traverse are presented in Table B-9. Note that the sugar beets were remarkably unpolarized.

TABLE B-9  
CALCULATED EMISSIVITIES FROM AVERAGE ANTENNA TEMPERATURES ON SITE 19  
( $45^{\circ}$  Viewing Angle)

<u>Radiometer</u>	<u>Polarization</u>	<u>Emissivity</u>
21-cm	Vertical	0.85
	Horizontal	0.85
2.2-cm	Vertical	0.95
	Horizontal	0.95
0.8 cm	Vertical	0.95
	Horizontal	0.95





3425/078

Figure B-23. Site 19

SITE 20 (7 JUNE 1968)

Site 20 was situated on a field of recently planted cotton on the west side of Highway 111, 5 miles south of Calipatria. The plants were small and afforded only 20-percent ground cover, Figure B-24. Soil moisture conditions were dry on the surface and only slightly moist at depth. The field had been recently tilled and small clods one to two inches in diameter were exposed in the furrows.

A traverse was made along the field parallel to the furrow direction, using a viewing angle of  $45^{\circ}$ . Antenna temperatures for all radiometers varied over a wide range. Maxima, minima, and average temperatures for the entire traverse are given in Table B-10.

TABLE B-10  
AVERAGE ANTENNA TEMPERATURES OF RECENTLY PLANTED COTTON ON SITE 20  
( $45^{\circ}$  Viewing Angle)

	<u>21-cm Sensor</u>		<u>2.2-cm Sensor</u>		<u>0.8-cm Sensor</u>	
	<u>Vert.</u> <u>Plzn.</u>	<u>Horiz.</u> <u>Plzn.</u>	<u>Vert.</u> <u>Plzn.</u>	<u>Horiz.</u> <u>Plzn.</u>	<u>Vert.</u> <u>Plzn.</u>	<u>Horiz.</u> <u>Plzn.</u>
Maximum	261	260	301	294	301	301
Minimum	246	228	283	282	277	275
Average	256	256	292	288	285	285

An important point to be noted from these measurements and from measurements taken in other areas with vegetation, is the unpolarized nature of the crops. Areas under cultivation measured at moderately-high viewing angles represent diffuse, unpolarized surfaces. This relationship is in agreement with analytical models where scattering due to the irregular crop surfaces is considered.

SITE 21 (7 JUNE 1968)

Site 21 was situated on a field of mature silage grass 0.5 miles west of Highway 111 on the north side of Hazard Road. The grass

Reproduced from  
best available copy.



3425/079

Figure B-24. Site 20

was 9-inches high with stalks 1/16-inch in diameter, Figure B-25. The grass covered 80 percent of the ground surface. Soil moisture conditions were dry at the surface, increasing to 6 percent immediately beneath the surface. At a depth of 6 inches, soil moisture was 23 percent and increased to 28 percent at 12 inches below the surface. Air temperature at the time of measurement was 26°C.

A traverse was taken along the south side of the field using a viewing angle of 45°. Only the 2.2-cm and 0.8-cm radiometers were operating during the traverse. Antenna temperatures averaged 301°K and 296°K for vertical and horizontal polarizations on the 2.2-cm radiometer. Slightly colder antenna temperatures were recorded for the 0.8-cm radiometer.

Calculated emissivities for the silage grass are presented in Table B-11.

TABLE B-11  
 CALCULATED EMISSIVITIES FOR SILAGE GRASS ON SITE 21  
 (45° Viewing Angle)

<u>2.2-cm Sensor</u>		<u>0.8-cm Sensor</u>	
<u>Vert.</u> <u>Plzn.</u>	<u>Horiz.</u> <u>Plzn.</u>	<u>Vert.</u> <u>Plzn.</u>	<u>Horiz.</u> <u>Plzn.</u>
1.0	0.99	0.98	0.98



3425/080

Figure B-25. Site 21

Reproduced from  
best available copy. 